Case II Sorption in Glassy Polymers: Penetration Kinetics

by

Jian-Xin Li

A thesis submitted in conformity with the requirements
for the degree of Doctor of Philosophy
Graduate Department of Pharmaceutical Sciences
University of Toronto

Dedicated to my family

Case II Sorption in Glassy Polymers: Penetration Kinetics

Doctor of Philosophy, 1998, Jian-Xin Li
Department of Pharmaceutical Sciences
Faculty of Pharmacy, University of Toronto

Abstract

The penetration kinetics of methanol in polymethyl methacrylate (PMMA) beads has been examined in detail, which reveals a size dependence in the induction time during the initial phase of the Case II sorption. In addition, the induction time and front penetration rate are inversely related. Similar size dependence and inverse relationship between induction time and front penetration rate have also been observed in several other systems including methanol in crosslinked PMMA beads, higher alcohols in uncrosslinked PMMA beads, and n-hexane in polystyrene (PS) beads. This suggests that the induction time is not a material constant as previously assumed by existing theories. A new phenomenological analysis of front penetration kinetics further substantiates that the induction time and front penetration rate are inversely related for any given system.

Our results also show that the volume swelling ratio in the swollen region of the bead remains constant during the propagation of the penetration front. This supports the notion of a uniform concentration distribution in the swollen region during Case II sorption. This volume swelling ratio also shows a slight increase with temperature.

As confirmed by SEM and AFM observations, the dependence of induction time on size is not caused by changes in surface morphology since there is no detectable difference in surface morphology for PMMA beads of different diameters.

The inverse relationship between induction time and penetration rate as derived from our phenomenological analysis is in agreement with that predicted from a molecular theory. The phenomenological analysis further confirms that the induction time and its relationship with the initial front penetration rate depend on both the geometry and dimension of the polymer specimen in the penetration direction. The length of induction time for slab and cylindrical geometry approaches that of the semi-infinite geometry more than that of the spherical geometry. Consequently, this size dependence may become insignificant when the dimension of the cylindrical discs and slabs is comparable to the diameter of the beads.

Based on our results, a quantitative criterion has been formulated for the occurrence of Case II sorption. A new phase diagram has also been constructed to predict the occurrence of Case II behavior. It provides a qualitative definition of the upper temperature limit for Fickian diffusion as well as a lower temperature limit for anomalous diffusion in glassy polymers.

Acknowledgments

I am very grateful to Professor Ping I. Lee for his patient, supportive and inspiring guidance, understanding and encouragement. He has won my admiration for his dedication and enthusiasm to academic research. His rich experience has enabled him to give me the best introduction and guidance to this fascinating and competitive field. His intellectual inspiration has been a vital source of my creativity.

It is very fortunate for me to have Professors Yu-Ling Cheng, Don E. Cormack, my former co-supervisor, and Peter S. Pennefather serving in my advisory committee. Thanks for the time they spent with me. They have been very helpful and friendly.

I am much obliged to both Professor Lee and Professor Cormack for their compassionate and generous support to finish my research related to my M. A. Sc. project while studying in this Faculty.

My sincere gratitude also goes to each member in our research group, and our friendly neighbors, diners in the Faculty Lounge for their friendship and help, which have made my life in this university both enjoyable and memorable. I am indebted to Drs. P. Wang in Germany and Q. Yang in England for helping me to obtain valuable copies of theses. I am grateful to the Van der Woods family for their constant emotional support during my program; to Dr. Thiessen, advisor for my comprehensive examination, for his friendship; to Lin Zhu for her love.

Finally, I wish to acknowledge the financial support from the University of Toronto.

The Tao that can be told of
  Is not the Absolute Tao;
The Names that can be given
  Are not Absolute Names.

The Nameless is the origin of Heaven and Earth;
The Named is the Mother of All Things.

Laotse

Table of Contents

Symbols

A	extrapolated normalized penetration
a	a constant
$a_o(0)$	initial radius of the sphere or cylinder or half-thickness
$a_o(t)$	radius of the sphere or cylinder or half-thickness at time t
$a_i(t)$	radius of the sphere or cylinder or half-thickness for the inner unswollen core
B	mobility coeffcient
b	a constant
C_e	equilibrium (maximum) concentration of the penetrant in the polymer which increase with increase in temperature
C_g	penetrant concentration at which the transition of polymer from glassy state into rubbery state occurs
C_l	minimum concentration at which the polymer change into liquid or the maximum concentration at which the polymer remains rubbery
C_t	local concentration of the penetrant inside the polymer at time t
c	concentration
c_c	the maximum concentration at the front
c_e	equilibrium surface concentration
c_i	instant surface concentration
c_s	surface concentration at t
c_p	critical penetrant concentration marking the position of plasticization front
c_∞	equilibrium concentration
D	diffusion coefficient
$d_o(t)$	diameter or thickness of the outer swollen core
$D(c)$	diffusion coefficient for the concentration dependent component
$D(c,\sigma)$	global diffusion coefficient
D_0	diffusion coefficient of the penetrant in the glassy region
D_r	diffusion coefficient of the polymer chains
$d_i(t)$	diameter or thickness of the inner unswollen core
$d_o(0)$	initial diameter or thickness
E	modulus of elasticity
$E(c)$	a concentration dependent coefficient
F	phenomenological coefficient correlating the effect of hydrostatic stress σ on the global diffusion coefficient
J	flux of the penetrant
K	a material constant,
K'	a material constant
k	mass transfer coeeficient in surface resistance boundary condition
k_b	Boltzmann constant
M	molecular weight of polymer
n_0	degree of polymerization
P	normalized front penetration
P'	normalized front penetration rate

R	absolute gas constant
$\langle R^2 \rangle$	mean-square end to end distance of the chains
S	partial stress tensor
s	a constant
T	temperature
T_g	glass transition temperature
T_α	temperature at which glass transition of polymer occurs when it is in equilibrium with the penetrant
T_β	temperature at the onset of β relaxation of the polymer
T_l	onset temperature at which polymer starts to flow
t	immersion time
V	specific molar volume of the penetrant
x	position
v_0	initial front penetration rate
α	a constant
β	inverse of the relaxation time
δ	thickness of the plasticizing zone
ε	a small parameter corresponding to the large diffusivity of the polymer in the plasticized state
ζ_0	friction coefficient per monomer unit
μ	chemical potential
Π	osmotic stress
ρ	global density
σ	hydrostatic stress
τ	relaxation time
τ_d	disentanglement time
τ_0	induction time
τ_r	the longest relaxation time of a polymer chain in Rouse equation

List of Tables

List of Figures

Chapter 1

Case II Sorption: A Review

1.1 Introduction

The diffusion of small molecules in a polymer occurs as a result of the random motions of individual molecules known as random walk or Brownian motion in the polymer. Therefore, the transport behavior of small molecules in polymers strongly depends on the polymer structure and mobility. As a result, small molecules can be used as a sensitive indicator to probe the polymer structure and state, and their dynamic changes. Diffusion in polymer is also one of the fundamental problems associated with a variety of industrial applications including controlled drug release, packaging, separation, and micro lithography.

Diffusion may not occur in pure form. In materials science, abundant examples exist supporting the notion that coupling of diffusion, phase transformation, structural relaxation and mechanical deformation, etc., are often the norm in reality. Diffusion of the fluid molecules in a polymer can be adequately described by Fick's law when the structure and mobility of the polymer are not significantly modified by the presence of the penetrant molecules in the polymer. Such premises may not be valid when a glassy polymer is exposed to a penetrant of high activity, where Fick's law fails.

Five major types of experimental results are commonly associated with non-Fickian or anomalous diffusion kinetics in glassy polymer: Case II behavior, Super Case II behavior, sample size effects, two stage sorption and sorption overshoot. It is conceivable

that material properties, both mechanical and physical in nature, may have to be considered in searching for an interpretation of the apparent anomalous behavior in the Fickian paradigm. Currently, there is no single universally accepted theory which could be used to describe all the diffusion anomalies.

Diffusion of penetrant molecules in a rubbery polymer generally follows Fickian diffusion or Case I diffusion, which is a limiting behavior for diffusion in polymers. In slab samples, such Case I diffusion is characterized by a linear increase of polymer weight gain as a function of the square root of sorption time. On the other hand, the sorption weight gain may deviate from the Case I diffusion behavior and increase linearly with time in glassy polymers. This phenomenon is known as Case II diffusion which has been regarded as another limiting case for diffusion in polymers, generally glassy polymers. Case I diffusion and Case II transport have characteristic activation energy ranging from less than 10 kcal/g-mol to 20-50 kcal/g-mol, respectively. Diffusion behavior which is intermediate between that of Case I or Case II is regarded as anomalous diffusion. Super Case II diffusion is characterized by an acceleration of absorption rate towards the end of the front penetration process.

The role of Case II diffusion as another limiting case of diffusion may be debated because of the controversy over the existence of Super Case II diffusion, and the fact that Case I diffusion generally precedes the onset of Case II diffusion. In addition, Case I behavior may reoccur in Case II diffusion when the sample dimension is large. Therefore, Case II diffusion may be more appropriately named as Case II transport or more precisely, Case II sorption. Case II sorption is uniquely characterized by a constant movement of penetration front after a glassy polymer is immersed in a non-dissolving liquid penetrant.

This linear behavior of front penetration kinetics has been proposed for the design of zero-order drug delivery systems (Hopfenberg and Hsu, 1978).

1.2 Literature Review

Case II behavior was first documented by Alfrey, Gurnee and Lloyd (1966). This transport mechanism is generally associated with liquid penetrant in glassy polymers. The unique attribute of this unsteady sorption is the constant movement of a sharp penetration front, separating highly swollen polymer shell from a nearly dry core, propagating slowly into the dry glassy core. The liquid mass uptake of a polymer slab increases linearly with time due to the stepwise concentration distribution. The transport process was strikingly distinct from normal diffusion. It has been actively investigated in the past three decades (Frisch, 1980; Windle, 1985; Lustig *et al.*, 1992; Kalospiros *et al.*, 1993; Durning *et al.*, 1996; Samus and Rossi, 1996). In this review, Case II transport, Case II sorption and Case II behavior are used interchangeably, so are fluid molecules, penetrant, diffusant and swelling agent; as well as internal stresses and differential swelling stresses.

1.2.1 Overview of Case II Sorption

The sorption method has been extensively used experimentally to study the unsteady diffusion of penetrant in polymers. Sorption kinetics is characterized by penetrant concentration distribution in the swelling polymer or the weight change of the polymer due to absorption. Differential or interval sorption takes place when the difference between the external penetrant activity and the equilibrium penetrant activity within the polymer is close

to zero. When the difference of penetrant activity is close to 1, the process is termed integral sorption.

Case II sorption only occurs during integral sorption of small molecules in glassy polymers (Windle, 1985) or during interdiffusion of polymers when only one of the polymers is in glassy state (Sauer and Walsh, 1991; 1994). The phenomenon is considered as nonlinear since it cannot be observed during differential sorption test (Billovits and Durning, 1990, 1993). The following key features are characteristic with Case II sorption:

- An induction time is needed to form the fluid penetration front;
- The front will move at a constant velocity;
- The induction time is inversely proportional to the front penetration rate;
- The penetrant concentration distribution in the swelling polymer is almost step-wise

As will be clarified later, the following observations are also associated with Case II sorption:

- The fronts are hallmark of heterogeneity of the swelling polymer;
- The rate controlling process occurs at the front;
- Case II sorption is nonlinear and irreversible;
- Case II sorption may be treated as a quasi-steady transport process

When a glassy polymer is immersed in an organic swelling agent of high activity, partial absorption will occur instantaneously to fill the unoccupied free volume at the polymer surface. Further absorption of diffusant will cause swelling or plasticization. The

swelling or plasticization of polymer is realized through the change of polymer conformation (chains or segments). This dynamics of conformational change is determined by the mobility of the polymer chain, which is hindered by intramolecular and intermolecular forces. The intramolecular and intermolecular forces can be altered by experimental temperature, type and concentration of diffusants. The conformational changes, which limit the kinetics of concentration changes, are not instantaneous; a long time interval is needed for the surface concentration of the diffusant to reach an equilibrium value.

Before the onset of Case II behavior, the surface concentration will first evolve to a threshold concentration prior to establishing the penetration front, then the surface concentration will approach an equilibrium value. Once the concentration in the surface layer reaches a critical threshold value (usually less than the equilibrium value), the swelling region would start to move into the core (Hui *et al.*, 1987a). An induction time corresponding to the time necessary for the polymer surface to reach this critical concentration is usually associated with this process.

The heterogeneous swelling polymer can be divided into three regions: a swollen region, a transitional swelling region and an unswollen region. Isotropic conformational changes of polymer chains due to penetrant swelling will cause lateral expansion parallel to the polymer surface, which will be constrained by the unswollen core through the adjacent unaffected chains and segments. The lowest energy path for such conformation change is in the direction perpendicular to the surface. Changes of polymer conformation and sample dimension are therefore anisotropic. This potentially unstable structure stores energy.

The swelling region is usually observed as an interface or a front separating the swollen from the unswollen region. However, this is not a pure geometrical plane. The thickness of the swelling region for poly (methyl methacrylate) (PMMA)/methanol was estimated to be 0.1-20 μm (Thomas and Windle, 1978; Durning *et al.*, 1995). Polymer relaxation (delayed response to stimulus) in response to the osmotic swelling stresses or plasticization is mainly involved in this region. The kinetics of relaxation or plasticization depends on the activity of diffusant available in this region and the morphology of the unswollen polymer adjacent to the region. Diffusion in this region is intermediate between Case I and Case II behavior. It is possible that mechanisms governing the movement of this transitional swelling region are also involved in the formation of the initial swollen surface layer during the induction period.

As a driving force in the swelling region, the osmotic stress is responsible for the transformation or plasticization of adjacent unswollen polymer, again embodied by the changes in polymer conformation. Generally, sample thermal and sorption history can result in modification of the polymer structure. Similarly, the sample geometry and size will affect the differential swelling stress. The nature and activity of diffusants, as well as temperature, can also influence the osmotic swelling pressure and the differential swelling stress. Generally, these factors will affect the time required for the surface layer formation and the migration speed of the swelling region.

When the swollen polymer is rubbery, a thermodynamic equilibrium state is generally reached, and the equilibrium concentration depends mainly on the interaction coefficient and the penetrant molar volume. On the other hand, the swollen polymer will be in a pseudo-equilibrium state when it is still glassy, since the glassy state is not in

thermodynamical equilibrium. The polymer-penetrant mixture can be effectively considered stable in the time scale of the experiments. The "equilibrium" concentration, different from its thermodynamic value, may depend on at least four factors: the polarity of the penetrant, its solubility parameter, molar volume and glass transition temperature (Bellenger *et al.*, 1997).

In the swollen region, the osmotic swelling pressure is superimposed with the differential swelling stress which is generally compressive in nature. When the swollen region is homogeneous, diffusion can be described by a modified Fick's law, with a stress and concentration dependent diffusion coefficient. The swollen polymer may be in the rubbery or glassy state, depending on the experimental temperature and diffusant concentration. Contrary to the assumption held by many investigators in this field, recent DSC results on PMMA/Methanol systems have demonstrated that the swollen PMMA may still be in the glassy state when sorption is conducted below 40°C (Lin *et al.*, 1990, 1991).

Depending on the level of tensile stress and plasticization due to the presence of penetrant, the unswollen glassy region can be either homogeneous or heterogeneous. The latter occurs when the tensile stress is above the yield strength of the unswollen polymer. In this case, crazing and cracking may result. Diffusion in this region can be Fickian or non-Fickian, depending on the morphology and the degree of mechanical damage in the unswollen core. Mechanical damage or failure of the core due to differential swelling stresses may lead to an accelerated migration of the swelling region when diffusional resistance is negligible.

It is known that a range of diffusion patterns can occur in the same polymer within a broad range of temperature, penetrant type and activity. This was proposed initially by

Alfrey *et al.* (1966) and latter described in more detail by Hopfenberg and Frisch (1969). Experimental work with glassy polystyrene (PS) by Enscore, Hopfenberg and Stannett revealed that sample dimension and history can also significantly alter the diffusion kinetics and equilibrium absorption of the penetrant (Enscore *et al.*, 1977a, 1977b; Hopfenberg, 1978). For example, absorption in submicron spheres is Fickian, whereas under the same boundary conditions, absorption in films (75 μm thick) and spheres (184 μm) are Case II. In addition thinner films (35 μm) may exhibit the so-called Super Case II behavior, whereas thick films (2000 μm) show Fickian behavior. The geometrical shape of specimen is another important factor that controls the sorption kinetics, concentration distribution and front penetration kinetics (Peterlin, 1980; Lee and Kim 1992).

1.2.2 Experimental Study of Case II Sorption

1.2.2.1 Concentration distribution

It is well established that the penetrant concentration profile is almost step-wise in typical Case II sorption, nearly constant behind the penetration front and negligibly low ahead of the front. The temporal evolution of concentration profile can be adequately determined by tracking the front movement, or by measuring the weight gain (Thomas and Windle 1978). The two most important parameters of Case II sorption, namely the induction time and front penetration rate, are generally obtained from such experiments. NMR imaging (Grinsted *et al.*, 1992), optical microscopy (Lee and Kim, 1992; Lee, 1993), laser interferometry (Durning *et al.*, 1995), and magnetic resonance imaging (Ercken *et al.*, 1996) have been employed in the non-destructive tracking of front movement. For rigid

slabs, cylinders and spheres, optical microscopy remains the simplest and most effective for such purpose. Confirmation of such step-wise concentration profile, and the relationship between induction time and front penetration rate can be derived from simple analysis of this phenomenon (see Chapter 2).

Results on the effect of sample thickness and temperature (Hopfenberg, 1978; Thomas and Windle, 1978) indicate that the front propagation rate may be reduced when the transport is rate-limited by diffusion in the swollen region as a result of an increase in the diffusion path length between the polymer surface and the swelling front as the front propagates inward. In this case, the penetrant concentration profile may not be step-wise, as experimentally demonstrated by following the penetrant color density distribution in the methanol-PMMA system using a microdensitometer (Thomas and Windle 1978).

For a more accurate understanding of Case II sorption, the concentration profile of the penetrant in the unswollen polymer during the induction period and front propagation needs to be determined. This generally requires a method with high spatial resolution and adequate penetration depth. Rutherford backscattering spectrometry (RBS) (Hui *et al.*, 1987a, b; Lasky *et al.*, 1988), and resonance nuclear reaction analysis (Umezawa *et al.*, 1992) have been employed for this purpose. The results demonstrate that the initial change of the penetrant concentration at the polymer surface is very slow prior to reaching a critical value and establishing a nascent concentration profile near the polymer surface. Subsequently, the penetrant concentration increases autocatalytically toward the saturation concentration, coincidental with the creation of a sharp concentration front and the termination of induction period. The front, with a penetrant precursor or Fickian tail, migrates into the unswollen core at a constant speed.

1.2.2.2 Micro-mechanism of Case II sorption

Although the penetrant molecules move more easily along their length rather than perpendicular to the molecular contour, experimental evidence does not support a simple reptation-like mechanism for the molecular motion of the penetrant in glassy polymer (Gall *et al.* 1990).

Case II behavior occurs in both linear and crosslinked polymers. The reptation of polymer chains may not be dominant in Case II sorption if the key parameters of Case II sorption are independent of the polymer molecular weight and its distribution as was concluded by Baird *et al.* (1971). However, contradictory observations were also reported for polymers of relatively low molecular weight (Bray and Hopfenberg, 1969; Papanu *et al*, 1990; Sauer and Walsh, 1991; 1994; Umezawa *et al.*, 1992). When the polymer is of high molecular weight (M_n ~ 200,000 for polystyrene (McGarel and Wool, 1987)), the frictional forces opposing the forced reptation of polymer chain are higher than the chain scission force well below T_g. Consequently there is no dependence on molecular weight since polymer chain scission is dominant in this situation (McLeish *et al.*, 1989; Plummer and Donald, 1990; Kausch and Plummer, 1994), though the forced reptation of fragmented chain segments may still take place. Observations of structural damage of the swelling polymer, such as crazing and fracture, were reported in some cases (Alfrey *et al.*, 1966; Jacques and Hopfenberg, 1974a; 1974b). If the surface energy required for the creation of craze or crack is large, simple homogeneous shear deformation will be favored (Kausch and Plummer, 1994)

As to the sorption kinetics, the swelling dynamics of ultra-thin film exposed to vapor can be monitored as a simulation of the critical plasticization process at the nanometer scale in the transitional swelling region. The effects of penetrant size, sorption temperature and the molecular weight of polymer on the swelling of PMMA thin films in alcohols were characterized by *in situ* ellipsometry (Papanu *et al.*, 1990). Surface-enhanced Raman scattering can be potentially used to monitor solvent progression within a polymer matrix in real time, which is capable of providing spectral information about polymer relaxation with spatial resolution under 300Å (Drake and Bohn, 1994). Similarly, surface plasmon resonance measurement was shown to be useful in the study of diffusion event in nanometer sized polymer films (Drake and Bohn, 1995; 1996). Attenuated total reflectance, FTIR (FTIR-ATR) spectroscopy was applied to provide information about molecular interaction in the swelling polymer (Fieldson and Barbari, 1995). In addition, relaxation time of polymer chains in the surface layer can be estimated from ellipsometry (Kip *et al.*, 1985).

It has long been recognized that the glass transition temperature of the swollen polymer can be higher than the experimental temperature in Case II sorption (Frisch *et al.*, 1969; Thomas and Windle, 1980; Brown, 1989; Samus and Rossi ,1996), *i.e.*, the swollen polymer may exist in glassy state as confirmed by experimental results (Janacek and Kolarik, 1976; Williams *et al.*, 1986; Lin *et al.*, 1990, 1991). Consequently, glass transition at the experimental temperature is not essential for the occurrence of Case II behavior. It has been proposed that β relaxation is associated with Case II sorption (Thomas, 1978). However, this idea has not been conclusively verified either experimentally or theoretically. Case II sorption has also been considered as a yielding or

creep phenomenon of the polymer in response to the osmotic stress of the penetrant. In this case, the polymer swelling rate is determined by the osmotic stress exerted on the polymer similar to the mechanical strain rate (Gall *et al.*, 1990). In addition to the proposed Case II sorption mechanisms based on glass transition and crazing, the interpretation based on plasticization and yielding, *i.e.*, chain solvation and molecular rearrangement through forced reptation of polymer chain, provides another alternative mechanism.

1.2.2.3 Effects of polymer history on diffusion

Unlike rubbery polymers, the structure and consequently the properties of glassy polymers depend strongly on the sample history. Such history effects need to be taken into account in the preparation of specimen and the interpretation of experimental sorption results. Considerable effort has been devoted to elucidate the history effects on penetrant diffusion by various investigators. One of the most extensively studied systems is the sorption of methanol in PMMA.

Methanol treatment has been observed to reduce the glass transition temperature (T_g) of a fully swollen PMMA below the experimental temperature when the sorption experiment is carried out at a temperature above 40°C (Lin *et al.*, 1990, 1991). Micro-cracks in PMMA have been observed to heal above 40°C with methanol treatment. It was also found that during cooling, desorption above T_g of the swollen PMMA may produce voids in the polymer and create an opaque appearance, due to the temperature dependence of the penetrant solubility in the polymer. This indicates that morphological changes can be induced by sorption/desorption. Furthermore, desorption and resorption rate can be considerably faster than the initial sorption rate (Lin *et al.*, 1990, 1991). All these facts

suggest that penetrant absorption and desorption processes in glassy polymer may not be reversible.

The removal of absorbed penetrant from a polymer below its T_g can also increase the porosity of the polymer. Experiments by Koenig's group indicated that cyclic absorption-desorption of methanol at room temperature has a more significant effect on diffusion kinetics in PMMA than that produced from temperature changes. During such cycling, the diffusion kinetics were changed from Case II to Case I, accompanied by an increased diffusion rate and equilibrium concentration (Grinsted *et al.*, 1992). This may be attributed to an increase in porosity.

PMMA can also be plasticized by water. As the initial water content in PMMA increases, the diffusion rate of methanol into PMMA will also increase. The room temperature diffusion coefficient with a water content of 1.25 wt % is increased by an order of magnitude over that of the original specimen. This indicates that water content, even though very low, has a significant effect on the diffusion of methanol in PMMA (Grinsted *et al.*, 1992).

In addition to sorption history, thermal history has also been reported to influence the diffusion kinetics. Front penetration in annealed samples is slower with a longer induction time, compared with the "as-received" samples. On the other hand, the front penetration rate in annealed samples increases significantly with increasing cooling rate through T_g (Windle, 1984). The height and depth of the precursor at the front are also sensitive to the quench scheme, especially at higher cooling rates. Although increased front sharpness has been associated with increased front penetration rate in annealed samples, the front sharpness can decrease when the thermal history is varied (Durning *et al.*, 1995).

1.2.2.4 Effect of experimental temperature and penetrant size

Polymeric materials can exist in different states ranging from rubbery to glassy state, depending on the experimental temperature with respect to the T_g of the polymer. Generally, diffusion in homogenous rubbery polymers is well described by the Fick's Law. Diffusion in glassy polymers, however, may show anomalous, also known as non-Fickian, behavior which cannot be adequately described by simple Fick's law.

Case II sorption only occurs when the unswollen polymer is in the glassy state. The behavior of Case II sorption is strongly influenced by the experimental temperature since the front velocity, diffusion coefficient and viscosity of the polymer all depend on thermally activated processes. The induction time is also influenced by temperature since the induction time and penetration rate are inversely related to each other (Rossi *et al.*, 1995; Friedman and Rossi, 1997; Chapter 2 and 3). In general, the front penetration rate increases, while the induction time decreases, with increasing experimental temperature. The apparent activation energy for Case II sorption is reported to be in the range of 20-50 kcal/g-mol, much greater than that for Case I diffusion (10 kcal/g-mol)(Thomas and Windle, 1978,1980; Lasky *et al.*, 1988b; Lee, 1993; Durning *et al.*, 1995).

Case II behavior typically takes place at temperatures lower than T_g of the unswollen polymer, with a nearly step-wise penetrant concentration distribution in the swelling polymer separated by a penetration front moving at constant velocity. The equilibrium concentration in the swollen region will increase with increasing temperature (Thomas and Windle, 1978). At temperatures above T_g, Case II behavior will be transformed to Fickian behavior. The penetrant concentration at the front and the front

penetration rate will decrease with increasing penetration depth at higher temperatures. It is reported that the front becomes sharper with increasing temperature at first, then loses its sharpness with further increase in temperature (Durning *et al.*, 1995).

The effect of increasing penetrant size is similar to the effect of decreasing temperature. Smaller molecules are more favorable kinetically, therefore, they penetrate at considerably higher rates (Gall *et al.*, 1990; Sarti and Doghieri, 1994). The effective cross section of a penetrant molecule has a more dominant influence on its penetration rate than its molecular weight (Papanu *et al.*, 1990). The flexibility and compactness of the diffusing species have a profound effect on the diffusive behavior (Arnould and Laurence, 1992).

Interdiffusion of miscible polymers may also exhibit Case II characteristics when one polymer is glassy and the other remains rubbery at experimental temperatures (Sauer and Walsh, 1991; 1994). The penetration rate will conformably depend on the thermal history of the glassy polymer. Unlike classical Case II sorption, the penetration rate of a rubbery polymer in a glassy polymer depends strongly on the molecular weight of the glassy polymer, which was attributed to the molecular weight dependence of the rate of swelling and dissolution of the glassy polymer in the swollen front.

1.2.2.5 Effect of external and internal stress

The effect of stress on diffusion has long been recognized (McAfee, 1958; Li, 1978; Larché and Cahn, 1982; Wilson and Aifantis, 1982; Unger and Aifantis, 1983 ; Neogi *et al.* 1986; Sih *et al.*, 1986; Klier and Peppas, 1987; Yaniv and Ishai, 1987; Weitsman, 1990; Gent and Liu, 1991). The stresses will influence diffusion kinetics through their influence on the free volume fraction of the polymer and the chemical potential of the penetrant

(Fahmay and Hurt, 1980; Larché and Cahn, 1982: Neumann and Marom, 1987). The coupling between a concentration field and a stress field is strongly governed by the nature of the boundaries (Larché and Cahn, 1982). The integral sorption process in solid materials is often accompanied by the existence of internal stress due to non-uniform swelling or the application of external stress.

In a glassy polymer undergoing Case II sorption, the low external stress may lead to an appreciable change in both the front penetration rate and the induction time. The application of compressive stress will produce an increase in induction time and a decrease in front penetration rate (More *et al.*, 1992), opposite to what would be expected for tensile stress (Brown, 1989). Higher stresses may produce more dramatic effects (More *et al.*, 1992). The external stresses were chosen to be well below the (unplasticized) yield stress to maintain the homogeneity of the specimen. The penetration front was sharp and parallel to the original edge of the specimen indicating that the change is not caused by local inhomogeneities.

During sorption, the specimen can be permanently deformed when the external stress exceeds the yield stress. It has been reported that pre-deformed samples absorb solvent at a higher rates than the undeformed sample, and Case II kinetics can be maintained only when the penetrant size is large or the temperature is low (Sarti and Doghieri, 1994). Resorption is faster than the original absorption for both deformed and undeformed samples. The results demonstrate that the effect produced by deformation is similar to that by cyclic sorption (Harmon *et al.*, 1987). For a ductile material such as PMMA, the change in penetration rate in the deformed specimen should depend on the

strain state of shear deformation in the polymeric glass. It is not directly related to the sign and magnitude of stress applied during straining process (Windle, 1984).

Integral sorption of high concentration of penetrant in glassy polymer may lead to a heterogeneous structure. The concentration distribution in the swelling polymer is stepwise since the diffusion coefficient in the swollen region is much greater than that in the unswollen region. The heterogeneous transport medium, analogous to composite material, can be divided into three regions: a swollen region, a transitional swelling region and an unswollen region. The geometrical continuity of the three is maintained by internal stresses (known as differential swelling stresses), more compressive in the swollen region, shear in the swelling region and tensile in the unswollen region. This will have indirect implications since the diffusion coefficient and equilibrium concentration of the penetrant are usually stress-dependent (Fahmay and Hurt, 1980; Neumann and Marom, 1987). The stress gradient in a swelling polymer acts as a negative driving force to the penetrant diffusion against the chemical potential gradient (Kim *et al.*, 1996). The internal stress induced by diffusion will always enhance diffusion (Li, 1978; Larché and Cahn, 1982). The anisotropic dimensional changes of the swelling polymer during Case II sorption is an obvious manifestation of the mechanical constraint of the unswollen region (Thomas and Windle, 1977). In Cohn and Marom's (1982, 1983) work on anisotropic dimensional changes in PMMA during Case II sorption, the swelling system was considered as a composite material with a stiff fiber embedded in a soft matrix. As a consequence, the size and the relative dimensions of the core would determine the anisotropic behavior.

1.2.3 Theories: Criterion and Modeling

Although experimental and theoretical efforts have been made to delineate the transport process involved in integral sorption, no practical set of criteria is available to predict the diffusion pattern in a systematic manner. It is understandable that current knowledge of Case II behavior is not sufficient to enable the universal prediction of experimental conditions under which Case II sorption will occur.

For anomalous swelling in a glassy polymer sheet, the swelling medium can be treated as a changing composite laminate or sandwich. The synergistic coupling of diffusion, relaxation and the resulting differential swelling stresses will determine the overall transport kinetics of the polymer when temperature, geometry and size of the polymer sample, type and activity of penetrant are specified.

Various approaches have been applied to describe or predict Case II behavior. Existing continuum models can be classified as phenomenological models, mechanistic models and thermodynamic models. No model has been established to predict the front penetration rate based on the molecular dynamics of polymers. Phenomenological models use formulations derived from intuitive or empirical approaches to describe the sharp penetration front with an initial constant rate. These can provide useful guide to better the understanding of Case II behavior. On the other hand, mechanistic models attempt to predict the key attributes of Case II behavior, namely the induction time and front penetration rate, via the introduction of non-Fickian mechanisms. These can provide insightful understanding of the transport behavior. In contrast, thermodynamic models are derived from the first principle, capable of validating the mechanistic models on a

theoretical basis. These are either based on linear irreversible thermodynamics or extended irreversible thermodynamics, all independent of the microscopic details of the system.

1.2.3.1 Criterion for the occurrence of Case II behavior

Case II sorption only occurs during integral sorption in a glassy polymer. It is considered as a manifestation of the coupling between diffusion and anelasticity or viscoelasticity (Durning *et al.*, 1996). The activity of the immersion fluid has to exceed a critical value to induce Case II behavior (Hopfenberg *et al.*, 1969). The penetrant volume fraction at the surface has to be greater than 0.1 for Case II behavior to begin (Lasky *et al.*, 1988a, Umezawa *et al.*, 1992). Those conditions alone, however, are insufficient to ensure a Case II behavior.

To maintain a constant front penetration rate, the rate controlling process should in principle be occurring at the front. Microscopically, it has been accepted that Case II behavior occurs when the mobility of the penetrant in the swollen region is much greater than the segmental relaxation rates at the front, and the relaxation at the front becomes the rate limiting step. No practical rule is available to guide the selection of a polymer/penetrant pair which will exhibit Case II behavior, as the mechanistic basis of Case II sorption is still not well understood. Therefore, it is not clear if Case II behavior occurs in any specific combination of a glassy polymer and penetrant under appropriate experimental conditions, or only to a limited combinations of polymer and penetrant due to their unique synergy.

Alfrey (1965), Hopfenberg and Frisch (1969) attempted to describe the full spectrum of the diffusion patterns for a given polymer-penetrant system in a phase diagram

with temperature and penetrant activity as independent variables. Their description for polystyrene, however, is incomplete, and is not universally consistent with other systematic experimental observations. The effect of sample size, sample history on diffusion pattern was not predicted in their phase diagrams.

Vrentas, Duda and co-workers correlated the appearance of non-Fickian behavior with a diffusional Deborah number $\theta=\alpha D/L^2$, the ratio of a characteristic relaxation time to a characteristic diffusion time (Vrentas *et al.*, 1975). Here, α is the mean relaxation time; D is a diffusion coefficient and L is a characteristic length. L^2/D represents a characteristic time for sorption determined by molecular mechanism. They showed that the anomalous behavior appears at intermediate Deborah numbers. The size of a swelling sample and the relaxation behavior of polymer will play an important role in determining the Deborah number and the corresponding transport kinetics. Although Deborah number diagrams were constructed to predict the diffusion pattern, they cannot be used to predict the occurrence of Case II behavior, because Deborah number can be well defined only in differential sorption, integral sorption cannot be characterized by a single Deborah number (Vrentas and Duda, 1977; Wu and Peppas, 1993). An integral Deborah number was defined as the ratio of the characteristic relaxation time in the glassy region to the characteristic time in the swollen region to characterize integral sorption with a single parameter (Wu and Peppas, 1993).

Although Deborah number has been widely used to interpret experimental observations, the soundness of these ideas has recently been challenged (Samus and Rossi, 1996). Deborah number diagram predicts that when a PMMA slab is immersed in methanol, Case II behavior will occur at room temperature for samples with a thickness of

1 mm, while Fickian behavior will take place when a sufficiently thick slab of PMMA is used; consequently, the front would either disappear or begin to move with a velocity proportional to the square root of time, simply because a thick slab of PMMA is employed. According to these ideas, systems such as natural rubber or polyethylene which exhibit Fickian behavior for film thicknesses of the order of 1 mm, should display "non-Fickian" or even Case II behavior if sufficiently thin films are used. This obviously is not realistic since Case II behavior only occurs in integral sorption when the polymer is in the glassy state. Therefore, the Deborah number diagram is limited in predictive value.

1.2.3.2 Phenomenological models

The kinetic features of Case I sorption is determined once the diffusion coefficient is known. This is true for Case II sorption when the induction time and front penetration rate are known. In this case, the sorption kinetics may be simpler than Case I sorption since the concentration distribution in a swelling polymer is almost stepwise (Alfrey, 1965).

Peterlin (1965,1969) presented an elegant phenomenological analysis of Case II behavior, assuming the existence of penetration front moving at constant velocity and an almost step-wise penetrant concentration distribution in a swelling polymer: a uniformly high concentration in the swollen region and a low Fickian concentration distribution in the unswollen region. Peterlin's model provided a useful concept that Case I and Case II behavior can occur simultaneously in a swelling system. It was predicted that the length of the Fickian tail, which should be inversely proportional to the front penetration rate, increases linearly with the diffusion constant.

Berens and Hopfenberg's (1978, 1979) phenomenological treatment of this anomalous diffusion problem employed a combination of Case I and Case II processes. With the assumption of a Fickian precursor extending into the glassy core, Super Case II behavior could be simulated by this approach. However, the overlap of the Fickian precursor is not a convincing explanation for Super Case II behavior, because this overlap also occurs in other situations which does not lead to Super Case II behavior.

Astarita and Sarti's (1978) phenomenological model is combined with a mechanistic criterion for occurrence of Case II behavior. It was assumed that two different physical processes, penetrant diffusion and polymer plasticization, take place during the sorption of penetrant into the sample. Diffusion of absorbed molecules occurs only in the plasticized region according to Fick's law (the diffusion coefficient in the glassy region is assumed to be zero). Polymer can only be plasticized if the volume faction of solvent exceeds a certain value, and the kinetics of the transition from the glassy to the rubbery state determines the equation for the velocity of the plasticization font. Constant front movement takes place only if such a limit exists. This approach was also successfully extended to correlate sample size effects on transport pattern (Astarita and Joshi, 1978), and the difference between sorption and desorption (Joshi and Astarita, 1979).

The existence of induction time can be quantitatively predicted in an extended treatment of Astarita and Sarti's model (Rossi *et al.*, 1995; Friedman and Rossi, 1997), which is consistent with a simpler phenomenological analysis of the front penetration kinetics (see Chapter 2). The main difference between the extended model and the original model is that in the penetration kinetics an upper limit is set for the front penetration rate rather than imposing a constitutive equation (Rossi *et al.*, 1995). The extended model

predicts a longer distance covered by the constant front (compared with the original model) before the crossover to Fickian behavior at later stage.

Case II sorption can also be formulated as a moving boundary problem with a surface resistance boundary condition. A universal effect of sample geometry on the trend of the front movement, which is independent of transport mechanism, was predicted and verified experimentally (Lee and Kim, 1992). It was demonstrated that the front penetration in cylindrical and spherical samples will accelerate towards the center, rather than remain constant, for a polymer/penetrant system exhibiting typical Case II behavior. This was shown to be a natural outcome of the radially symmetric geometry and not a Super Case II phenomenon. The transport characteristics is independent of the sample geometry only in the initial stage of the front penetration. The understanding of this geometry effect helps to clarify the confusion in the interpretation of some experimental observations.

In a series of papers by Cohen *et al.* (Cox and Cohen, 1989; Cohen and White, 1989; Cohen and Erneux, 1990; Cox, 1990; Hayes and Cohen, 1992; Edwards and Cohen, 1995a, 1995b; Witelski, 1996; Edwards, 1996), the governing equations for the generation and penetration of the front were derived from a diffusion equation with stress gradient as a second driving force for penetrant flux in addition to the classical Fickian flux due to concentration gradient. The mathematical framework is essentially presented as a moving boundary problem. The stress evolves with a relaxation time according to a concentration-dependent equation, analogous to Maxwell or Kelvin-Voigt viscoelastic models. Prediction of induction time and surface concentration effects were neglected in their treatment. Although a constant front rate was not considered as *a priori*, their approach is

essentially phenomenological. Their *ad hoc* analysis involving glass transition can be extended to Case II sorption without glass transition.

With quasi-steady state approximation, a constant front movement in Case II sorption can be predicted, though short time prediction of front movement does not agree with experimental observation (Cohen and Erneux, 1990). Based on an *ad hoc* assumption of the involvement of glass transition and related dependence of relaxation time, some general features of Case II behavior have been simulated with great simplification of the actual phenomenon (Hayes and Cohen, 1992). With emphasis on the effect of the nonlinear viscoelastic term, a constant movement of the front can be predicted from asymptotic solutions. It was also predicted that there is a self-regulating mass uptake which is determined by the properties of the polymer but independent of the externally imposed boundary conditions (Edwards and Cohen, 1995a, 1995b). Asymptotic and numerical solutions were obtained to correlate the front speed and mass transport with dimensionless groups which were identified to measure the relative effects of different dynamic processes. It was demonstrated that the concentration profile can change its concavity in a certain parameter range (Edwards, 1996). Several trends were predicted to occur with the increase of thickness in the transitional swelling layer. For example, the front penetration rate will gradually increase, and the stress profile will be broadened, and the position of increasing maximal stress will be further extended into the glassy region ahead of the front (Witelski, 1996).

To account for the "non-Fickian" features of the sorption curves by using constitutive relations for the local flux different from Fick's law, Camera-Roda and Sarti (1990) divided the overall flux into a Fickian term and a relaxation term. The Fickian term

implicitly assumes an instantaneous response of the diffusion flux to the concentration gradient, while the relaxation term takes into account of the delayed response of the diffusion flux to the concentration gradient. The delayed response can be attributed to molecular rearrangements or morphological changes under internal stresses associated with diffusant transport. The time scale was represented by a Deborah number. Physical parameters such as modulus and diffusion coefficient were assumed to depend on concentration which is influenced by time-dependent solubility. The effects of relaxation was lumped into the constitutive equation for diffusion flux. The model is formulated to give qualitative representation of various anomalous transport behaviors, with front moving at a concentration dependent velocity. Fickian behavior can be recovered if the delay is too short or too long in regard to diffusion time.

The success of Fick's law relies on the fact that the relaxation time for ordinary materials can be effectively taken as zero. In contrast, the relaxation times of glassy polymers can be comparable to the experimental time scale. Maxwell first included a relaxation time in the heat flux equation in 1867 to avoid infinite propagation speed of heat waves or thermal impulses. The idea was then neglected until the formulation of Maxwell-Cattaneo equation in 1949. For mass flux, it takes the form:

$$J + \tau \frac{\partial J}{\partial t} = D \frac{\partial c}{\partial x} \qquad (1.1)$$

where τ is the relaxation time, c, D, and J are concentration, diffusivity and flux respectively.

Kalospiros *et al.* (1991,1993) attempted to develop a universal diffusion model based on Maxwell-Cattaneo equation with two adjustable parameters, coupled with a description of the intrinsic swelling kinetics. The governing equations can then provide

discontinuous solutions for the chemical potential and local penetrant concentration. The model can only give qualitative prediction for the anomalous patterns, including Case II behavior, due to the assumption of oversimplified constitutive equations with constant parameters. It was shown that Case II sorption will be slower than would be predicted on the basis of Fickian diffusion. The relaxation time was shown to be crucial to the development of front.

The phenomenological approaches reviewed thus far are assumed to be valid throughout the sample and usually include one or more (often vaguely defined) relaxation times, which may or may not be different from mechanical relaxation time. In Case II sorption, it was argued that the only obvious "violation" of Fick's law occurs at the penetration front, where a different phenomenon (plasticization) occurs. When the kinetics of plasticization is taken into account, such as imposing an upper limit on the flux into the glassy material, the validity of Fick's law can still be retained (Samus and Rossi, 1996).

1.2.3.3 Mechanistic phenomenological models

Over the past decades, several mechanistic models were developed to describe the observed Case II sorption in PMMA and PS sheets. Long and Richman (1960) experimentally demonstrated that the surface concentration is time-dependent and reaches the equilibrium values very slowly. Time-dependent surface concentration boundary condition and a constant diffusion coefficient were used to describe the non-Fickian sorption to obtain solutions to the diffusion equation. Their successful approach delineates an important link between sorption and molecular relaxation process, and demonstrates the significant effect of boundary conditions on transport behavior.

Crank proposed a theory based on the influence of differential swelling stresses on diffusion coefficient. With the use of simplified linear elasticity, Crank assumed that this differential swelling stress only affects the diffusion coefficient while the cross section area of the swelling slab remains uniform throughout the sample thickness (Crank, 1953). Crank also proposed the use of a time and concentration dependent diffusion coefficient to deal with the non-Fickian problem. Such an approach may yield a good fit with experimental data but it does not provide additional insight into the underlying physical process.

As an improvement of Crank's theory, Petropoulos and Roussis treated the polymer as a linear viscoelastic material (Petropoulos and Roussis, 1978). The diffusion coefficient was considered to depend on both concentration and stress. This, when combined with Fick's second law, produced some features of Case II diffusion. Under well defined conditions, this model could also predict the existence of Super Case II diffusion and an increased desorption rate. The model was improved later by making the diffusion coefficient and equilibrium concentration both stress and time dependent. However, the existence of a sharp diffusion front and the associated kinetics can not be predicted by this model.

In an earlier work of Gostlic and Sarti (1983), sorption rate was considered to be controlled by both swelling kinetics and penetrant diffusion through the swollen layer. The sum of osmotic swelling stress and differential swelling stress, exerted on the glassy core in the swelling region, was considered to be the driving force for swelling. It was demonstrated that during the sorption process, the osmotic swelling stress in the swelling region would decrease, due to an increase in diffusional resistance. As a result, the

differential swelling stress in the core would increase, which lead to the acceleration of front velocity. Their general ideas are reasonable, however, the assumption that swelling kinetics is determined by the rate of mechanical crazing appears to be *ad hoc*. In addition, solubility and diffusion coefficient were assumed to be constant, and linear viscoelasicity was employed in the model.

The most well known model is that of Thomas and Windle (T-W) (1978, 1981, 1982). According to this model, the penetrant chemical potential is a function of both concentration and osmotic pressure. The osmotic pressure is related to the local concentration by a viscous response model. The swelling kinetics is obtained for a thin film without diffusional resistance with the assumption that the local normal strain is proportional to the local penetrant concentration. The swelling kinetics is then combined with Fick's law to predict the typical features of Case II sorption. The T-W model uses a simple viscous response model as the stress-strain constitutive equation; consequently it cannot encompass the polymer relaxation time.

Anisotropic swelling during Case II diffusion in slab samples was reported by several groups (Thomas and Windle, 1978; Cohn and Marom, 1982). This effect has been related to the stress state in the swelling sheet. In T-W models, the dimensional changes and diffusion kinetics were treated separately without the inherent connection governed by differential swelling stress. As a result, differential swelling stress will affect the dimensional changes, but not the diffusion kinetics in the T-W model. Such neglect of the contribution of the differential swelling stress to diffusion kinetics is not justified based on physical considerations. Similarly, T-W model does not distinguish between the penetrant-induced osmotic pressure and the stresses in the polymer, even though the former is a scalar

and the latter is a tensor. Furthermore, the local strain is not used in the calculation of the swelling or deformation of the polymer, despite the fact that the increasing diffusional resistance due to swelling in the rubbery region can cause a significant error if the swelling is extensive. Also, the theoretical assumption that the swollen region is in a rubbery state may not be valid based on recent experimental evidence (Lin *et al.*, 1990, 1991).

It was noted in Thomas and Windle's experiments that changes in diffusional resistance in thick specimen (>3 mm) or at elevated temperature (>40°C) can significantly influence the whole diffusion process. Their kinetic model is based on the coupling of Fickian diffusion (represented by a concentration dependent diffusion coefficient) with the viscous response of the polymer chain (represented by concentration dependent viscosity) to the osmotic swelling stress of the penetrant in the swelling region. The rate-controlling step in the swelling region is the Newtonian viscous flow of the polymer under osmotic swelling stress (creep or tensile flow). Although the theory includes Case II sorption as a limiting case, paradoxically it also seems to predict the existence of Super Case II transport. Although the theory could reproduce some of the Case II features, it does not predict the sample size effect on penetration kinetics. Its agreement with some experimental results might be considered fortuitous as acknowledged by Thomas and Windle. The merit of the model is in the theoretical treatment of relaxation contribution and induction time. However, the effect of relaxation may not be the only factor responsible for the Case II behavior as commonly believed. It appears that the constant front velocity may not be governed by a single mechanism. It is more likely the synergistic result of several different factors, such as diffusion, relaxation and differential swelling stress.

The T-W model was further refined and tested by Hui *et al.* (1987a, 1987b) and Lasky *et al.* (1988a, 1988b). The agreement between theory and experiment on surface layer swelling is poor. This was attributed to the oversimplification of T-W model. The Newtonian fluid assumption was believed to lead to an underestimation of front velocity. Their model can predict most essential features of Case II sorption, but it cannot properly predict the linear viscoelastic limit (Durning *et al.*, 1985). Astarita and Sarti's model and T-W model were considered complementary (Billovits and Durning, 1988): Astarita and Sarti's model gives analytical asymptotic solutions and simple phenomenological understanding of the behavior, while T-W model provides a more detailed mechanistic interpretation of Case II behavior, and a prediction of front penetration rate which Astarita and Sarti's model fails to provide.

1.2.3.4 Thermodynamic models

Fick's law can be derived from the thermodynamics of irreversible process. Similarly, the phenomenological and mechanistic models for Case II sorption can also be derived from irreversible thermodynamics (Jou *et al.*, 1996).

Frisch, Wang and Kwei (1969) took the partial stress of the penetrant as the second driving force, in addition to the gradient of chemical potential. Based on the thermodynamics of irreversible process, the basic transport equation for the flux of the penetrant takes the form

$$J = -Bc\left(\frac{\partial \mu}{\partial x} - \frac{1}{c}\frac{\partial S}{\partial x}\right) \tag{1.2}$$

where B is the mobility coefficient, μ the chemical potential and S the partial stress tensor in one dimension, proportional to the total uptake of penetrant. The generalized diffusion equation is expressed as

$$\frac{\partial c}{\partial t} = \frac{\partial}{\partial x}\left[D(c,x,t)\frac{\partial c}{\partial x} - B(c,x,t)sc \right] \qquad (1.3)$$

where s is a constant and the convection velocity $v=Bs$. Case II behavior can be predicted when the effect of stress gradient dominates the chemical potential. The phenomenological model of Peterlin (1965,1969) can be derived by this approach.

Glassy polymers are in a nonequilibrium state, with a very slow rate of change towards equilibrium. It takes a finite time for the polymer to reach equilibrium because of the entanglement of polymer chains. In a consideration of sorption-equilibrium boundary conditions, Frisch (1964) derived the relationship for the time-dependent surface concentration observed by Long and Richman (1960). He also justified the use of history-dependent diffusivity of glassy polymers based on thermodynamic analysis of isothermal diffusion.

The time dependence of diffusivity and solubility was also derived from classical formalism of linear irreversible thermodynamics by Neogi (1983), based on the formulation of Larché and Cahn (1982). The chemical potential was used to obtain a phenomenological expression for diffusive flux. However, the relaxation mechanism cannot explain the sigmoidal sorption (Neogi, 1983), and Case II behavior cannot be explained with the swelling effect (Kim and Neogi, 1984). It was recognized that anomalous diffusion may be induced by either swelling or relaxation, or generally, a combination of both (Neogi *et al.* 1986). The chemical potential of the penetrant in the polymer depends on both the

penetrant concentration and stress in the polymer. Swelling induces time-dependent internal stress that affects the chemical potential of the solid, similar to the effect of pressure. Consequently the surface concentration will be time-dependent since the chemical potential of the penetrant in the polymer remains the same as that in the fluid reservoir, which is constant.

Brochard and de Gennes (1983) suggested that the swelling of the polymer due to the influx of penetrant molecules will result in an elastic-like orientational stress opposing the osmotic stress (the mixing term) and consequently resisting further influx of the fluid. The stress accompanying the swelling of polymer can be dealt within the reptation model (Herman and Edwards, 1990). The swelling of polymer will induce a non-random distribution of orientations for the segments in the primitive chain, which contribute to the free energy and chemical potential of the polymer and the penetrant. When this contribution is large enough compared with the ordinary mixing terms, phase separation may take place. The sharpness of the phase boundary between the polymer and the concentrated solution is likely to be dictated by the nature of the polymer. Case II behavior would take place when the contour relaxation time of the polymer chain is long in the unswollen glassy region, while it is very short in the swollen region compared with swelling time.

Under certain conditions, a relaxing or rate-dependent driving force for mutual diffusion may come from the stored free energy in a deformed polymer structure due to the interdiffusion of polymer and fluid. Durning and Tabor (1986) developed a nonequilibrium thermodynamic theory for the limiting case of linear viscoelastic diffusion, *i.e.* differential sorption, with a simple functional form for the nonequilibrium free energy consistent with

well accepted molecular-level models for concentrated polymer solutions based on reptation theory. When the initial disturbance from equilibrium is infinitesimal, as in the case of differential sorption, the transient network and reptation models can provide expression for the chemical potential of the solute, which is then employed to generate a simple expression for the diffusive flux containing a memory integral associated with the deformation of the polymer structure, and the resultant integrodifferential equation is linear, with the diffusion coefficient and the polymer relaxation time reasonably assumed to be constant. The diffusive flux is proportional to the gradient of the chemical potential for small driving forces and small strain histories. This is a linear initial-value problem, or a formulation of interdiffusion in the linear limit. The relation between osmotic pressure and the stresses on the polymer was analyzed by a force balance. A diffusional Deborah number was obtained by arranging the model equations in dimensionless form. Model simulations showed the typical two-stage sorption behavior.

Fu and Durning (1993) rederived the Thomas-Windle's model for Case II sorption from the results of this linear irreversible thermodynamic treatment of Durning and Tabor (1986) by introducing a concentration dependence of physical properties in the fluid flux expression. The polymer relaxation time could be defined since the viscous model in the Thomas-Windle model was replaced with the Maxwell viscoelastic model. They demonstrated that Thomas-Windle model is a small Deborah number limit of the more general theory of Durning and Tabor (1986), contrary to the conventional expectation that anomalous behavior occurs when Deborah number is close to one. Strong nonlinearities in both diffusivity and viscosity are considered essential for the prediction of Case II sorption from Thomas-Windle model. Thomas-Windle's model was also analyzed by a singular

perturbation technique. The analysis shows that relaxation has a significant effect on the unswollen region ahead of the moving front (Durning *et al.*, 1996). Both Thomas-Windle's model and Durning and Tabor's model can be derived from extended irreversible thermodynamics as limiting cases (Jou *et al.*, 1991). Here, extended irreversible thermodynamics is more appropriate than linear irreversible thermodynamics for the description of integral sorption.

The derivation of the continuum thermodynamic theory of diffusion in a viscoelastic polymer extended the original theory of mixtures developed by Truesdell (1984) to situations where one of the components of the mixture is a viscoelastic solid with relaxation time depending on the local temperature and concentration history (Lustig *et al.* 1992). In this comprehensive theory, the fluxes can be driven by chemical-potential gradient, elastic and viscoelastic stresses, and thermal diffusion. The anomalous transport behavior, including Case II behavior, is caused by the negative driving force to the penetrant diffusion due to the polymer stress gradient against the chemical potential gradient (Kim *et al.*, 1996). For one dimensional sorption, the theories of Durning and Tabor (1986) and Lustig *et al.* (1992) can be considered equivalent (Cairncross and Durning, 1996).

Carbonell and Sarti (1990) postulated that the chemical potential of the penetrant depends on the instantaneous value of the stress, which can be correlated to the deformation history and concentration fields based on the constitutive equation for the Helmholtz free energy of the mixture. The constitutive equation for stress is represented by a standard linear viscoelastic model where the polymer is assumed to have one single relaxation time. A new expression for the diffusive flux is then obtained by this approach

to account for the effect of stress on diffusion in a viscoelastic solid. The expression used for the chemical potential and the constitutive equation of stress are thermodynamically consistent, because they are all based on the Helmholtz free energy. Similar to other viscoelastic models, it may lead to unrealistic prediction of desorption fluxes out of a dried polymer matrix (Doghieri *et al.*, 1993).

The constraints imposed by the second law of thermodynamics on viscoelastic-rate-type constitutive equations for the diffusive flux has been analyzed (Doghieri *et al.*, 1993). It was found that the steady-state diffusivity and relaxation time cannot be chosen independently of each other because the precise relationship between them and the equilibrium entropy. When this constraint is imposed on situations close to low concentration limit, the relaxation time approaches zero, and Fickian behavior is predicted.

1.2.4 Current Status

The failure of classical Fick's law in describing anomalous diffusion reveals that Fick's law and consequently Fourier's law are not universally observed. They can only be used as a first approximation for simple diffusion process. Like Newton's law, the adoption of the first derivative is not supported by any universal principle or method. They are macroscopically descriptive or purely phenomenological because they do not have a microscopic basis.

Despite intensive research effort in this area, it is generally agreed that a complete physical picture of diffusion in glassy polymer is not yet available. It should be emphasized here again that glass transition is not essential for the occurrence of Case II behavior. The exact nature of relaxation involved in Case II sorption is still not clear, though it has been

unduly associated with glass transition. Since the front penetration rate remains constant as the distributions of internal stresses change, the effect of internal stresses might not be dominant in Case II sorption. Systematic and creative experimental investigations are needed to quantitatively test some of the existing models and theories, to examine the synergy among relaxation, swelling (internal stress or gradient of internal stress) and diffusion, to elucidate the micro-mechanism or macro-mechanism of Case II behavior, and ultimately to establish a criterion for the occurrence of Case II behavior.

Existing theories are generally *ad hoc* and the predicted trends are only in qualitative agreement with some experiments. The seemingly controversial or intriguing experimental results have not been explained by a consistent theory. So far, no model can predict both qualitatively and quantitatively the observed Case II behavior. There is still a need to develop a realistic physical picture for Case II sorption in glassy polymer. Both the boundary conditions and governing equations need to be re-formulated according to the physical scenario of Case II behavior, consistent with the spectra of anomalous transport behaviors as a whole. The theory for Case II sorption preferably should be a special case of a unified theory for anomalous transport.

The practical exploitation of Case II behavior for the design of zero-order drug release device is questionable, since the transport process in drug release from glassy hydrogels is more likely to be multi-components diffusion, involving a mechanism different from typical Case II sorption; and the drug release rate from such devices may be too slow to be practical at body temperature for drugs of high molecular weight, such as polypeptides. Moreover, zero-order release is not necessarily the optimal profile to be pursued *in vivo* as has been demanded by chronopharmacokinetics.

1.3 Hypothesis

The induction time and front penetration rate are correlated to each other. The induction time is not a material constant. It will depend on sample size and geometry when the sample dimension is considered small.

1.4 Objectives

1). To propose criteria for the occurrence of Case II sorption;

2). To establish correlation between key parameters of Case II sorption;

3). To provide mechanistic interpretation of micro-events.

1.5 Selection of Model System

Due to complexities involved in the physical process of anomalous diffusion, a well developed and characterized polymer is more desirable for experimental work to further characterize Case II transport. Although Case II diffusion can occur in a variety of glassy polymer-swelling solvent systems (PS in acetone and in n-alkanes, crosslinked epoxies in benzene and PMMA in alcohols), PMMA is used as model system in this work as more data on PMMA is available.

PMMA is widely used as structural, optical and biomedical materials (Mark, 1985). The wide application of PMMA is due to its excellent transparency, good biocompatibilty and balanced mechanical properties. It has been used as bone cement to deliver antibiotics to prevent deep wound infection. It can potentially be used to deliver various agents including proteins (Downes, 1991). The relationship between cement preparation, morphology and drug release characteristics has been extensively studied. The research

work is generally empirical. The study of diffusion in PMMA may help to improve our understanding of the drug release process. Although the effects of water and sample history (including physical aging) deserve special attention in controlled release of drugs, they will not be included in the present treatment as it is outside the scope of the present investigation.

Spherical beads have the simplest geometry. No anisotropic dimensional change will occur in beads during swelling. The simple sample geometry helps to simplify the mathematical problem. PMMA beads used in our experiment were prepared by suspension polymerization. Because diffusion in polymers is closely related to the physical structure of the material, diffusion studies will also help to evaluate the material for quality control and to optimize the conditions of suspension polymerization.

Chatper 2

Phenomenological Penetration Kinetics of Case II Sorption

2.1 Introduction

Diffusion of small organic molecules in glassy polymers is commonly encountered in many different fields ranging from controlled release, separation and micro lithography. The resulting penetration kinetics cannot be adequately described by the classical Fick's law and, therefore, has been the subject of numerous research publications over the past three decades. One limiting case which has attracted significant attention is the so-called Case II sorption behavior.

Case II sorption is phenomenologically characterized by an induction time and a linear penetration kinetics of the solvent penetrating front (or a linear weight gain as a result of uniform concentration distribution in the swollen region of a slab). For modeling purpose, Case II sorption, like other anomalous diffusion phenomena, may be considered as a moving boundary problem (Lee and Kim, 1992). The evolution of the position of the front and the concentration field, in theory, could be predicted by solving the transport equation with appropriate surface flux boundary conditions. The expression of "Case II sorption" or "Case II transport" is preferred over "Case II diffusion" because the penetrant transport in glassy polymers is not a pure diffusion process.

Various theories have been developed to describe Case II sorption. In the well known Thomas-Windle theory (Thomas and Windle, 1978, 1981,1982; Windle. 1985), the induction

time and front penetration rate were treated as material properties of the polymer. As a result, the behavior of Case II sorption was regarded as a material property independent of sample size and geometry for quite some time. As an improvement to and a further elucidation of Thomas and Windle work, Lasky *et al.* treated Case II sorption as a moving boundary problem (Hui *et al*, 1987a, 1987b; Lasky *et al.*, 1988a, 1988b). Their prediction of the velocity of front movement is not satisfactory in general, especially for penetrant of high activity. The paradoxical agreement of Thomas and Windle's simplified theory with the complex physical phenomena involved in Case II sorption reveals our limited understanding of the underlying mechanisms.

As for the existing interpretations of Case II sorption, the following aspects still remain to be addressed:

1) It is widely believed that a physical transition from the glassy to rubbery state during the swelling and diffusion processes is the central feature for the occurrence of Case II sorption. This concept, however, has neither been well established experimentally, nor well defined conceptually. For example, an obvious glassy to rubbery transition is involved during the swelling of a glassy hydrogel, such as PHEMA in water, no true Case II sorption behavior has been reported for PHEMA hydrogels. On the other hand, no glass transition is involved in a methanol-swollen PMMA polymer exhibiting Case II behavior over a wide range of temperatures (Janacek and Kolarik, 1976; Williams *et al.*, 1986; Lin *et al.* 1990, 1991), since the swollen polymer is not in the rubbery state. Therefore, the widely held concept of glass transition in determining Case II behavior is questionable.

2) What happens at the swelling front is critical in determining the overall transport characteristics. However, the appearance of a moving front is not limited to Case II sorption alone. For example, penetrating fronts are also observed during Fickian or other anomalous sorption processes. Although the osmotic pressure gradient present at the front has been cited to explain the characteristics of Case II sorption, it does not offer further understanding as to why Case II sorption will not occur in other similar systems.

3) Internal stresses and their non-uniform distribution will inevitably be generated in a swelling polymer due to non-uniform swelling resulting from the presence of an unswollen core. These stresses occur in both Fickian and anomalous diffusion. It is therefore obvious that the mere existence of stresses alone does not produce a Case II sorption behavior.

In contrast to the mechanistic models, such as that of Thomas and Windle, pure phenomenological model may provide a useful framework to further the understanding of Case II behavior. As will be shown later, an important conclusion of our phenomenological analysis is that the induction time depends on the dimension of the polymer sample, rather than being a material constant.

Our recent experimental results on spherical PMMA beads demonstrate a significant dependence of induction time and penetration rate on sample dimension, which contradicts the predictions of Thomas-Windle's theory and is not apparently predicted by other existing theories on Case II sorption. In this study, a simple reciprocal relationship between the induction time and penetration rate for Case II sorption is deduced, and experimentally confirmed. The evaluation of the volume swelling ratio confirms an important aspect of Case II sorption regarding the uniform penetrant concentration profile in the swollen shell. It has

also been found that this volume swelling ratio only marginally increases with increasing swelling temperature. The dependence of both the induction time and front penetration rate on the cooling rate of the PMMA beads after annealing has been investigated experimentally, the result of which can be interpreted by changes in the free volume fraction. The effect of penetrant size has also been investigated using alcohols of different chain lengths as penetrants. The results show similar trend as those observed with methanol as the penetrant.

2.2 Phenomenological Penetration Kinetics

It can be shown that the normalized penetration rate depends on sample size as a consequence of its definition

$$P' = \frac{dP}{dt} = \frac{d\left(\frac{a_o(0) - a_i(t)}{a_o(0)}\right)}{dt} = \frac{d[a_o(0) - a_i(t)]}{a_o(0)dt} = -\frac{da_i(t)}{a_o(0)dt} \qquad (2.1)$$

where P, P' and t are respectively the normalized front penetration, normalized front penetration rate and immersion time. $a_o(0)$ is the initial radius of the sphere or cylinder, or the half-thickness of the film, and $a_i(t) = \frac{d_i(t)}{2}$ is the corresponding radius or half-thickness for the inner unswollen core and $d_i(t)$ is the diameter or thickness, as shown in Figure 2.1. If the true penetration rate is defined as

$$v_0 = -\frac{da_i(t)}{dt} = -\frac{1}{2}\frac{d[d_i(t)]}{dt} \qquad (2.2)$$

then

$$P' = -\left(\frac{da_i(t)}{a_o(0)dt}\right) = \frac{v_0}{a_o(0)} \qquad (2.3)$$

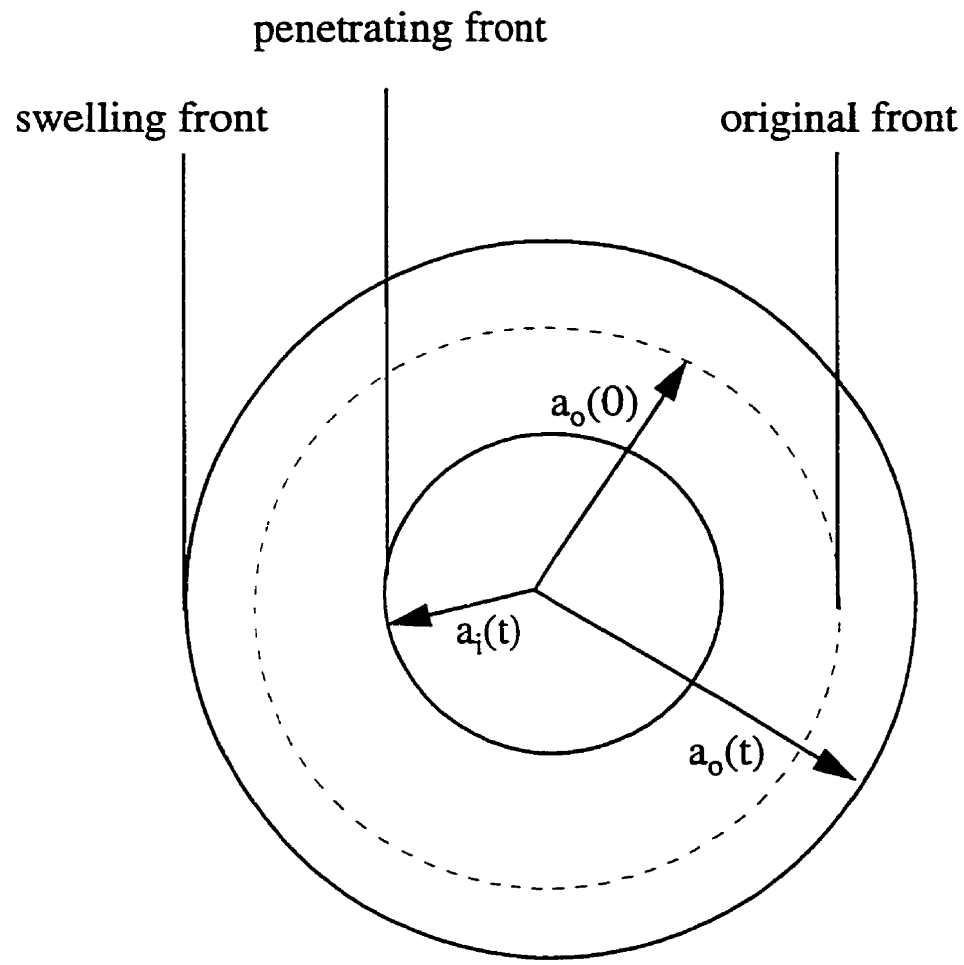

Figure 2.1 Schematic diagram of a swelling PMMA bead

where v_0 can be adequately regarded as a material constant. It is obvious from Equation (2.3) that normalized penetration rate will be affected by the original dimension of the polymer sample. Experimentally, Case II sorption is characterized by a linear penetration kinetics, which can be represented by

$$P = -A + P't \qquad (2.4)$$

Where A is the extrapolated normalized penetration. Induction time is the extrapolated time of onset of front penetration ceases to be zero. From the definition of induction time, a reciprocal relationship between the induction time τ_0 and the normalized penetration rate P' can be obtained from Equation (2.4) by setting $P = 0$ at t = τ_0:

$$\tau_0 = \frac{A}{P'} = \frac{a_o(0)A}{v_0} \qquad (2.5)$$

This relationship is similar to the phenomenological prediction reported by Li and Lee for various other geometries (see Chapter 3).

It can easily be seen from Equations (2.3) and (2.5) that both the induction time and normalized penetration rate depend on the size of the sample. This relationship may imply that similar mechanisms are involved in the formation of the initial swollen surface layer and the propagation of the swelling region, as is also evident from the similar activation energies reported for the induction time and normalized penetration rate of the methanol front in PMMA (Thomas and Windle, 1978; Lee, 1993)

2.3 Experimental

2.3.1 Synthesis of Polymer Beads

The synthesis of PMMA beads and their purification in methanol have been described in details elsewhere (Lee, 1993). Briefly, free radical suspension polymerization of freshly distilled methyl methacrylate were employed to prepare PMMA beads at 70°C for 3 hr. using t-butyl peroxy-2-ethylhexanoate as the initiator and freshly precipitated $Mg(OH)_2$ as the suspending agent. After polymerization was completed, concentrated HCl was added to

remove the suspending agent. The beads obtained by filtration were then extracted in a Soxhlet with methanol before being dried to a constant weight in a vacuum oven, typically at 70-80°C for 3-5 days. Based on intrinsic viscosity measurement in acetone obtained on a Ubbelohde viscometer, the average molecular weight of the PMMA beads was estimated to be about 5.2×10^5 according to the Mark Houwink equation. The heat treatment of PMMA beads was performed using a Perkin-Elmer DSC-2. The beads were heated to 130°C at 320°C/min and kept at 130°C for three hours under nitrogen gas purge, then cooled down to room temperature at different programmed rates. Samples without heat treatment are those oven dried at 70-80°C for 3-5 days right after the purification process.

2.3.2 Swelling Test

The penetration of methanol and ethanol into PMMA beads was measured in a sealed quartz cuvette at room temperature (25°C) and observed with a Wild M420 polarized light stereomicroscope equipped with a digital optical measuring accessory (Wild MMS235; accurate to ±0.001mm). The penetration of n-propanol, iso-propanol, and n-butanol was conducted in cuvettes immersed in water bath with temperature maintained at 50 ±0.2°C. All solvents used were reagent grade. Methanol was obtained from by Caledon Laboratories LTD, anhydrous ethanol from Commercial Alcohol Inc., iso-propanol from Caledon Laboratories LTD, 1-propyl alcohol from ACP chemicals Inc., and butanol-1 from BDH Inc..

2.4 Results and Discussion

2.4.1 Penetration Kinetics

Typical methanol penetration curves for an annealed PMMA bead sample are illustrated in Figures 2.2-2.5. The annealed samples were cooled down to room temperature at a rate of 5°C/min. Figure 2.2 shows the change of the outer diameter, $d_o(t)$, as a function of immersion time as swelling proceeds. It can be seen that the change of diameter starts immediately before the development of a visible penetration front. This swelling can only be attributed to Fickian diffusion within the surface region. Therefore, $d_o(t)$ continues to increase smoothly during the propagation of the front. However, the rate of increase of $d_o(t)$ gradually diminishes due to the decreasing diffusional driving force as well as the area at the front. For Case II sorption of methanol in PMMA, $d_o(t)$ ceases to increase once the fronts have met at the center ($d_i(t)$=0), suggesting a negligible concentration gradient behind the swelling front (Lee, 1993).

As can be seen from Figure 2.3, the diameter of the unswollen core decreases at a constant rate for the major portion of the penetration process. The front propagation accelerates shortly before the complete disappearance of the unswollen core. This acceleration of front propagation has been shown to be a natural consequence of the spherical geometry (Lee and Kim, 1992). When the linear portion of the penetration curve is extrapolated to zero time, an extrapolated bead diameter consistently 1.2 times that of the initial diameter $d_o(0)$ for beads of various sizes is obtained, in agreement with the fact that front propagation does not start immediately after immersion of the sample. This ratio of the extrapolated diameter to the

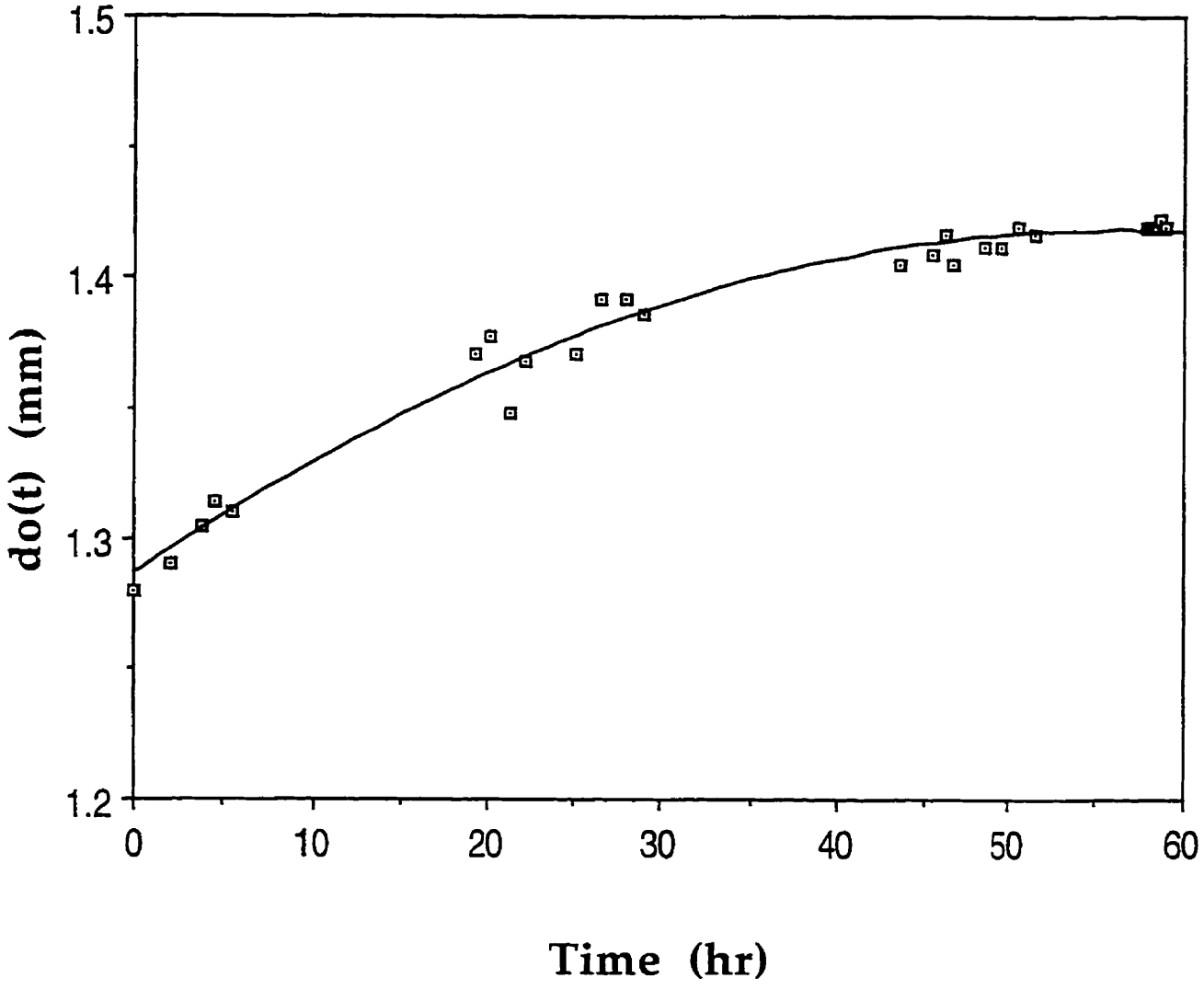

Figure 2.2 Outer diameter of a swelling PMMA bead in methanol as a function of time at 25°C. The uncrosslinked PMMA bead was annealed at 130°C and cooled to room temperature at 5°C/min ($d_o(0)$=1.280mm)

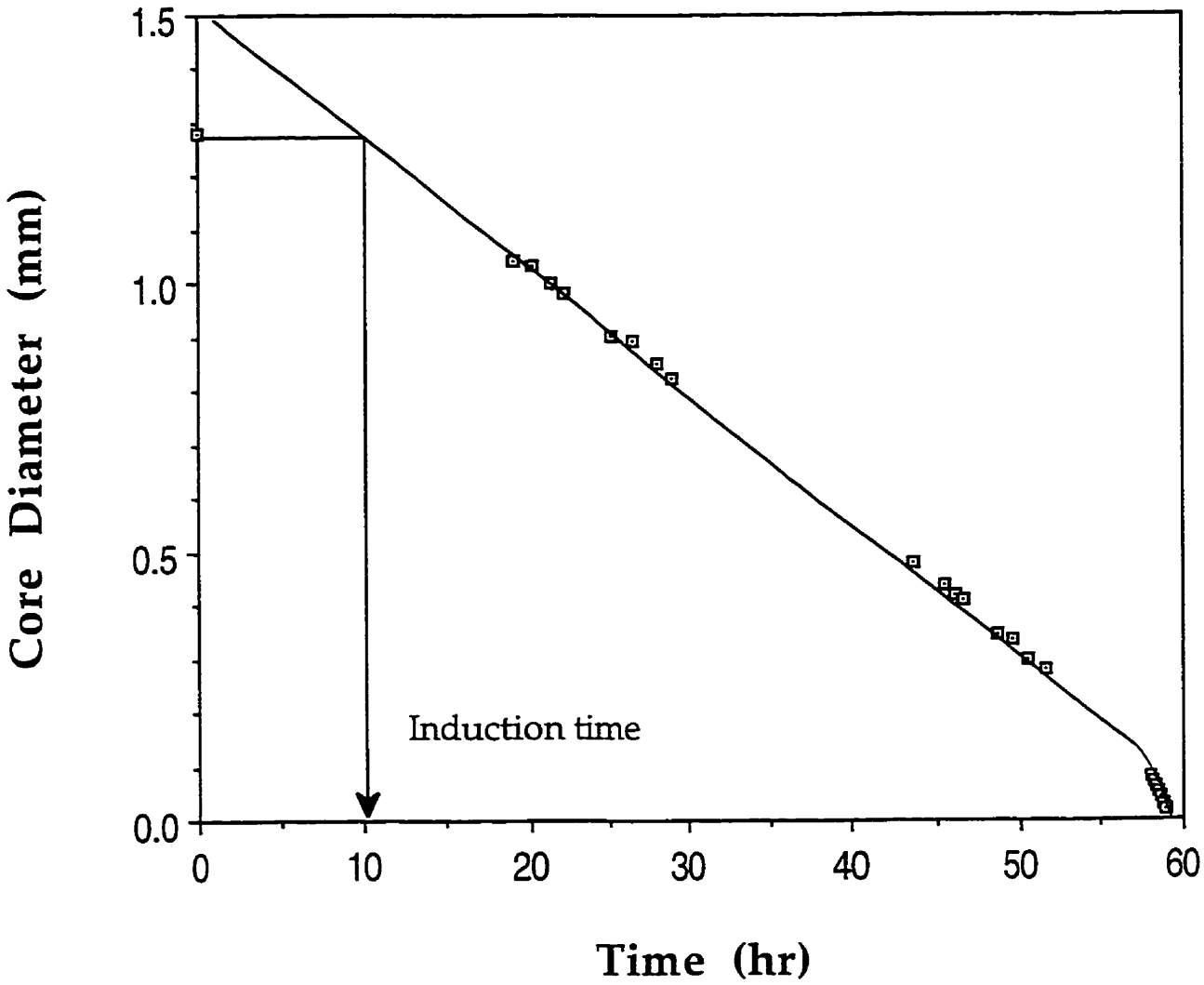

Figure 2.3 Diameter of the inner unswollen core of a PMMA bead in methanol as a function of time at 25°C. The uncrosslinked PMMA bead was annealed at 130°C and cooled to room temperature at 5°C/min ($d_o(0)$=1.280mm)

original diameter also equals the ratio of the diameter of a completely swollen bead to its original diameter.

As shown in Figure 2.4. the volume swelling ratio, defined as $\frac{a_o^3(t)-a_i^3(t)}{a_o^3(0)-a_i^3(t)}$, does not change with time once the front starts to propagate. This agrees with the fact that the penetrant concentration in the swollen region is nearly constant, and the gradual decrease of compressive stress in the swollen region is not significant enough to cause an increasing trend in the volume swelling ratio. It is reasonable that the volume swelling ratio reported in Figure 2.4 is not a step function of time, since the evolution of the Fickian tail in the surface layer during the induction period also contributes to the gradual establishment of a constant volume swelling ratio during the front propagation period. Through proper data analysis it may be possible to estimate the effective Fickian tail layer thickness.

There are two different definitions for the normalized penetration thickness, referenced either to the initial surface position of the unpenetrated beads by $\frac{a_o(0)-a_i(t)}{a_o(0)}$ or the changing outer surface of the swelling sphere by $\frac{a_o(t)-a_i(t)}{a_o(t)}$. The former should be preferable because a simple relationship may exist between normalized penetration P and normalized penetration rate, $P' = \frac{dP}{dt} = -\frac{1}{d_o(0)}\frac{d[d_i(t)]}{dt} = -\frac{1}{a_o(0)}\frac{da_i(t)}{dt}$, and only one time dependent variable is included in P'.

Two normalized penetration curves are shown in Figure 2.5. In the initial part of the curve, the normalized penetration is a linear function of time. The slope of this linear portion gives the normalized penetration rate, P'. The extrapolation of this linear

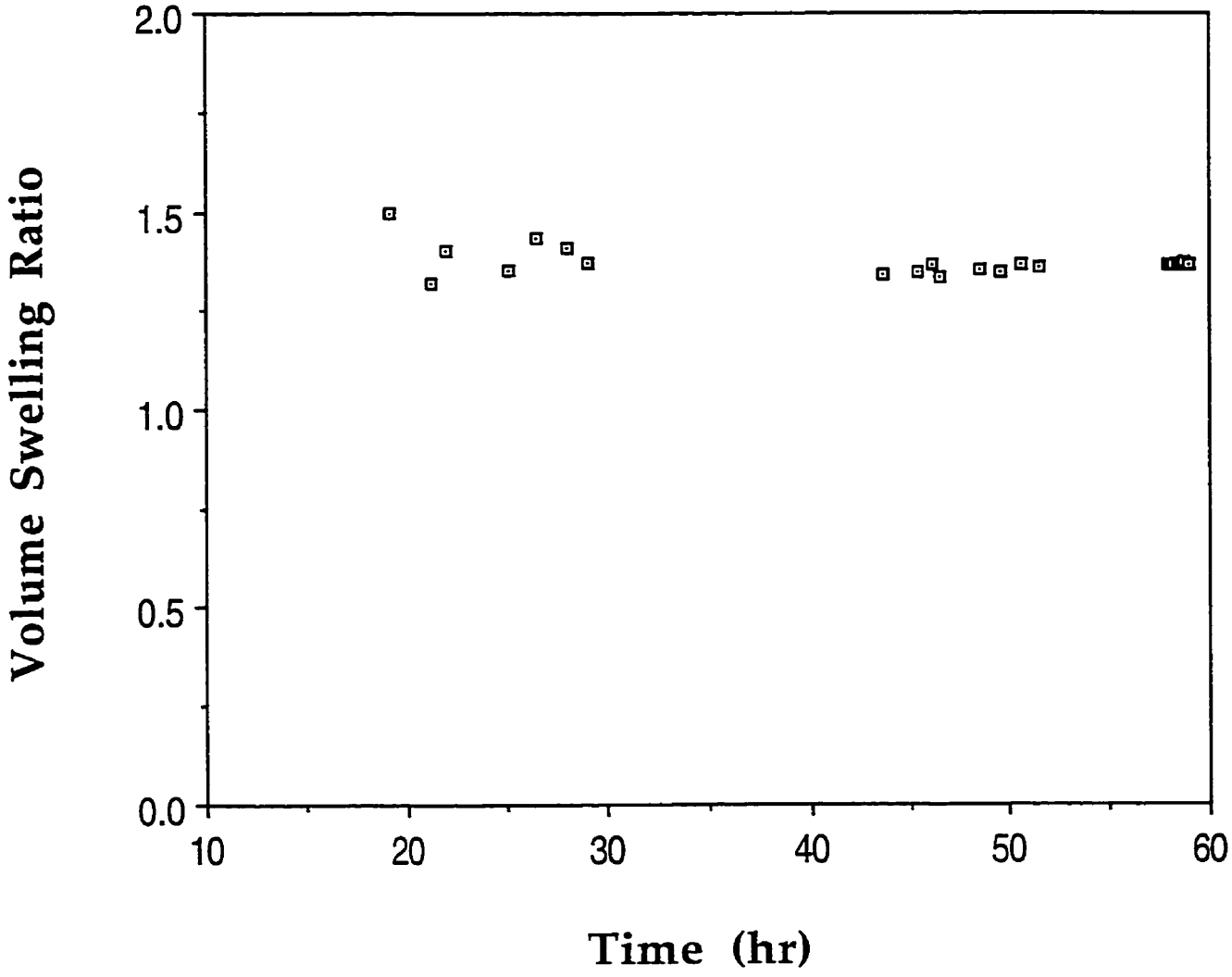

Figure 2.4 Volume swelling ratio during the penetration period. The uncrosslinked PMMA bead was annealed at 130°C and cooled to room temperature at 5°C/min and immersed in methanol at 25°C ($d_o(0)$=1.280mm)

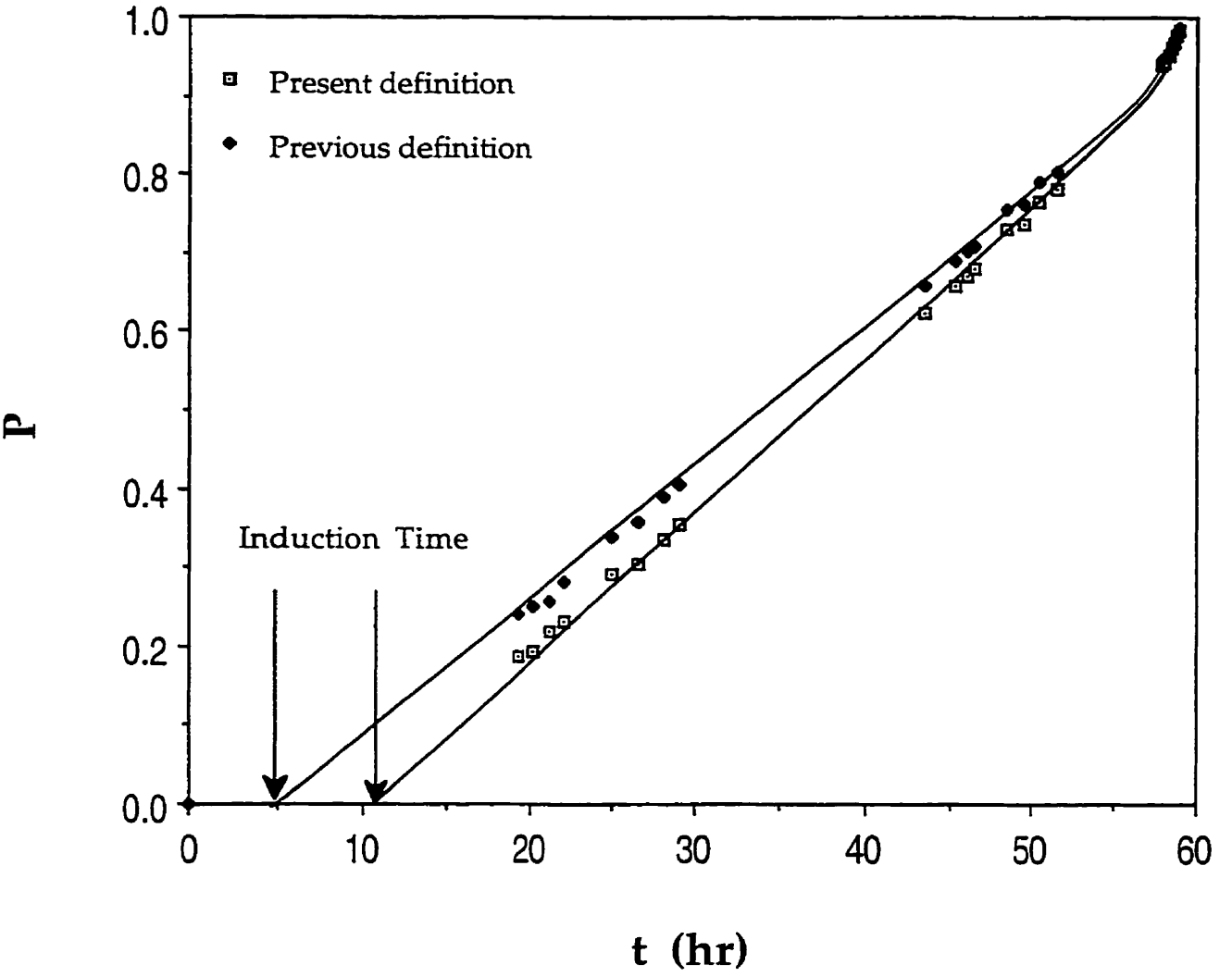

Figure 2.5 Complete time course of normalized penetration with different definitions. The uncrosslinked PMMA bead ($d_o(0)$=1.280mm) was annealed at 130°C and cooled to room temperature at 5°C/min and immersed in methanol at 25°C

relationship to the two axes (zero penetration and zero time) provides two important parameters, the induction time τ_0 and the extrapolated normalized penetration, A. The induction time based on the present definition using the initial surface position as the reference agrees well with the actual experimental time of onset at which the migration of penetration front from the sample swelling surface was first observed.

2.4.2 Effects of Sample Size

In Figures 2.6 and 2.7, the estimated induction time τ_0 and the reciprocal of normalized penetration rate $1/P'$ were plotted against the original bead diameter, based on results collected on 80 beads annealed at 130°C cooled at 5°C/min to room temperature. Each point represents the average result obtained from 3 to 20 beads. As expected from Equations (2.3) and (2.5), both τ_0 and $1/P'$ are linearly proportional to the original diameter of the beads. This is at least a good first approximation. The dependence of $1/P'$ on $D_o(0)$ is a natural consequence of the definition of P'. However, the dependence of induction time on sample size is not predicted by existing theories on Case II sorption.

According to Rossi *et al.* (1995) and Astarita and Sarti (1978), the diffusive flux into the glassy region is limited or equal to the product of front penetration rate and critical penetrant concentration, $v_0 c_p$, as dictated by plasticization kinetics during the induction period. The greater the dimension of the specimen, the longer it is required for the surface to reach the threshold or critical concentration, when the dimension of the beads is in intermediate range (see Chapter 3).

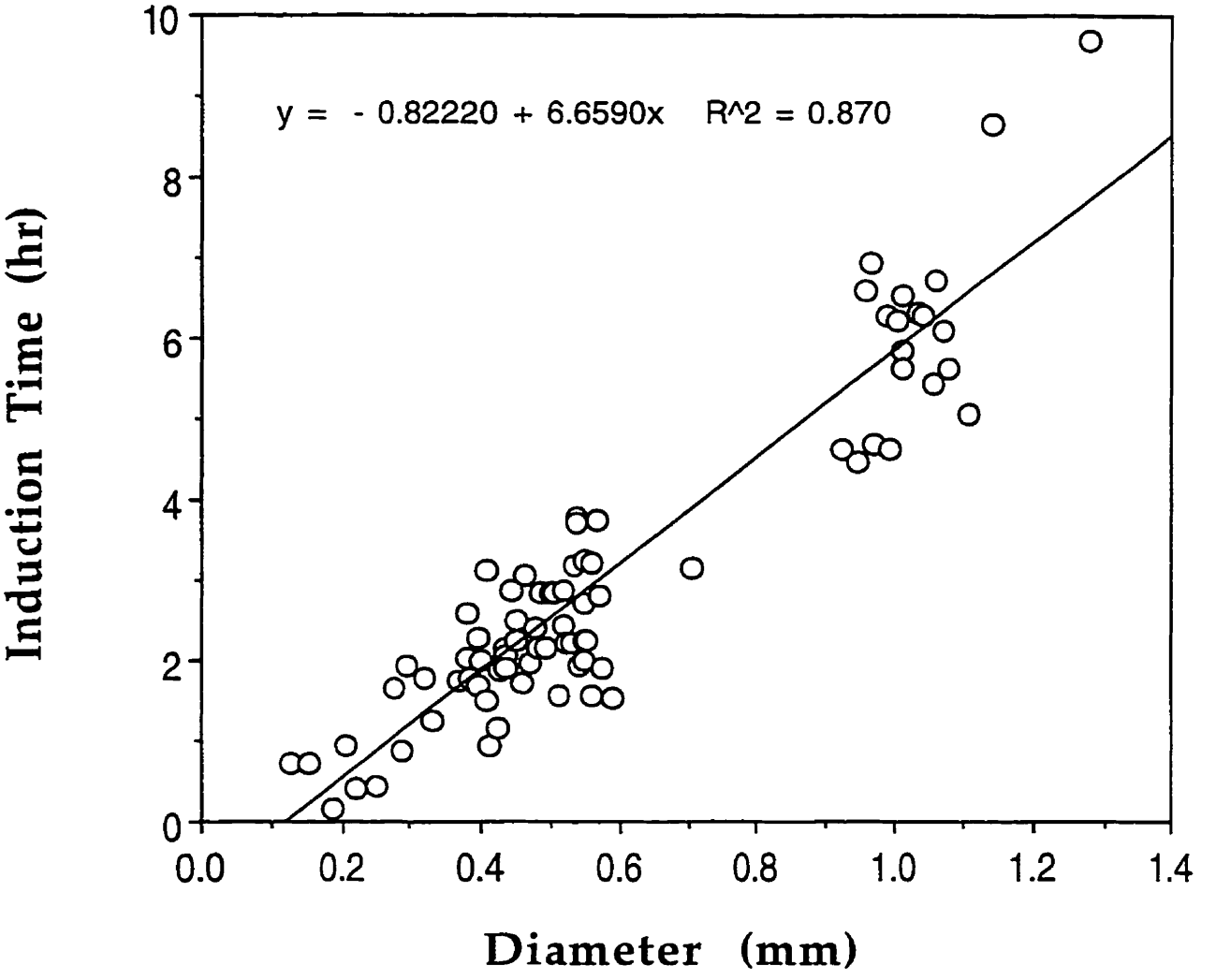

Figure 2.6 Effect of specimen size on induction time. The uncrosslinked PMMA beads were annealed at 130°C and cooled to room temperature at 5°C/min and immersed in methanol at 25°C

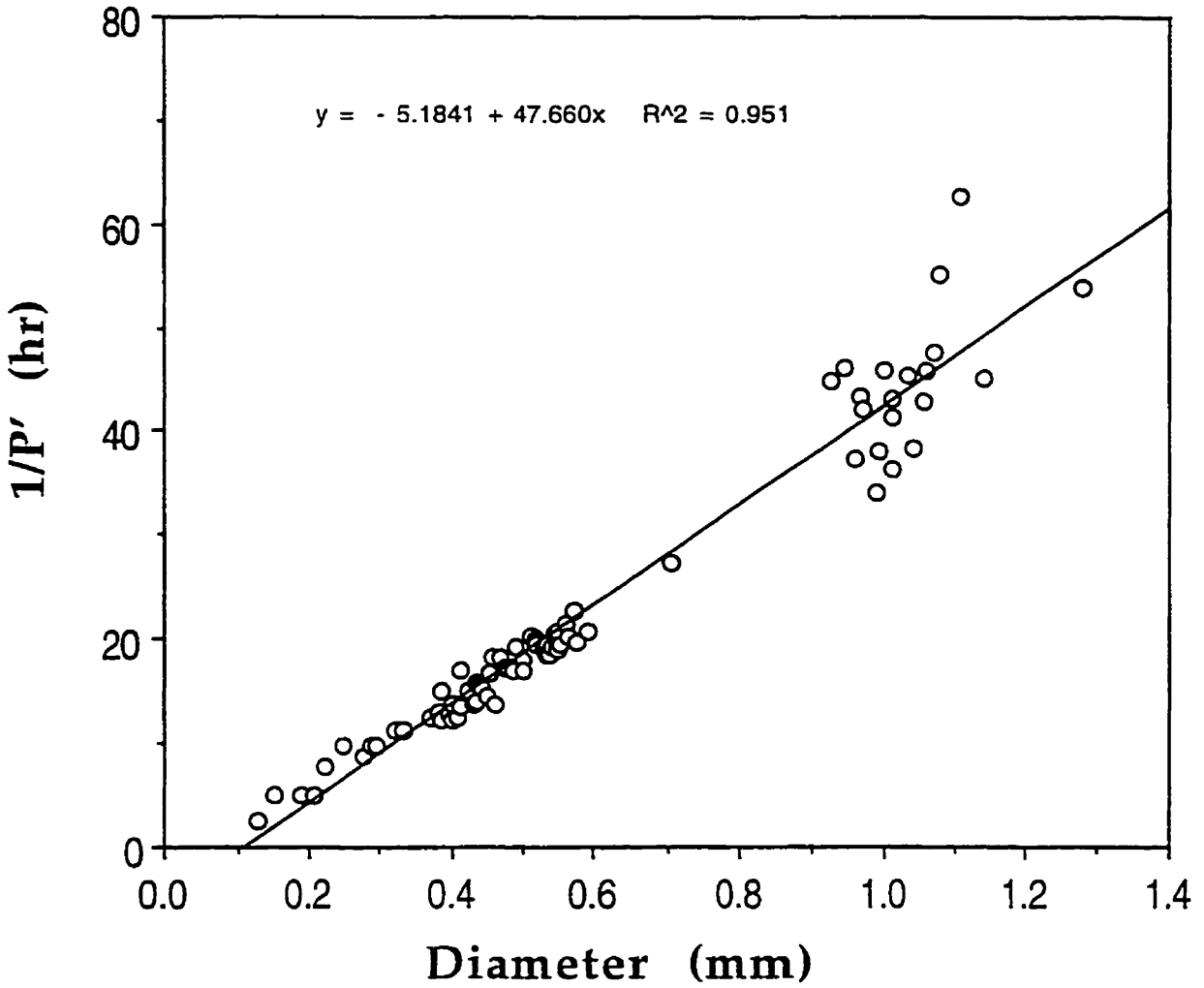

Figure 2.7 Effect of specimen size on normalized penetration rate. The uncrosslinked PMMA beads were annealed at 130°C and cooled to room temperature at 5°C/min and immersed in methanol at 25°C

On the other hand, the increase in penetrant concentration gives rise to an increase in volume of the swelling layer which is further constrained by the compressive stresses exerted by the rigid unswollen core. The second possible scenario is that the effective thickness for the Fickian tail region is the about the same for PMMA beads of different sizes during the induction time. It is conceivable that the larger the bead diameter, the smaller the fraction of the Fickian tail region, and therefore the higher the constraint which will suppress the diffusivity and equilibrium concentration, leading to a longer induction time.

As a result of either of these possible scenarios or a combination of both. it requires longer time for larger beads to reach a constant volume swelling ratio before front propagation starts. The induction time is consequently longer because front would not propagate until the concentration in the effective Fickian tail region reaches the threshold level (Lasky *et al.*, 1988a).

According to the alternative phenomenological analysis proposed by Li and Lee (see Chapter 3), the relationship for a spherical geometry is:

$$\tau_0 = \frac{a_0}{3v_0}\left(1 - \frac{a_0 v_0}{5D_0}\right) \tag{2.6}$$

From Equation (2.6), the extrapolated normalized penetration for spherical sample is expressed as:

$$A = \frac{1}{3}\left(1 - \frac{a_0 v_0}{5D_0}\right) \tag{2.7}$$

Figure 2.8 shows a plot of the extrapolated normalized penetration, A, against the original diameter of the beads. It can be seen that within experimental error, A appears to be almost independent of bead size.

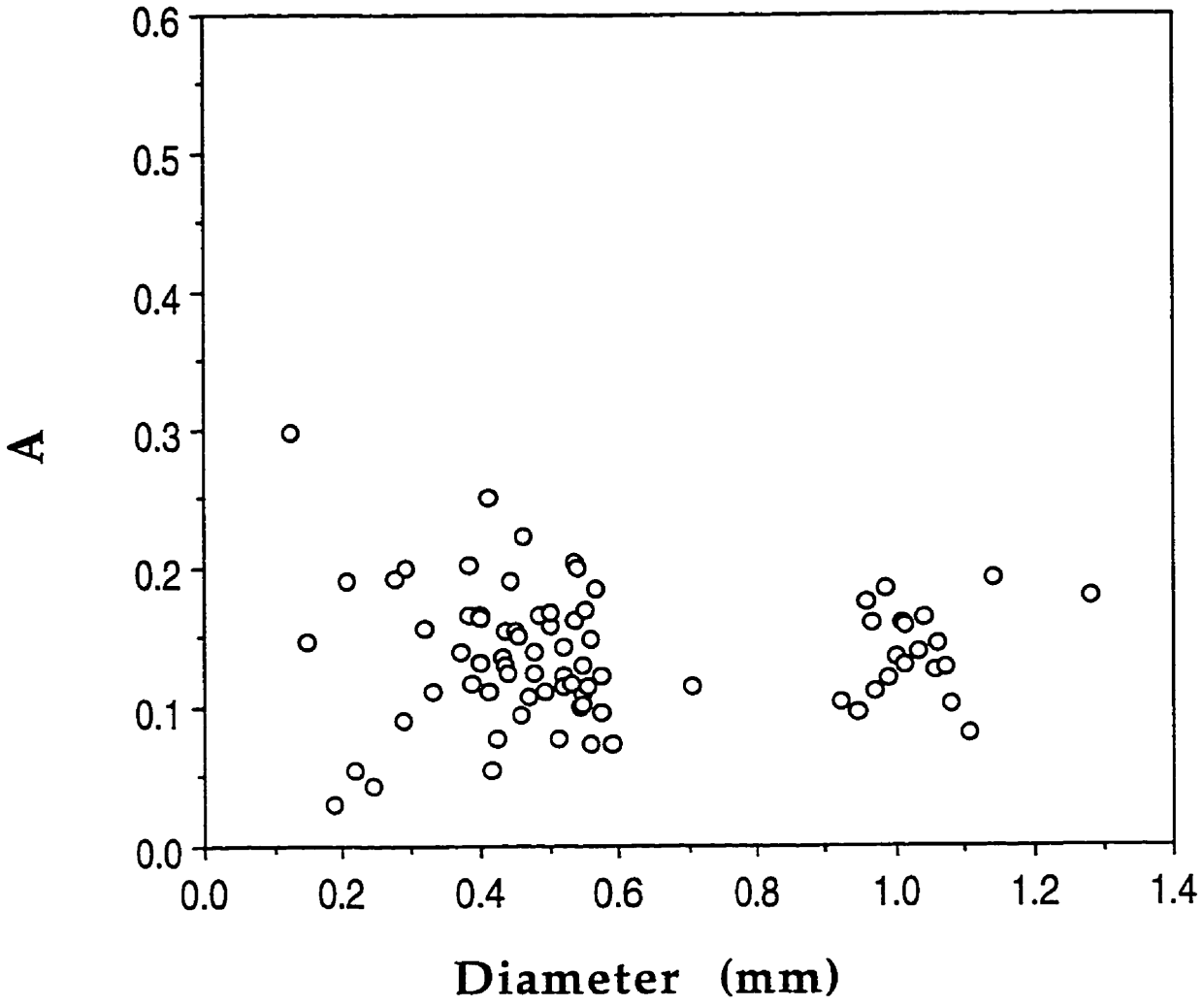

Figure 2.8 Size effect on the product of induction time and normalized penetration rate. The uncrosslinked PMMA beads were annealed at 130°C and cooled to room temperature at 5°C/min and immersed in methanol at 25°C

The dependence of penetration rate v_0 and scaled induction time $\tau_0/d_o(0)$ on bead diameter is shown in Figures 2.9 and 2.10. The results on the penetration rate show a slight decreasing trend with increasing bead diameter. This is matched by an increasing trend in the scaled induction time *vs.* $d_o(0)$ plot. as would be expected from Equation (2.5) with A being constant. This may also be attributed to the stress effect. The larger bead will produce a higher compressive stresses in the swollen region and the swelling region, thereby decreasing the penetrant diffusion coefficient and the mobility of the polymer chain, as well as producing a decrease in the penetration rate.

Experimentally, it has been demonstrated that external stress can be applied to modify the characteristics of Case II sorption (Harmon *et al.*, 1987; More *et al.*, 1992). It is therefore not surprising that the inherent stress produced during the swelling process may modify the characteristics of Case II sorption. The stress effect on diffusion generally results from its effect on free volume fraction (Smith and Adam, 1981; Neumann and Marom; 1987). The magnitude and distribution of the internal stress, also known as differential swelling stress, have been shown to depend on size (Crank, 1953; Cohn and Marom, 1982,1983; Klier and Peppas, 1987; Fu *et al.*, 1991). Therefore, the observed size effect may also be a natural outcome of the size dependent effect of internal stress on diffusion.

The volume swelling ratio in the swollen shell appears to be relatively independent of sample sizes, and maintains almost the same value throughout the sorption process. This implies that the effect of internal stresses on equilibrium solvent concentration in the swollen shell may not be significant.

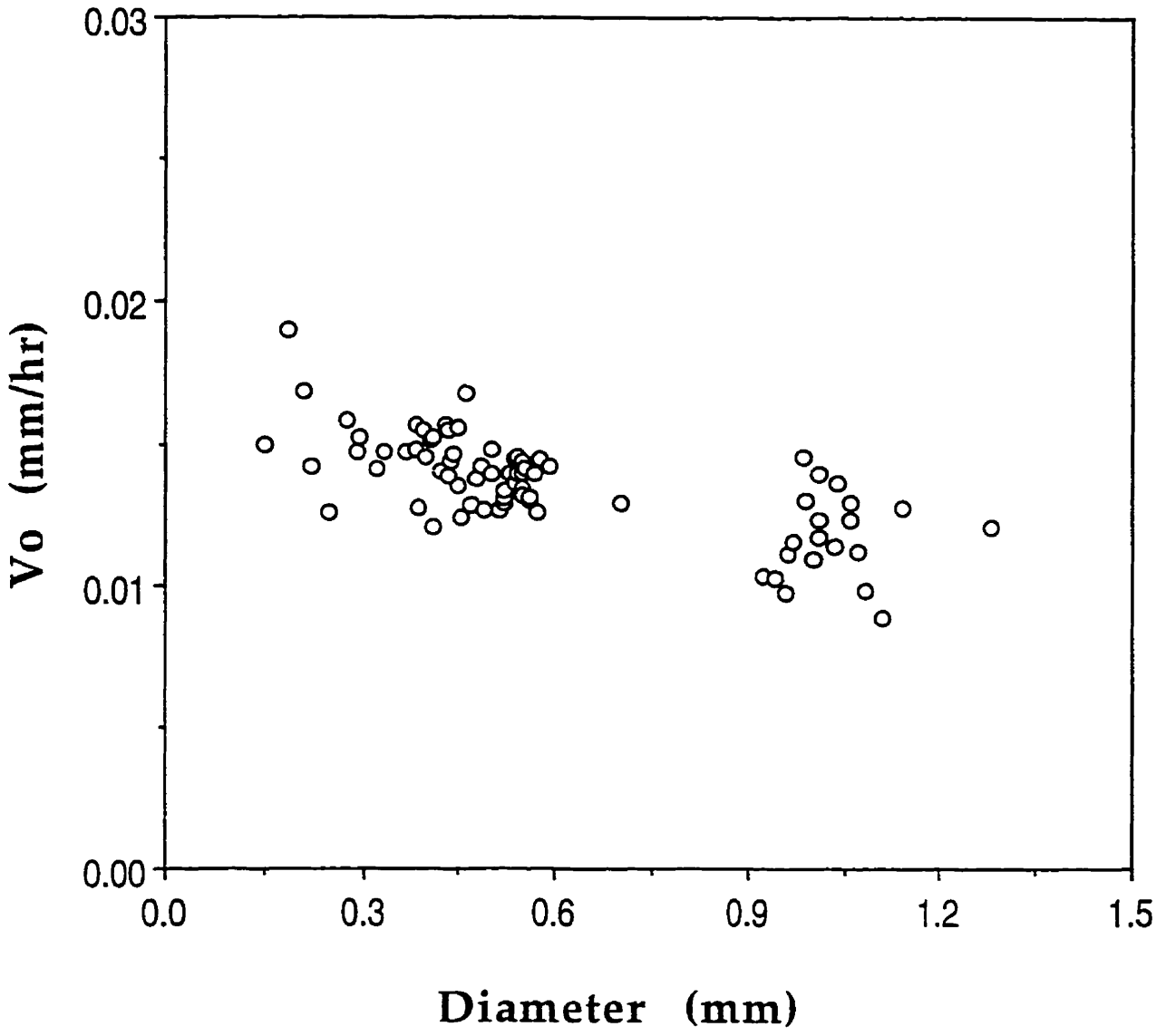

Figure 2.9 Averaged results for size effect on penetration rate. The uncrosslinked PMMA beads were annealed at 130°C and cooled to room temperature at 5°C/min and immersed in methanol at 25°C

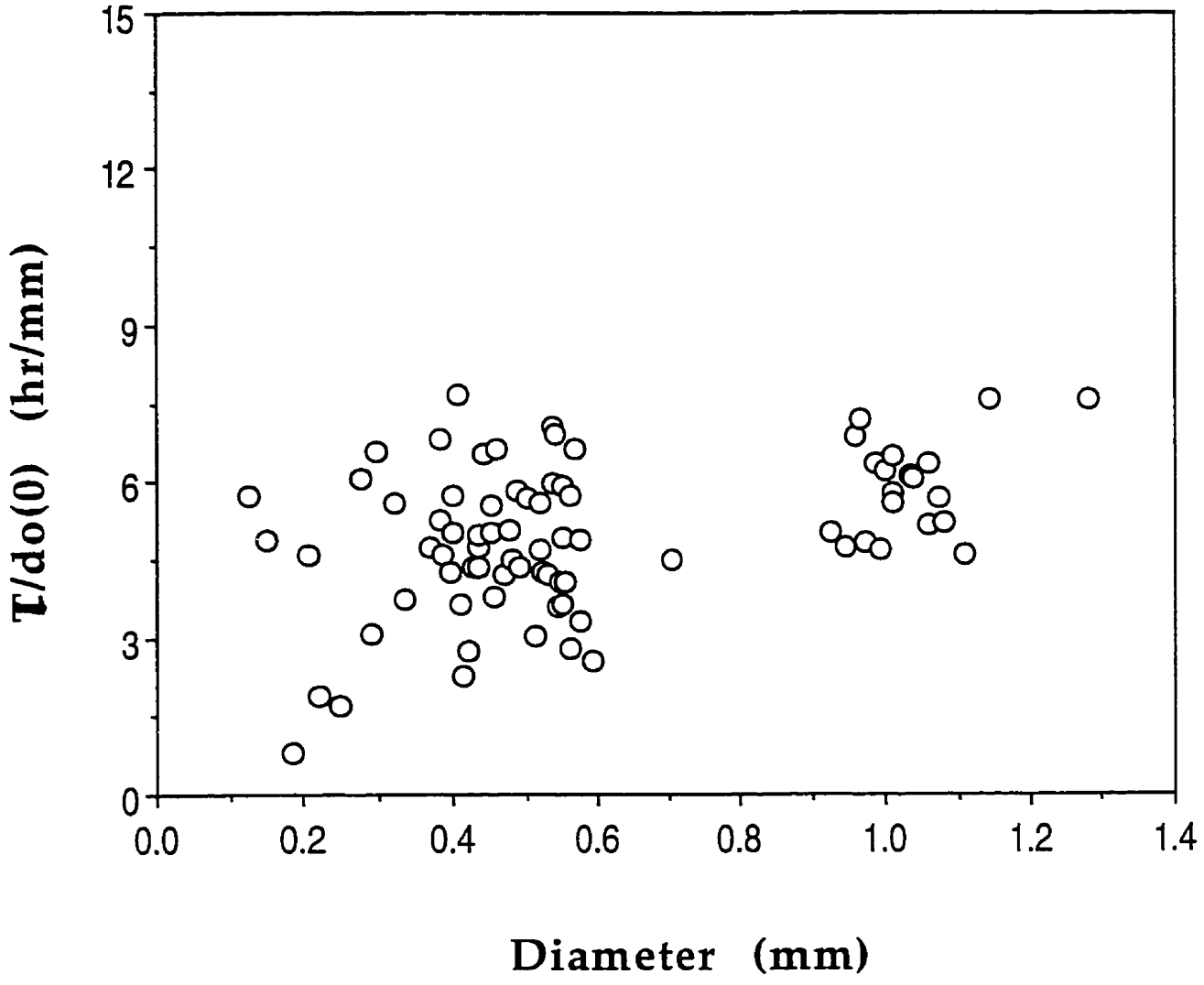

Figure 2.10 Averaged results for size effect on scaled induction time. The uncrosslinked PMMA beads were annealed at 130°C and cooled to room temperature at 5°C/min and immersed in methanol at 25°C

2.4.3 Effect of Sample History

The combined effects of size and cooling rate on normalized penetration rate and induction time for annealed beads are illustrated in Figures 2.11 and 2.12 respectively. The results for samples without heat treatment are also included to demonstrate the effect of sample thermal history. The cooling rate traversing the glass transition region of the polymer is critical in determining the free volume fraction of the polymer. The lower the cooling rate, the higher would be the packing density of the beads. A higher cooling rate will result in a larger free volume fraction in the polymer. This will increase the mobility of the polymer chain and the diffusion coefficient of the penetrant, especially at the swelling front, and consequently will result in a shortened induction time and an increased normalized penetration rate.

It should be noted that, due to the relatively low thermal conductivity of PMMA, a higher external cooling rate does not necessarily result in a higher cooling rate inside the beads. This helps to explain the closeness of the results at cooling rate of 20°C/min and 320°C/min.

The samples without annealing exhibit a very high free volume ratio because drying at 70-80°C after purification of the beads in methanol is an irreversible desorption process for the swollen beads, which should yield a morphologically more porous polymer (Lin *et al.*, 1990,1991). This porosity cannot be reduced by drying below the glass transition temperature. The density of the dried polymer is closer to the swollen rather than the annealed polymer and consequently, the induction time is very short and penetration rate is high. The observed increases in normalized penetration rate and the observed decreases in induction

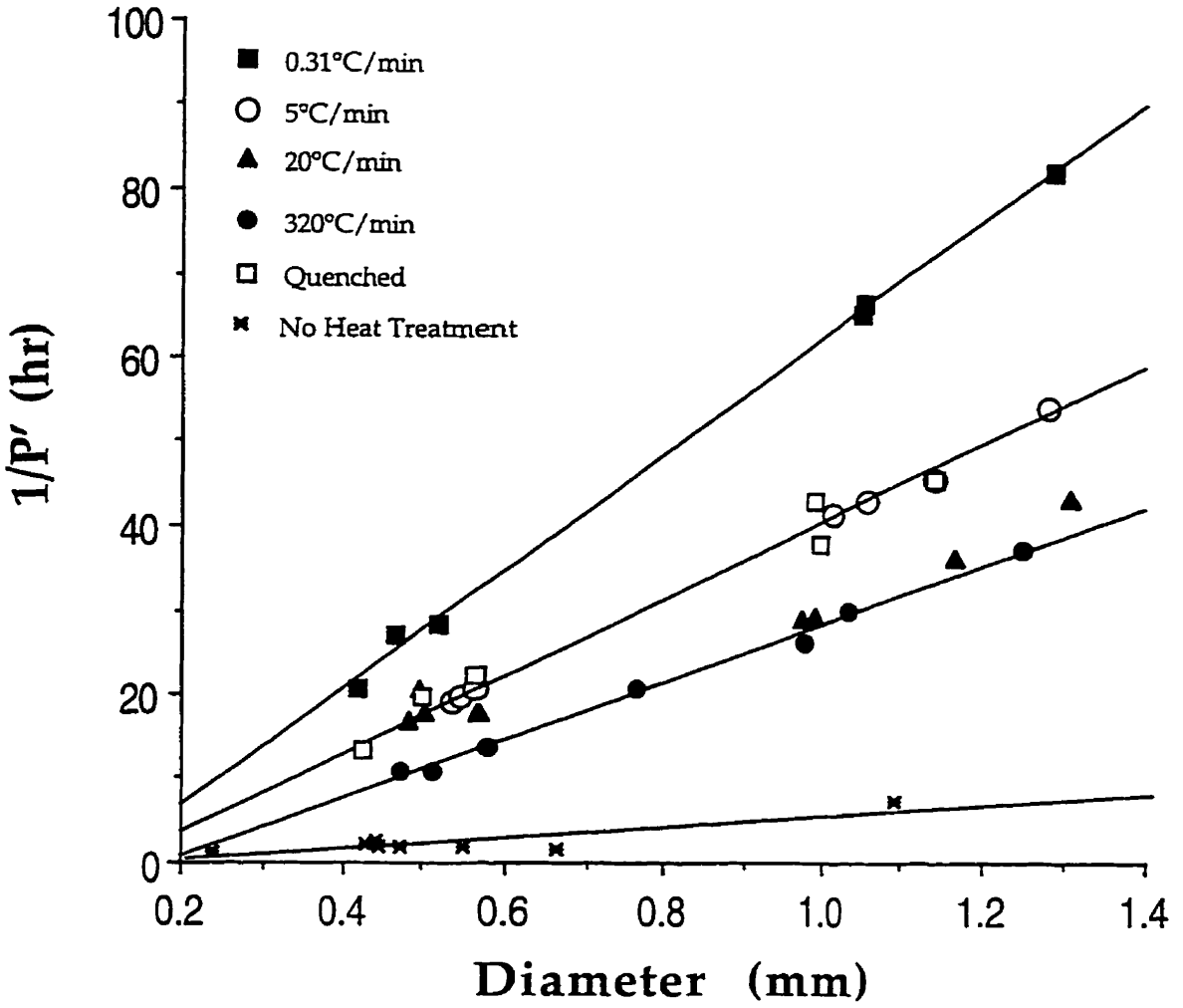

Figure 2.11 Effect of size and sample history on normalized penetration rate. The uncrosslinked PMMA beads, immersed in methanol at 25°C, were either without heat treatment or annealed at 130°C and cooled to room temperature at different rates

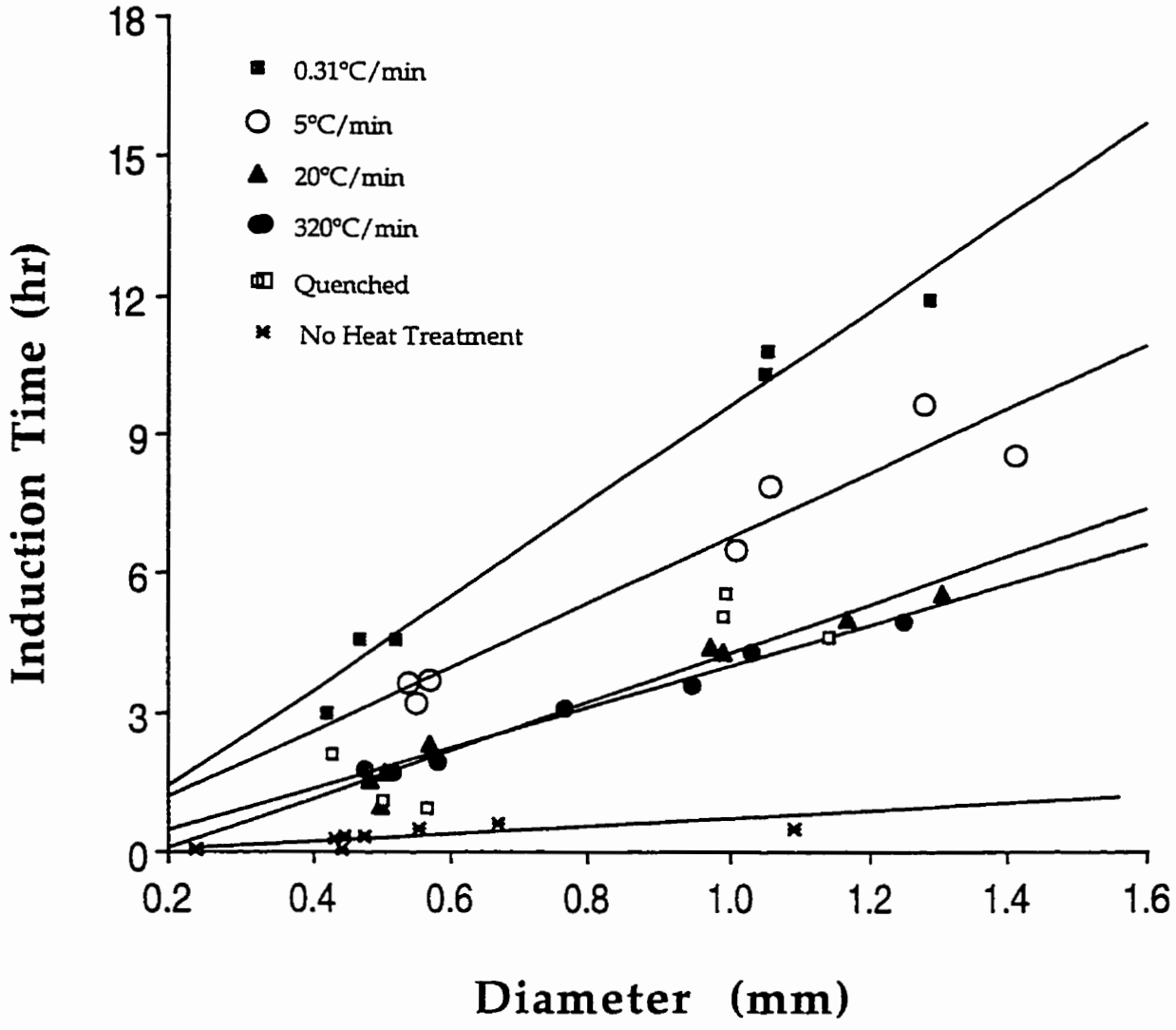

Figure 2.12 Effect of size and sample history on induction time. The uncrosslinked PMMA beads, immersed in methanol at 25°C, were either without heat treatment or annealed at 130°C and cooled to room temperature at different rates

time are consistent with the above interpretation based on the free volume consideration.

Within experimental error, the volume swelling ratio shows no discernible trend with the change of sample thermal history. The sensitive dependence of penetration rate v_0 on the thermal history of the glassy polymer is well known (Alfrey *et al.*, 1966). Its dependence on cooling rate is shown in Figure 2.13, which shows the same trend as reported by Windle (1985). As can be seen in Figure 2.14 that, within experimental error, A can be considered as independent of cooling rate or at best a very weak function of the cooling rate. However, possibly due to the random inhomogeniety of unannealed samples, a larger scatter of A was obtained.

2.4.4 The influence of Swelling Temperature

The temperature effect on Case II sorption was reported in a previous publication (Lee, 1993). The penetration rates consistently increase with increasing swelling temperature, corresponding to a decreasing trend in the normalized induction time. In this case, A should only decrease slightly with increasing temperature, as would be expected from the activation energy values for induction time and penetration rate. In Figure 2.15, the volume swelling ratio shows a marginally increasing trend with increasing temperature, which is consistent with the results of Thomas and Windle (Thomas and Windle, 1978).

2.4.5 Effect of Penetrant Size

Comparison of penetration kinetics of alcohols with different molecular weight was conducted at elevated temperature to facilitate the absorption of alcohols having higher molecular weight.

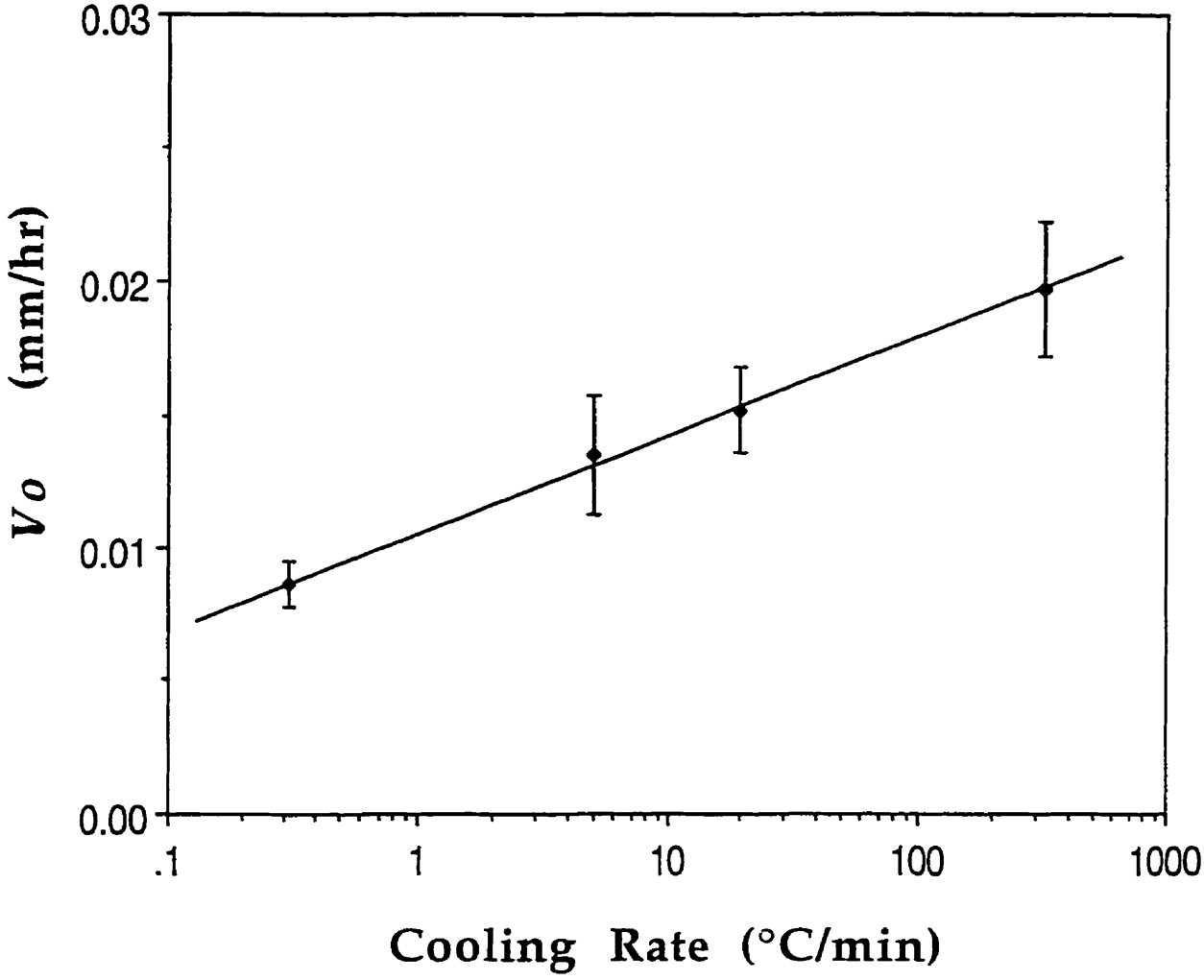

Figure 2.13 Effect of cooling rate on the penetration rate of methanol in PMMA beads at 25°C. The uncrosslinked PMMA beads were annealed at 130°C and cooled to room temperature at different rates

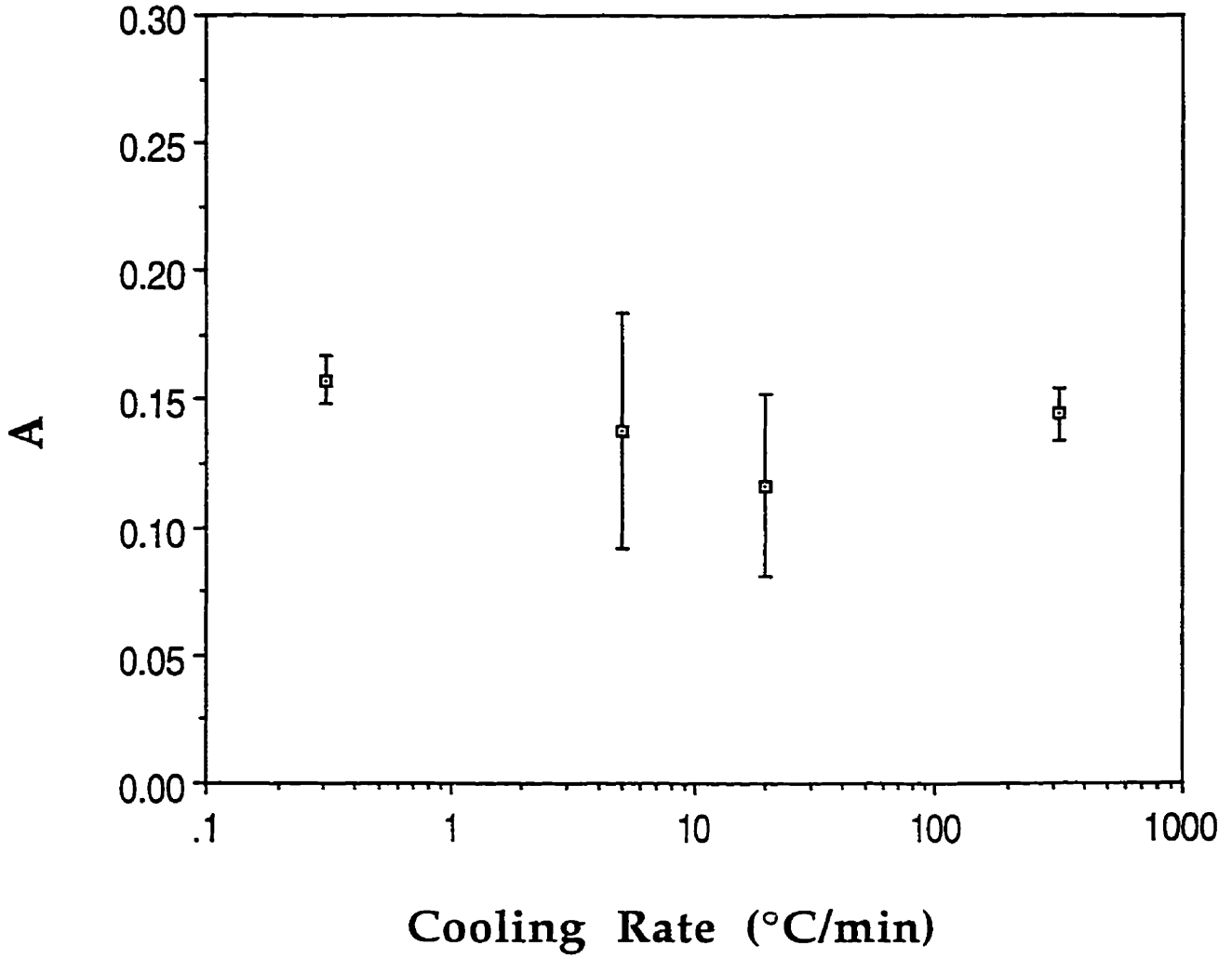

Figure 2.14 Dependence of parameter *A* on cooling rate. The uncrosslinked PMMA beads were annealed at 130°C and cooled to room temperature at different rate prior to immersion in methanol at 25°C

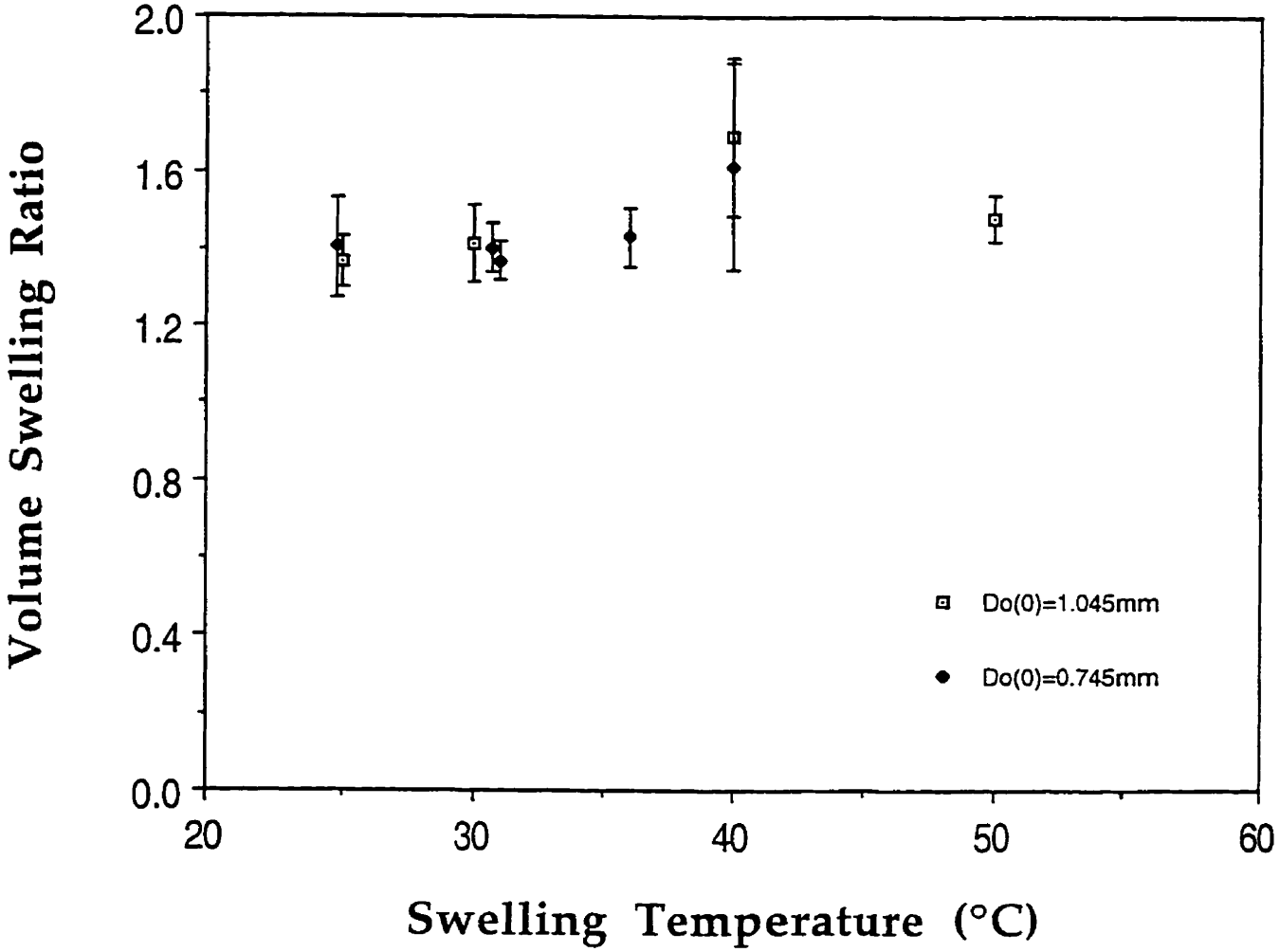

Figure 2.15 Dependence of volume swelling ratio on temperature. The uncrosslinked PMMA beads were annealed at 130°C and cooled to room temperature under ambient conditions

Penetration observed at 50°C exhibits typical Case II behavior for the alcohols used, except that the penetration front is less sharp when the penetrant is iso-propanol. The induction time increases with an increase in the molecular size of the penetrant as well as the bead size of samples having identical thermal history. The results are summarized in Figures 2.16 and 2.17.

At room temperature, there is no significant dependence of penetration rate on the size of the beads. However, the penetration rate depends strongly on the molecular size of the alcohols; the higher the molecular weight of the penetrant, the slower the front movement. The penetration rate was reduced roughly one order of magnitude by each increase of carbon atom as shown in Table 1. Although the penetrant molecules move more easily along their length rather than perpendicular to the molecular contour, experimental evidence does not support a simple reptation-like mechanism for the molecular motion of small penetrant in glassy polymer (Gall *et al.* 1990). Interestingly, no significant dependence of volume swelling ratio on the molecular size of the alcohols has been observed.

Table 2.1. Effects of Molecular Size of Alcohols on Case II Transport in PMMA Beads at 50°C

	Penetration Rate (mm/hr)	Induction Time (hr) (Dia.≈0.50mm)	Volume Swelling Ratio
MeOH	0.266±0.04	0.0504	1.46±0.05
Et OH	0.0143±0.0008	1.3139	1.49±0.08
n-PrOH	0.0019±0.0006	7.4651	1.61±0.08
i-PrOH	0.003±0.003	6.471	1.6±0.1
n-BuOH	0.00033±0.00004	26.435	1.5±0.1

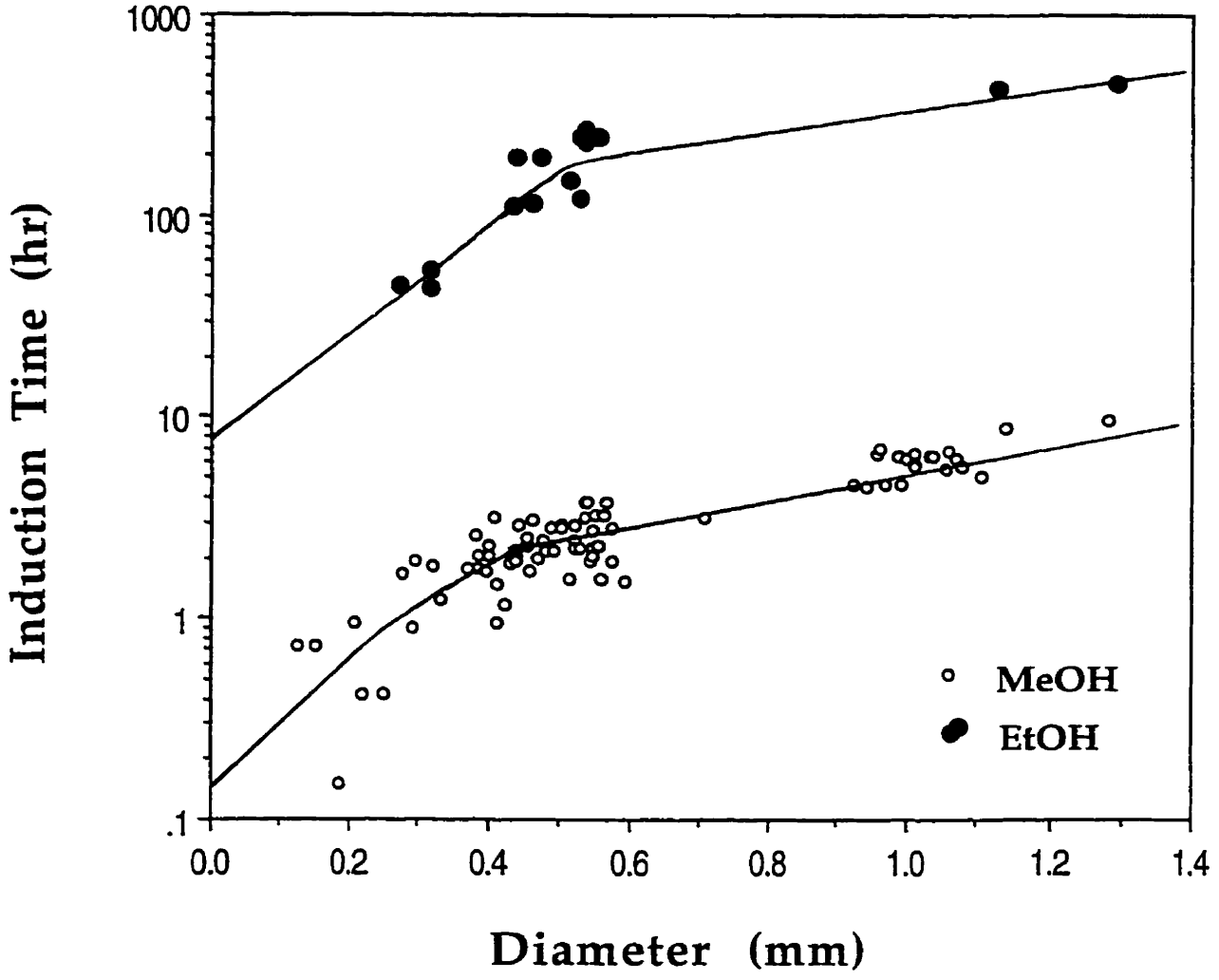

Figure 2.16 Effect of the molecular size of the penetrant MeOH and EtOH. The uncrosslinked PMMA beads were annealed at 130°C and cooled to room temperature at 5°C/min and immersed in the penetrant at 25°C

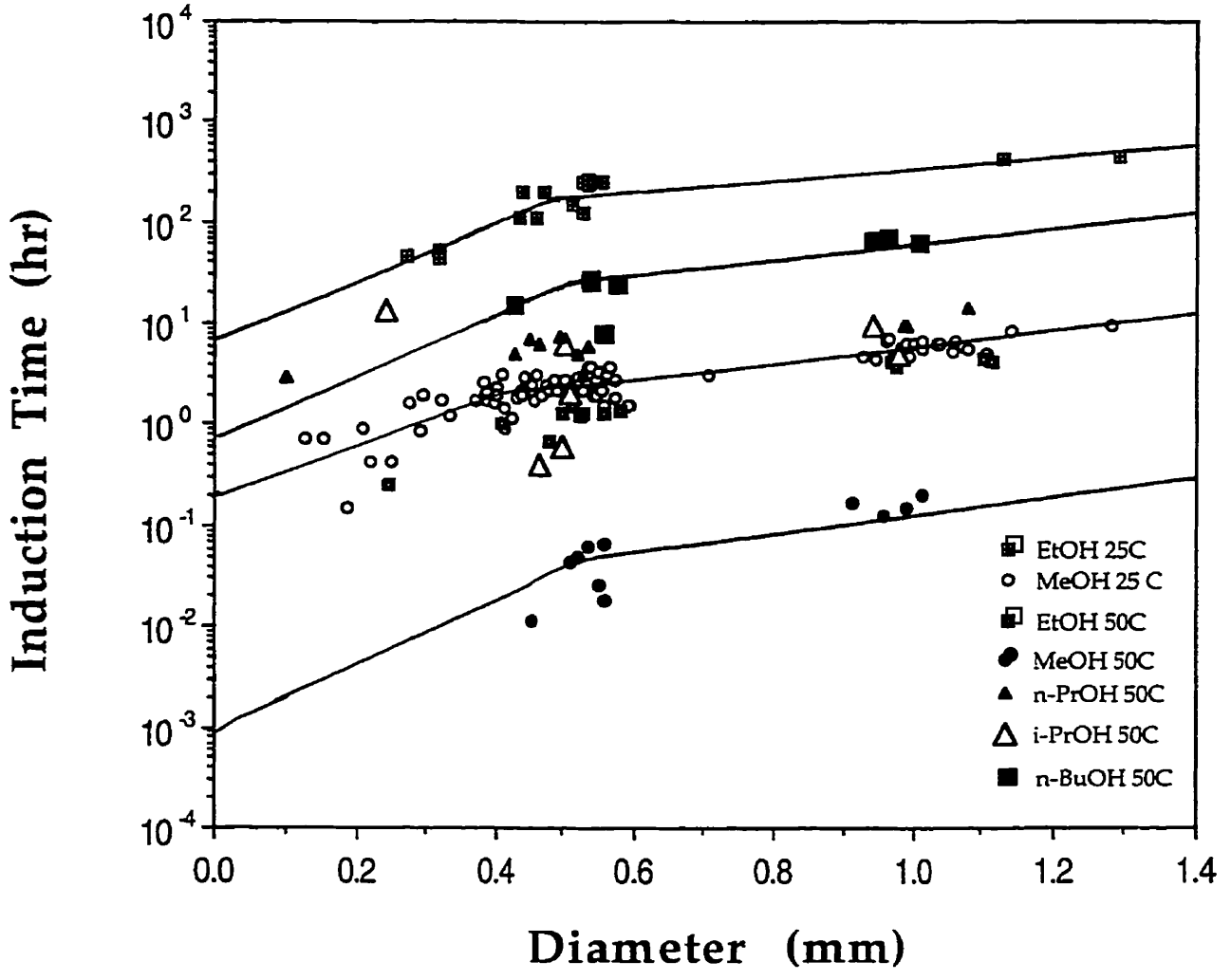

Figure 2.17 Effect of the molecular size of the penetrant, MeOH, EtOH, i-PrOH, n-PrOH, n-BuOH. The uncrosslinked PMMA beads were annealed at 130°C and cooled to room temperature at 5°C/min and immersed in the penetrant at 25°C and 50°C

2.5 Conclusions

The induction time and penetration rate in methanol-PMMA system were observed to vary with the diameter of bead samples undergoing Case II sorption. Being not predicted by existing theories, this observation implies that the characteristic parameters for Case II sorption are not material properties. The induction time and penetration rate were also observed to depend on sample history; the induction time increases with decreasing cooling rate, while the penetration rate shows the opposite trend. This history dependence can be well interpreted in terms of the free volume theory.

A phenomenological relationship between induction time and front penetration rate has been proposed and experimentally verified. The induction time and front penetration rate are inversely related by the extrapolated normalized penetration, which appears to be independent of the bead size and cooling rate.

The volume swelling ratio in the swollen region of the bead remains constant during the propagation of the penetration front, which offers another supporting evidence for the uniform penetrant concentration distribution in the swollen region during Case II sorption. This volume swelling ratio also shows a slight increase with the swelling temperature. In the case of alcohol penetrants, no significant dependence of volume swelling ratio on the molecular size of the alcohols was observed.

In all cases, the internal stresses may be a dominant factor in determining the dependencies of the induction time and penetration rate on sample size. However, their effect on the volume swelling ratio does not appear to be significant.

Chapter 3

Prediction of the Behaviors of Case II Sorption in Glassy Polymers

3.1 Introduction

Case II sorption, uniquely characterized by a constant movement of the fluid penetration front and a uniform high concentration of the penetrant in the swollen polymer shell, occurs when a non-solvent penetrant is absorbed by a glassy polymer. The swelling penetrant concentration leads to a plasticization of the polymer and generates differential swelling stress. Thus, Case II sorption has been considered as a result of stress-coupled diffusion. The effects of osmotic stress, differential swelling stress and its gradient on diffusion have been incorporated in various theoretical approaches to predict the Case II behavior (Crank, 1953; Alfrey *et al.*, 1966; Frisch *et al.*, 1969; Petropoulos and Roussis, 1978; Thomas and Windle, 1978; Gostlic and Sarti, 1983; Neogi *et al.*, 1986; Klier and Peppas, 1987; Cohen and White, 1989; Cox and Cohen, 1989; Carbonell and Sarti, 1990; Cohen and Erneux, 1990; Cox, 1990; Hayes and Cohen, 1992; Lustig *et al.* 1992; Govindjee and Simo, 1993; Edwards and Cohen, 1995a, 1995b; Edwards, 1996; Witelski, 1996). It is well recognized that the differential swelling stress and the viscoelastic behavior of polymers play a critical role in the self-modulation of penetrant fluxes. As has been demonstrated by phenomenological models, Case II behavior can also be produced

when the surface flux of penetrant is limited (Lee and Kim, 1992; Rossi, Pincus and de Gennes. 1995).

Historically, Case II sorption in polymers is often associated with the glassy to rubbery transition induced by the penetrant swelling (Alfrey, 1965; Windle, 1985). However, as has been demonstrated experimentally, glass transition is not a prerequisite for the occurrence of Case II behavior. For example, Case II behavior may occur while the swollen polymer shell is still in the glassy state, similarly absorption in glassy polymers involving glass transition may not produce Case II characteristics (Frisch *et al.*, 1969; Janacek and Kolarik, 1976; Thomas and Windle, 1980; Williams *et al.*, 1986; Lin *et al.*, 1990, 1991; Samus and Rossi, 1996). The only possible relaxation involved in Case II sorption is the β relaxation in the glassy state with an activation energy of 20 kcal/mol, close to that for solvent front penetration. It is believed that this β relaxation is also involved in the yielding of polymers and the nucleation of crazing or the generation of a microcavity. On the other hand, disentanglement of polymer chains may occur during polymer swelling. This disentanglement is mobilized by forces exerted on polymer chain rather than Brownian motion. Forced reptation of polymer chain is also involved in the yielding of polymers under stress, and the development of crazing under stress or due to solvent attack (Brown, 1989; McLeish *et al.*, 1989; Herman and Edwards, 1990; Plummer and Donald, 1990).

In order to gain a better understanding of Case II sorption in glassy polymers, it is useful to first define the criteria for its occurrence. To this end, it is necessary to analyze the physics involved in the two characteristic parameters of Case II sorption, namely the

induction time and the front penetration rate, based on an improved understanding of polymer dynamics. Incorporating appropriate boundary conditions with these results, the evolution of Case II sorption in a swelling glassy polymer can then be formulated as a generalized moving boundary problem.

In this paper, the relationship between induction time and penetration rate is first established from a molecular theory. It is further demonstrated that the induction time depends on both the geometry and size of the polymer specimen. A simple relationship between the induction time and initial front penetration rate will be established for a glassy polymer with various finite geometries. Here, Case II sorption is treated as a pseudo steady state transport process. The flux of the penetrant into the glassy polymer is assumed to be limited to a much lower finite value, due to the synergy of diffusion, plasticization kinetics and differential swelling stress in a viscoelastic glassy polymer.

3.2 The Relationship between Induction Time and Penetration Rate

Case II sorption can be characterized by two parameters, namely the induction time and the front penetration rate. To better describe these characteristics of Case II sorption, it is essential to provide theoretical predictions on the induction time and front penetration rate and their relationship based on known physical parameters.

Based on Thomas-Windle's theory, the front penetration rate v_0 can be simply represented by (Brown, 1989; Gall *et al*, 1990):

$$v_0 = \left[\left(\frac{D_0}{c_c}\right)\frac{dc}{dt}\right]^{\frac{1}{2}} = \left[\left(\frac{D_0}{c_c}\right)\frac{(\Pi + S)}{\eta}\right]^{\frac{1}{2}} \qquad (3.1)$$

where D_0 is the diffusion coefficient of the penetrant in the glassy region, c_c the threshold penetrant concentration, Π the osmotic stress and S the trace of stress tensor. According to Equation (3.1), the front penetration rate is expected to depend on the molecular weight of the polymer in low molecular weight ranges because the viscosity η depends on molecular weight of the polymer. When the molecular weight is too high, polymer chain scission, rather than forced reptation of the whole chain, will take place. Consequently, the front penetration rate loses its dependence on the molecular weight of polymer.

Although the microscopic scenario of relaxation during swelling in Case II sorption has not been well established, it can be understood intuitively that in order for the progression of the penetration front and the polymer swelling to occur, rearrangement of polymer chains must take place in the transitional region between the swollen shell and the unswollen core. This rearrangement can be realized by the stressed diffusion or forced reptation of polymer chains (McLeish *et al.*, 1989; Plummer and Donald, 1990). The rearrangement and consequently the penetration rate should be proportional to the square root of translational diffusion coefficient D_r of the polymer chain (or broken segments) for forced reptation, similar to the relationship for D_0 suggested by Equation (3.1). Since $\eta \propto 1/D_r$ and D_r can be considered as similar to the diffusion coefficient of polymer chain for Brownian or diffusive reptation (Graessley, 1982),

$$v_0 = K\left[(\Pi + S)\, D_0 D_r\right]^{1/2} \propto K\left((\Pi + S) D_0 \frac{k_b T}{nf}\right)^{1/2} \qquad (3.2)$$

where K is a material constant, k_b Boltzmann constant, T the temperature, n degree of polymerization, and f the friction coefficient per monomer unit. Here, as is consistent with experimental observations, the front penetration rate increases with the experimental temperature and decreases with increasing molecular weight of the polymer. However, the front penetration rate does not depend on the molecular weight of the polymer due to polymer chain scission when the molecular weight is high.

The induction time τ_0 is intuitively related to the disentanglement time τ_d or the time required for the complete rearrangement of polymer chains during the formation of the initial swollen skin layer, prior to the front propagation. This disentanglement time is characterized by the relaxation time τ_r of the polymer chain (Graessley, 1982)

$$\tau_0 = K' \tau_d \approx K' \tau_r \propto \frac{K'\langle R^2 \rangle}{6\pi^2 D_r} \propto M^3 \qquad (3.3)$$

where K' is also a dimensionless material constant, $\langle R^2 \rangle$ the mean-square end to end distance of the chains, and M the molecular weight of polymer chain. From Equations (3.2) and (3.3), a new expression relating the induction time and penetration rate can be obtained

$$\frac{\tau_0 v_0^2}{D_0} \propto \frac{K^2 K' (\Pi + S)\langle R^2 \rangle}{6\pi^2} \qquad (3.4)$$

As a first approximation, $\frac{\tau_0 v_0^2}{D_0}$ is expected to be a material constant, determined once the condition of sorption is specified, regardless of the exact form of the translational diffusion coefficient. This predicted relationship between induction time and penetration

rate is similar to that given by Rossi *et al.* (1995) for situations where the effect of geometry and size of the samples can be neglected.

According to Rossi *et al.* (1995), penetrant diffusion is the only process within the polymer before the plasticization front is established, and the diffusion in this induction period is governed by Fick's law; a constant flux boundary condition at the penetrant-polymer interface is adopted to account for the kinetics of the plasticization process at the polymer surface. Induction time is the time when the surface concentration reaches the critical penetrant concentration c_p. For a semi-infinite, initially dry glassy polymer, the relationship between the induction time τ_0 and penetration rate v_0 has been given by Rossi, Pincus and de Gennes as (Carslaw and Jaeger, 1959; Rossi, Pincus and de Gennes, 1995; Friedman and Rossi, 1997):

$$\tau_0 = \frac{\pi D_0}{4 v_0^2} \tag{3.5}$$

where D_0 is diffusion coefficient of the penetrant in the glassy region. This is obtained by defining the induction time as the time for the surface concentration to reach c_p according to

$$c(x,t) = \frac{v_0 c_p}{D_0} \int_x^{\infty} erfc\left(\frac{\xi}{2\sqrt{D_0 t}}\right) d\xi \tag{3.6}$$

as the surface concentration is given by (Carslaw and Jaeger, 1959a)

$$c(0,t) = 2 v_0 c_p \left(\frac{t}{D_0 \pi}\right)^{\frac{1}{2}} \tag{3.7}$$

The induction time τ_0 is defined as the time when $c(0,t) = c_p$. Other details of the derivation of Equation (3.5) are included in Appendix A. Another correlation for induction time, $\tau_0 = \frac{\pi D_0}{4k^2}$, a form similar to Equation (3.5), can be derived from the more general surface resistance boundary conditions when the sample can be considered as semi-infinite, as is shown in Appendix B. The relationship expressed by Equation (3.5) is preferable since front velocity can be easily determined experimentally, while the value of k from the surface resistance boundary condition is unknown, despite the fact that it has a dimension of front penetration rate.

Contrary to the assumption adopted by Rossi *et al.* (1995), the sample dimension in the penetration direction during Case II sorption is usually finite. In this case, the semi-infinite plate assumption is not appropriate since the induction period is generally long. For large slabs, long cylinders and spheres with finite thickness or radius, the more appropriate relationship between induction time and penetration rate can be derived from concentrated solutions for large value of $\frac{D_0 t}{a_0^2}$ or small value of a_0 in a similar approach with the induction time τ_0 defined as: $c(a_0, \tau_0) = c_p$

For large slabs (Crank, 1975a),

$$\tau_0 = \frac{a_0}{v_0}\left(1 - \frac{a_0 v_0}{3D_0}\right) \tag{3.8}$$

as a result of rearrangement of

$$c(a_0,t) = \frac{v_0 c_p a_0}{D_0}\left\{\frac{D_0 t}{a_0^2} + \frac{1}{3} - \frac{2}{\pi^2}\sum_{n=1}^{\infty}\frac{1}{n^2}\exp\left(-\frac{D_0 n^2 \pi^2 t}{a_0^2}\right)\right\} \tag{3.9}$$

For long cylinders (Crank, 1975b),

$$\tau_0 = \frac{a_0}{2v_0}\left(1 - \frac{a_0 v_0}{4D_0}\right) \tag{3.10}$$

as a result of rearrangement of

$$c(a_0,t) = \frac{v_0 c_p a_0}{D_0}\left\{\frac{2D_0 t}{a_0^2} + \frac{1}{4} - 2\sum_{n=1}^{\infty}\frac{1}{\alpha_n^2}\exp\left(-\frac{D_0\alpha_n^2 t}{a_0^2}\right)\right\} \tag{3.11}$$

where α_ns are the positive roots of

$$J_1(\alpha) = 0$$

For spheres (Crank. 1975c),

$$\tau_0 = \frac{a_0}{3v_0}\left(1 - \frac{a_0 v_0}{5D_0}\right) \tag{3.12}$$

as a result of rearrangement of

$$c(a_0,t) = \frac{v_0 c_p a_0}{D_0}\left\{\frac{3D_0 t}{a_0^2} + \frac{1}{5} - 2\sum_{n=1}^{\infty}\frac{\exp\left(-D_0\alpha_n^2 t\right)}{\alpha_n^2 a_0^2}\right\} \tag{3.13}$$

where the $\alpha_n a_0$ s are the positive roots of

$$\alpha_n a_0 \cot \alpha_n a_0 = 1$$

As a first approximation, higher order terms in the infinite series have been neglected in arriving at Equations (3.8), (3.10) and (3.12). This is certainly justified for large values of $\frac{D_0 t}{a_0^2}$. As shown in Figure 3.1, Equations (3.8), (3.10) and (3.12) provide a good approximation to the exact numerical solution when the dimension in the penetration direction is small in comparison with the induction time. It is obvious from Figure 3.1 that both the dimension and size of the sample will have a significant effect on the induction

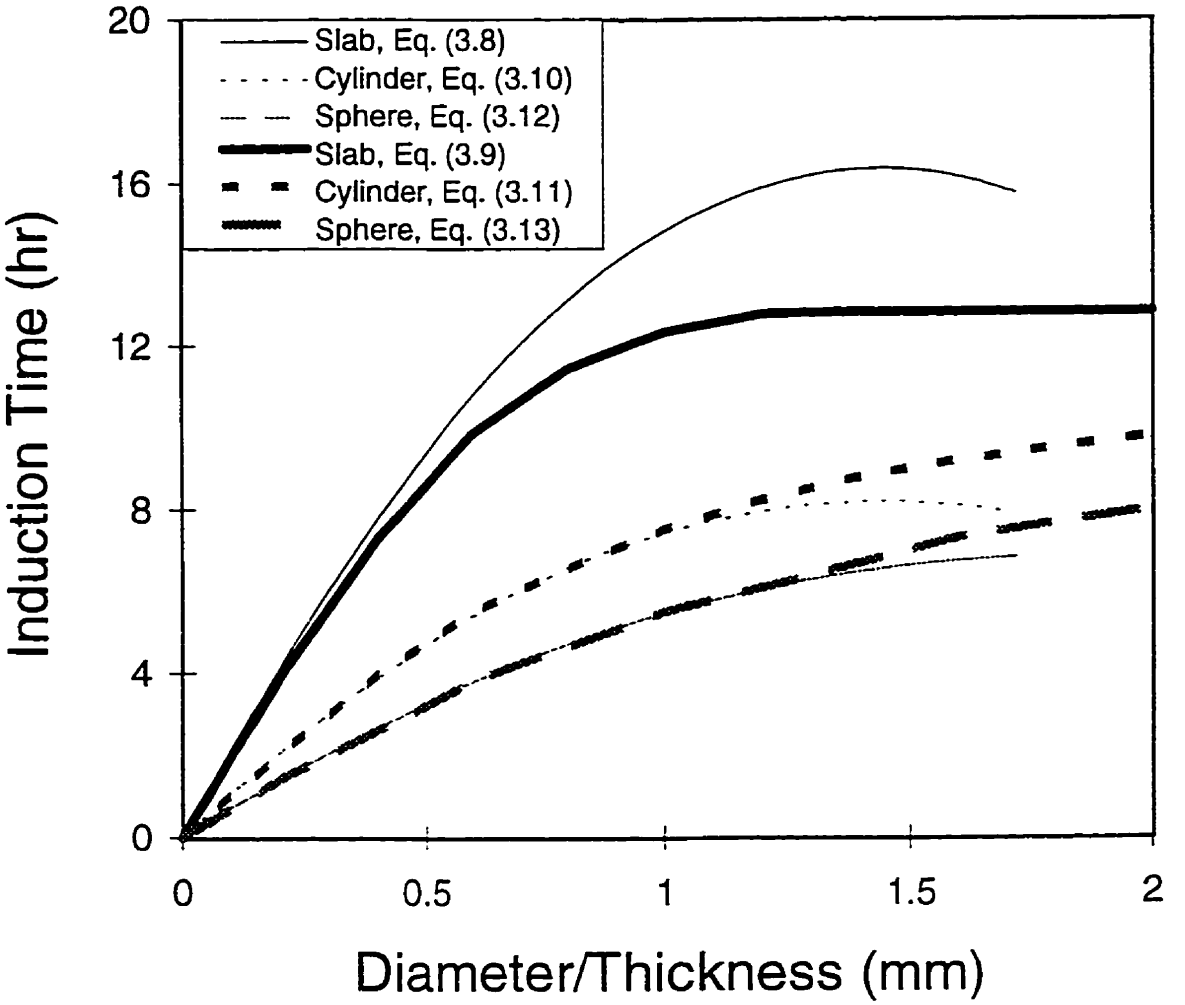

Figure 3.1 Prediction of induction time based on Equations (3.8), (3.10) and (3.12) in comparison with numerical solutions based on Equations (3.9). (3.11) and (3.13) for slab, cylinder and sphere, respectively. D_0 is assumed to be 2.2×10^{-12} m^2/s and $v_0 = 6.11\times10^{-9}$ m/s.

time. The size dependence of induction time is consistent with the prediction that surface concentration will also depend on both the diffusion coefficient and dimension of the sample based on the surface resistance model (Shankar, 1982). The size and geometry dependence of surface concentration, and consequently that of the induction time, is an essential feature of the diffusion process regardless of the exact form of the boundary conditions. Figure 3.1 also suggests that the dependence of induction time on size may not be observed in thick slabs. The trend of the size dependence may also depend on the diffusivity and front penetration rate. As is shown in Figure 3.2 and 3.3, an approximate linear dependence of induction time on size can be achieved in the small sample size range with a proper choice of parameters. It is further noted that the room temperature experimental results of Case II sorption of methanol in PMMA beads (Figure 3.4) agree well with the prediction based on Equation (3.12).

3.3 Discussion

3.3.1 Relationship between Induction Time and Penetration Rate

When the sorption time is short, or when the induction time is very small, the concentration profiles for specimens with finite dimension can be effectively treated as equivalent to those of the semi-infinite plate, as represented by the small $\frac{D_0 t}{a_0^2}$ solutions for various geometries. This is also true when the dimension of the specimens is very large

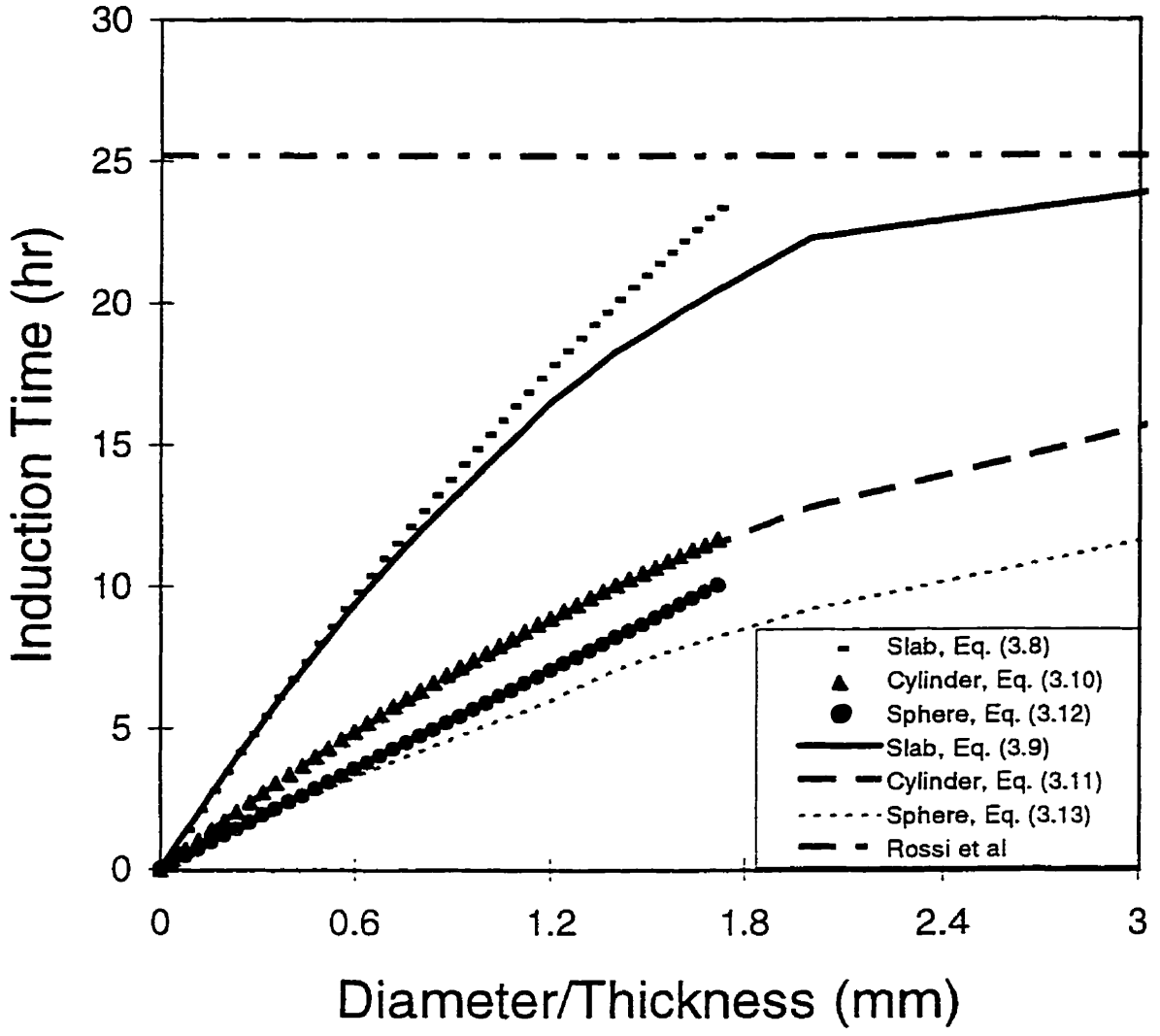

Figure 3.2 Prediction of induction time based on Equations (3.8), (3.10) and (3.12) in comparison with numerical solutions based on Equations (3.5), (3.9), (3.11) and (3.13) for semi-infinite plate, slab, cylinder and sphere, respectively. D_0 is assumed to be 7×10^{-12} m^2/s and $v_0 = 7.78\times10^{-9}$ m/s.

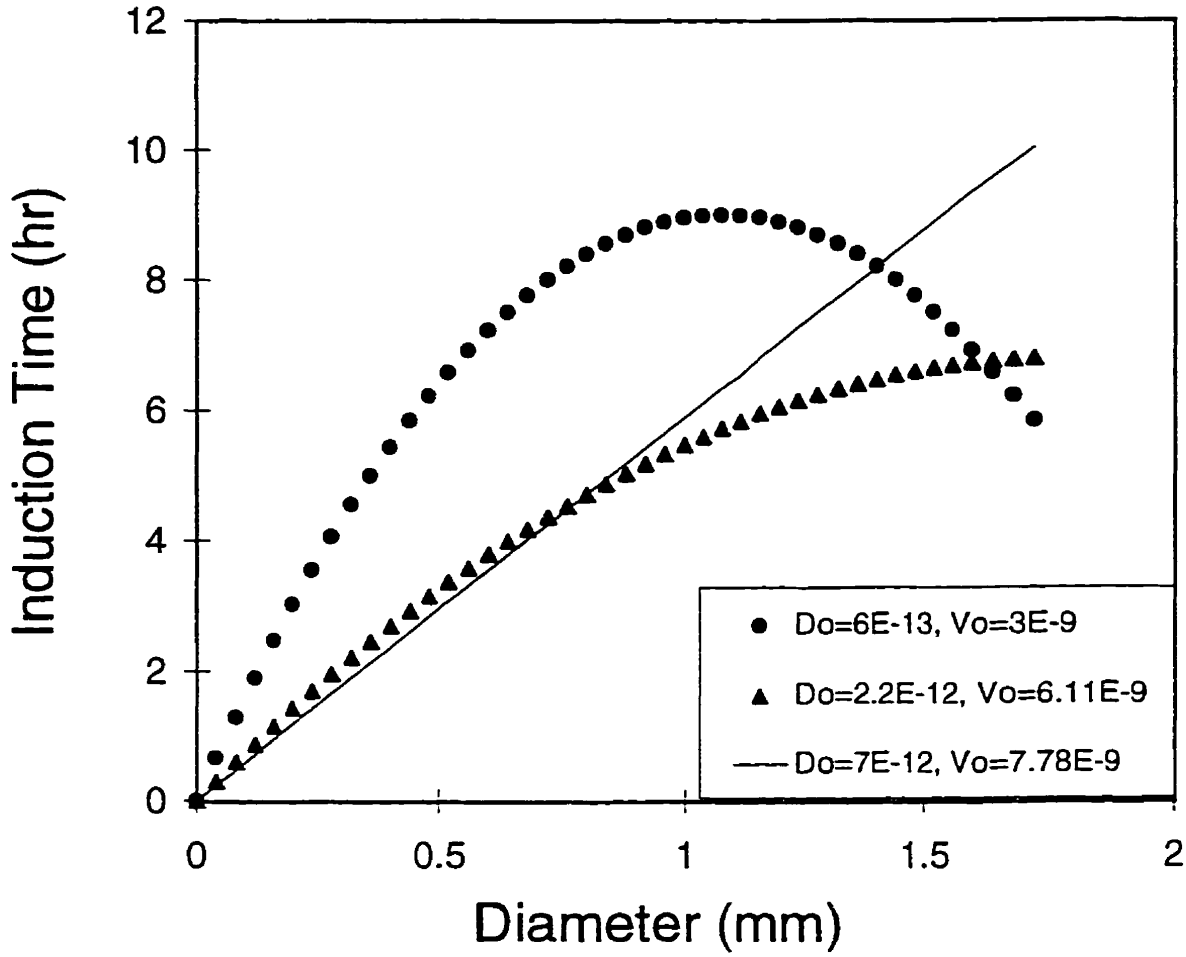

Figure 3.3 Prediction of size effect on induction time based on Equation (3.12). Various D_0 and v_0 are used to demonstrate their effects on the size dependence

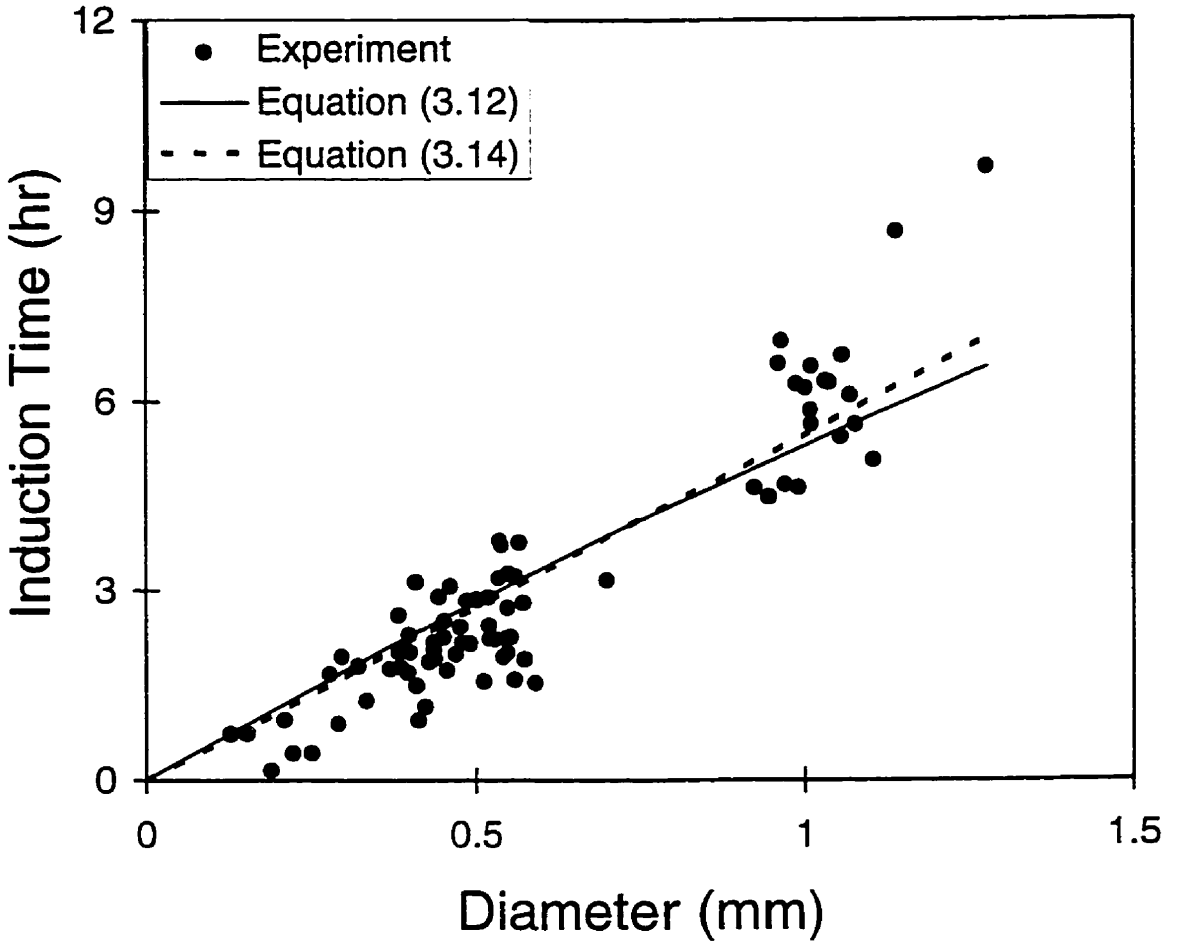

Figure 3.4 Experimental results of Case II sorption of methanol in PMMA beads at room temperature in comparison with the prediction based on Equations (3.12) and (3.14). D_0 is assumed to be 7×10^{-12} m^2/s, $v_0 = 7.78\times10^{-9}$ m/s and A=0.306

which gives a small $\frac{D_0 t}{a_0^2}$. In this case, the solution for induction time again converges to that of Rossi, Pincus and de Gennes for semi-infinite samples, namely Equation (3.5) (Carslaw and Jaeger, 1959b, Crank, 1975b). Detailed derivation of this is given in Appendix A.

The relationship between the induction time and front penetration rate expressed in Equation (3.5) has not been reduced to the simplest form since the front penetration rate depends on the diffusivity of the penetrant in the polymer D_0 according to Equation (3.2). By combining Equations (3.2) and (3.5), the induction time becomes independent of D_0 . In reality, however, factors which affect D_0 will affect the induction time indirectly through their influence on the friction coefficient f. For example, a less compact polymer structure would produce a smaller value of f, the mobility of the polymer chain, as well as that of the penetrant, is less restricted, and consequently induction time is shorter while D_0 is higher. Therefore, the applicability of Equation (3.5) due to Rossi, Pincus and de Gennes is limited because the specimen size in most experiments cannot be treated as semi-infinite and the fact that the induction time is affected by the penetrant diffusivity D_0 .

To overcome this drawback, more accurate expressions, Equations (3.8), (3.10) and (12), are derived for samples with finite geometries. Here, the induction time-front penetration rate relationship depends on both the size and geometry of the sample. Again, Equations (3.8), (3.10) and (3.12) hold only when $\frac{D_0 t}{a_0^2}$ is large.

From the phenomenological definition of induction time, a reciprocal relationship between the induction time and initial front penetration rate can be easily deduced from individual penetration curves for specimens of finite sizes (see Chapter 2):

$$\tau_0 = \frac{a_0 A}{v_0} \tag{3.14}$$

where a_0 is either the radius of a sphere or cylinder, or the half thickness of the slab, A is the extrapolated normalized penetration. The value of A depends on the geometry of the sample as is clearly seen from Equations (3.8), (3.10) and (3.12). It has been experimentally demonstrated that A may be independent of the sample size (see Chapter 2). The relationship expressed in Equation (3.14) cannot be reduced to a simpler form. It may be considered as a simpler alternative expression for Equations (3.8), (3.10) and (3.12) in the small dimension range as clearly suggested by a comparison of Equations (3.12) and (3.14) with experimental results shown in Figure 3.4.

The expression for the front penetration rate in Equation (3.2) can also be incorporated to Equations (3.8), (3.10) and (3.12) to predict the effect of sample size and geometry on induction time.

3.3.2 Boundary Condition

The boundary condition is a manifestation of the interaction between the polymer and the penetrant. It can be characterized by the surface concentration or flux of the penetrant at the surface, both of these are generally time-dependent. Experimentally, it has been established that during Case II sorption, the surface concentration of the penetrant will not reach the equilibrium concentration instantaneously (Hui *et al.*, 1987a, b; Lasky *et*

al., 1988; Umezawa *et al.*, 1992). Therefore, a constant surface concentration is not a realistic assumption during the induction period.

When a non-porous glassy polymer is in contact with a non-solvent penetrant, a concentration gradient of the penetrant will be present in the polymer as a result of the diffusion of penetrant into the polymer. Contrary to the prediction of Fick's law, the initial influx of the penetrant into the polymer can be finite, despite the fact that the concentration gradient is infinitely large initially. This suppression of initial influx is closely related to the nature of the glassy polymer. *First of all*, the surface concentration of penetrant reaches the equilibrium concentration in an incremental rather than instantaneous manner, due to the viscoelastic behavior of the polymer, which is also true for the concentration change in the interior of the polymer (Long and Richman, 1960; Shankar, 1982). *Secondly*, a compressive hydrostatic stress exists in the swollen shell as a requirement of geometric compatibility due to constraint of the rigid unswollen core (Klier and Peppas, 1987). In this case, the penetrant influx will be reduced because of the concomitant reduction of both diffusion coefficient and equilibrium concentration of the penetrant caused by the compressive stress (Fahmay and Hurt, 1980; Larché and Cahn, 1982; Neumann and Marom, 1987). *Thirdly*, a stress gradient is generated due to differential swelling of the polymer adjacent to the surface or the moving front. The stress gradient, which relates to the concentration gradient of the penetrant, will produce a flux in a direction opposite to that of the flux due to concentration gradient (Kim *et al.*, 1996). When the swollen polymer is relatively rigid, and neither mechanical failure nor significant structural damage is produced by the osmotic pressure generated by the

concentration gradient, a flux with a finite magnitude should be expected throughout the diffusion process. As a consequence, Case II sorption can be effectively regarded as a pseudo-steady state transport once the front is established (Gall *et al,* 1990)

The response of stress to the gradual and rapid change of concentration is viscoelastic, which can be represented by (Hayes and Cohen, 1992):

$$\frac{\partial \sigma}{\partial t} + \beta\sigma = a\frac{\partial c}{\partial t} + bc \tag{3.15}$$

where a and b are constants, and β, the inverse of the relaxation time, is a function of the penetrant concentration.

The diffusion of penetrant in a glassy polymer is governed by (Wilson and Aifantis, 1982; Neogi, 1993):

$$J = -D(c,\sigma)\left(1 - E(c)\frac{\partial \sigma}{\partial c}\right)\frac{\partial c}{\partial x} \tag{3.16}$$

where E(c) is a phenomenological coefficient correlating the effect of stress gradient; $D(c,\sigma) = D(c) + F\sigma$ is the global diffusion coefficient; F is a phenomenological coefficient correlating the effect of hydrostatic stress σ on the global diffusion coefficient; $D(c)$ is the concentration dependent component of the diffusion coefficient expressed as (Witelski, 1996):

$$D(c) = \frac{1+\varepsilon}{2\varepsilon} + \frac{1-\varepsilon}{2\varepsilon}\tanh\left(\frac{c - c_p}{\delta}\right) \tag{3.17}$$

Here, $0<\varepsilon \ll 1$, is a small parameter corresponding to the large diffusivity of the polymer in the plasticized state; $c_p < c_e$, is the critical penetrant concentration marking the position

of plasticization front; δ is the thickness of the plasticizing zone. The contribution of stress gradient is related to the concentration gradient by (Neogi, 1993):

$$E(c)\frac{\partial \sigma}{\partial c} = \frac{VE}{3\rho RT}c \tag{3.18}$$

where V is the specific molar volume of the penetrant; E is the modulus of elasticity; ρ is the density of polymer-penetrant mixture.

From Equations (3.15) and (3.17), it is reasonable to expect that the initial penetrant flux into the glassy polymer will be limited to a finite value, due to the coupling of diffusion and differential swelling stress in the polymer. As governed by the kinetics of plasticization, the initial flux of the penetrant at the polymer surface during the induction period will not exceed $v_0 c_p$, (Rossi, Pincus and de Gennes, 1995).

At the polymer surface, combination of Equations (3.16) and (3.18) provides a quantitative criterion for the occurrence of Case II sorption:

$$1 = \frac{VE}{3\rho RT}c_p \tag{3.19}$$

since $v_0 c_p = 0$. The calculated values of this dimensionless parameter are shown in Table 3.1.

Table 3.1 The Evaluation of Equation (3. 19)

Polymer + Penetrant	V (m^3/mol)	E (GPa)	ρ (kg/m^3)	c_p (kg/m^3)	$\frac{VE}{3\rho RT}c_p$
PMMA + MeOH	4.07E-05	2.75	1109.32	157.32	2.13254
PMMA + EtOH	5.84E-05	2.75	1109.8	157.8	3.082621
PMMA + PrOH	7.5E-05	2.75	1112.32	160.32	4.013608
PMMA + BuOH	9.15E-05	2.75	1114	162	4.939647
PS + Hexanes	0.000131	3.34	975	131.8	7.984373
Nylon + MeOH	4.07E-05	1.9	1069.32	157.32	1.82241
Natural rubber + MeOH	4.07E-05	1.05E-04	0.88532	157.32	0.000126

The volume fraction of the penetrant was assumed to be 0.2 for all penetrant/ polymer pairs in the calculation of c_p. The magnitude of this dimensionless parameter for glassy polymer is close to 1, rather than exactly equal to 1, since approximate values of the parameters were used in the calculation. Better agreement might be achieved when the exact values of the parameters are used in the evaluation. Since the magnitude of the dimensionless parameter for natural rubber is significantly lower than those of the glassy polymers, this demonstrates that the criterion may be useful in excluding system which does not exhibit Case II behavior.

Based on generalized surface resistance conditions, Lee and Kim (1992) showed that solutions to the associated moving boundary diffusion problem predict accurately the sample geometry effect on Case II front movement. Such size and geometry dependence is also expected to affect the induction time as illustrated above. The constant flux boundary condition approximation is employed because it is a special case of the more general surface resistance boundary condition and provides a useful correlation between induction time and front penetration rate. This boundary condition can be considered as a natural outcome of Case II sorption once the front is established since the transport behavior during front propagation is effectively equivalent to steady state diffusion (Gall *et al.*, 1990).

For a more general solution, one needs to incorporate the stress effect described in Equations (3.15)-(3.18) into the moving boundary diffusion problem and to employ the surface resistance boundary condition. In this case, numerical procedures would be needed to generate appropriate solutions.

3.4 Conclusions

The initial flux of penetrant into a glassy polymer during the induction period is limited to a finite value due to the coupling between diffusion and differential swelling stress in a viscoelastic glassy polymer. Our modeling of Case II sorption suggests that the induction time of Case II sorption depends on the geometry and size of the glassy polymer. This suggests that the induction time should not be considered as a material constant. It has been predicted that the induction time is proportional to the size of the sample in the small size range. This prediction agrees well with our experimental observations. The simple relationship between induction time and penetration rate derived from a molecular theory in the present analysis agrees with the phenomenological results of Rossi, Pincus and de Gennes. Furthermore, a quantitative criterion is proposed for the occurrence of Case II sorption.

Appendix 3A

Derivation of induction time for semi-infinite solid and other finite geometries with small $\frac{D_0 t}{a_0^2}$ and constant surface flux

As dictated by the kinetics of plasticization, the penetrant flux at the polymer surface (x=0) during the induction period may not exceed $v_0 c_p$, where v_0 is the front penetration rate in an initially dry glassy polymer (Rossi, Pincus and de Gennes, 1995).

$$-D_0 \frac{\partial c}{\partial x} = J(0,t) \leq v_0 c_p \qquad \text{(A1)}$$

The surface flux is assumed to be no larger than $v_0 c_p$ during the induction period. Fick's first law and second law state that

$$J(x,t) = -D_0 \frac{\partial c}{\partial x} \tag{A2}$$

$$\frac{\partial J(x,t)}{\partial x} = \frac{\partial c}{\partial t} \tag{A3}$$

and consequently $J(x,t)$ satisfies the same differential equation as $c(x,t)$

$$\frac{\partial J(x,t)}{\partial t} = -D_0 \frac{\partial^2 J(x,t)}{\partial^2 x} \tag{A4}$$

since

$$\frac{\partial J(x,t)}{\partial t} = -D_0 \frac{\partial^2 c}{\partial x \partial t} = -D_0 \frac{\partial^2 J(x,t)}{\partial^2 x} \tag{A5}$$

For semi-infinite solid, the solution of $J(x,t)$ with $J(0,t) < v_0 c_p$ is similar to the solution of $c(x,t)$

$$J(x,t) \le v_0 c_p \, erfc \frac{x}{2\sqrt{D_0 t}} \tag{A6}$$

From (1)

$$c(x,t) \le \frac{v_0 c_p}{D_0} \int_x^\infty erfc \frac{x}{2\sqrt{D_0 t}} dx = 2 v_0 c_p \sqrt{\frac{t}{D_0}} ierfc \frac{x}{2\sqrt{D_0 t}}$$

or
$$c(x,t) \le 2 v_0 c_p \sqrt{\frac{t}{D_0}} \left(\frac{1}{\sqrt{\pi}} e^{\frac{x^2}{4 D_0 t}} - \frac{x}{2\sqrt{D_0 t}} erfc \frac{x}{2\sqrt{D_0 t}} \right) \tag{A7}$$

which yields
$$c(0,t) \le 2 v_0 c_p \sqrt{\frac{t}{\pi D_0}} \tag{A8}$$

The induction time τ_0 is defined as the time when $c(0,t) = c_p$

$$\tau_0 \geq \frac{\pi D_0}{4 v_0^2} \tag{A9}$$

The solutions at small $\frac{D_0 t}{a_0^2}$ for large slabs and infinite cylinders are respectively (Carslaw and Jaeger, 1959b, Crank, 1975b):

slabs: $$c(x,t) \geq 2 v_0 c_p \sqrt{\frac{t}{D_0}} \sum_0^{\infty} \left(ierfc \frac{(2n+1)a - x}{2\sqrt{D_0 t}} + ierfc \frac{(2n+1)a + x}{2\sqrt{D_0 t}} \right)$$

cylinders: $$c(x,t) \geq \frac{v_0 c_p}{D_0} \left(2 \left(\frac{D_0 a t}{r} \right)^{\frac{1}{2}} ierfc \frac{a - x}{2\sqrt{D_0 t}} + \frac{D_0 t (a + 3r)}{2 a^{\frac{1}{2}} r^{\frac{3}{2}}} i^2 erfc \frac{a - x}{2\sqrt{D_0 t}} \right)$$

These result in the same equation for induction time (A9) as that of the semi-infinite solid at $c(0,t) = c_p$.

Appendix 3B

Induction time for semi-infinite solid with a surface resistance boundary condition

During the induction period, the surface penetrant flux can be expressed as (Lee and Kim, 1992):

$$-D_0 \frac{\partial c}{\partial x}(0,t) = J(0,t) = k(c_\infty - c_s) \tag{B1}$$

The solutions for small and large value of time are treated differently.

3B1 Small time solution

The concentration distribution under this boundary condition is (Crank, 1975d)

$$\frac{c(x,t)}{c_\infty} = erfc\frac{x}{2\sqrt{D_0 t}} - \exp(hx + h^2 D_0 t)erfc\left[\frac{x}{2\sqrt{D_0 t}} + h\sqrt{D_0 t}\right] \qquad \text{(B2)}$$

where $h=k/D_0$

at the surface $\frac{c_s}{c_\infty} = \frac{c(0,t)}{c_\infty} = erfc(0) - \exp(h^2 D_0 t)erfc\left[h\sqrt{D_0 t}\right]$ (B3)

The induction time τ_0 is defined as the time when $c_\infty = c_s$

This yields $1 = 1 - (1 + h^2 D_0 \tau_0)\left[1 - \frac{2}{\sqrt{\pi}} h\sqrt{D_0 \tau_0}\right]$ (B4)

or $1 - 2h\sqrt{\frac{D_0 \tau_0}{\pi}} = 0$ (B5)

and $\tau_0 = \frac{\pi}{4h^2 D_0} = \frac{\pi D_0}{4k^2}$ (B6)

The same equation can also be derived from the small time solution for the slab and cylindrical geometry under the same boundary condition (Crank, 1975e; 1975f).

3B2 Large time solution

The solution at large time is given by (Carslaw and Jaeger, 1959c)

$$\frac{c_s}{c_\infty} = \frac{1}{h\sqrt{\pi D_0 t}}\left[1 - \frac{1}{2h^2 D_0 t} + \frac{3}{4h^4 D_0^2 t^2} - \cdots\right] \qquad \text{(B7)}$$

The induction time τ_0 is also defined as the time when $c_\infty = c_s$

This gives $1 = \frac{1}{h\sqrt{\pi D_0 \tau_0}}$ (B8)

or $\tau_0 = \frac{D_0}{\pi k^2}$ (B9)

Chapter 4

Elucidation of the Cause of the Observed Size Effect in Case II Sorption

4.1 Introduction

The first and foremost feature of Case II sorption is the constant inward movement of the fluid penetration front after a glassy polymer is immersed in a non-dissolving liquid penetrant. Before the onset of Case II behavior, the surface concentration will evolve slowly to a threshold concentration. The induction time is defined as the time necessary for the polymer surface to reach this critical concentration.

Essential to various theories developed to describe Case II sorption, the behavior of Case II sorption has been considered as a material property independent of sample size and geometry. Consequently, both the induction time and front penetration rate were solely treated as material properties of the polymer. The validity of such assumptions was supported by experimental observations based on samples of thick slab geometry or thin films with similar thicknesses (Thomas and Windle, 1978, 1981,1982; Windle, 1985; Hui *et al*, 1987a, 1987b; Lasky *et al.*, 1988a, 1988b; Papanu *et al.*, 1990).

Our recent experimental results, however, showed a positive correlation of induction time with bead diameter (0.2-1.5 mm) for the penetration of methanol into PMMA beads, and the induction time is inversely proportional to penetration rate (see Chapter 2). This phenomenon is not predicted by current theories of Case II sorption.

Various mechanistic interpretations can, therefore, be proposed as possible as the basis of alternative models of Case II sorption. To investigate the underlying mechanisms for this size dependence and to verify the physical basis for our newly developed model (see Chapter 3), an experimental approach is necessary.

In the present work, experiments were carried out to verify that the size effect is not caused by differences in surface morphology, molecular weight and its distribution, heterogeneity of the beads, and differential swelling stress in the polymer. Samples with different geometries and chemical composition were also tested to examine the generality of this size effect. The disappearance of this size effect in cylindrical discs and slabs with dimension comparable to that of the beads in the front penetration direction can be explained by a new model developed by Li and Lee (see Chapter 3).

4.2 Experimental

4.2.1 Materials

The synthesis of PMMA (polymethyl methacrylate) beads and their purification in methanol have been described in details elsewhere (Lee, 1993). Free radical suspension polymerization of freshly distilled methyl methacrylate was employed to prepare PMMA beads at 70°C for 3 hr. with t-butyl peroxy-2-ethylhexanoate as the initiator and freshly precipitated $Mg(OH)_2$ as the suspending agent. EGDMA (ethyleneglycol dimethacrylate) was used as crosslinking agent to prepare crosslinked PMMA beads. After polymerization was completed, concentrated HCl was added to remove the suspending agent. The beads obtained by filtration were then extracted in a Soxhlet with methanol before being dried to

a constant weight in a vacuum oven, typically at 70-80°C for 3-5 days. Based on the intrinsic viscosity measurement in acetone obtained on a Ubbelohde viscometer, the average molecular weight of the PMMA beads was estimated to be about 5.2×10^5 according to the Mark Houwink equation.

The PS (polystyrene) beads were obtained from Polyscience. (MW 125,000 - 250,000). PMMA sheets were obtained as Plexiglas from Rohm-Haas and cut into slabs.

4.2.2 Sample Treatment

The heat treatment of PMMA and PS beads was performed on a Perkin-Elmer DSC-2. The beads were heated to 130°C at 320°C/min and kept at 130°C for three hours under nitrogen gas purge, then cooled down slowly to room temperature at 5°C/min.

All Plexiglas slabs were annealed at 130°C for 3 hrs before each penetration test, then cooled down at 0.5°C/min through the glass transition temperature. The penetration test was done at ambient temperature (25°C). Extraction of impurities was done in the Soxhlet extraction apparatus following the penetration test. Desorption of methanol from the extracted slabs was conducted in the fumehood.

4.2.3 Swelling Test

The penetration of methanol into crosslinked PMMA beads was performed in a sealed quartz cuvette at room temperature (25°C) and observed with a Wild M420 polarized light stereomicroscope equipped with a digital optical measuring accessory (Wild MMS235; accurate to ±0.001mm).

For polystyrene beads, n-hexane (99% of n-hexane, Sigma Chemical Co.), was employed as penetrant with experiments conducted at room temperature (25°C). The number of beads tested was about 50.

4.2.4 Dissolution Test

Dissolution of uncrosslinked PMMA beads in acetone and acetic acid was conducted at 25°C in a quartz cuvette. All solvents used were reagent grade. The diameter of the undissolved beads was measured by the stereomicroscope equipped with a digital optical measuring accessory (Wild MMS235; accurate to ±0.001mm).

4.2.5 SEM and AFM Observation

Polymer beads were sputter-coated with gold for SEM (scanning electron microscopy) observation. AFM (atomic force microscopy) images of the polymer beads were obtained from Nanoscope III at ambient environment. All images were taken from the top position of the beads.

4.3 Results and Discussion

4.3.1 Effect of Molecular Weight

The individual dissolution profiles of uncrosslinked PMMA beads in acetone and acetic acid are shown in Figure 4.1. The dissolution of PMMA beads in those two solvents started immediately once the beads were immersed in the solvents. No swelling or penetration front was observed in PMMA beads during dissolution at 25°C. The

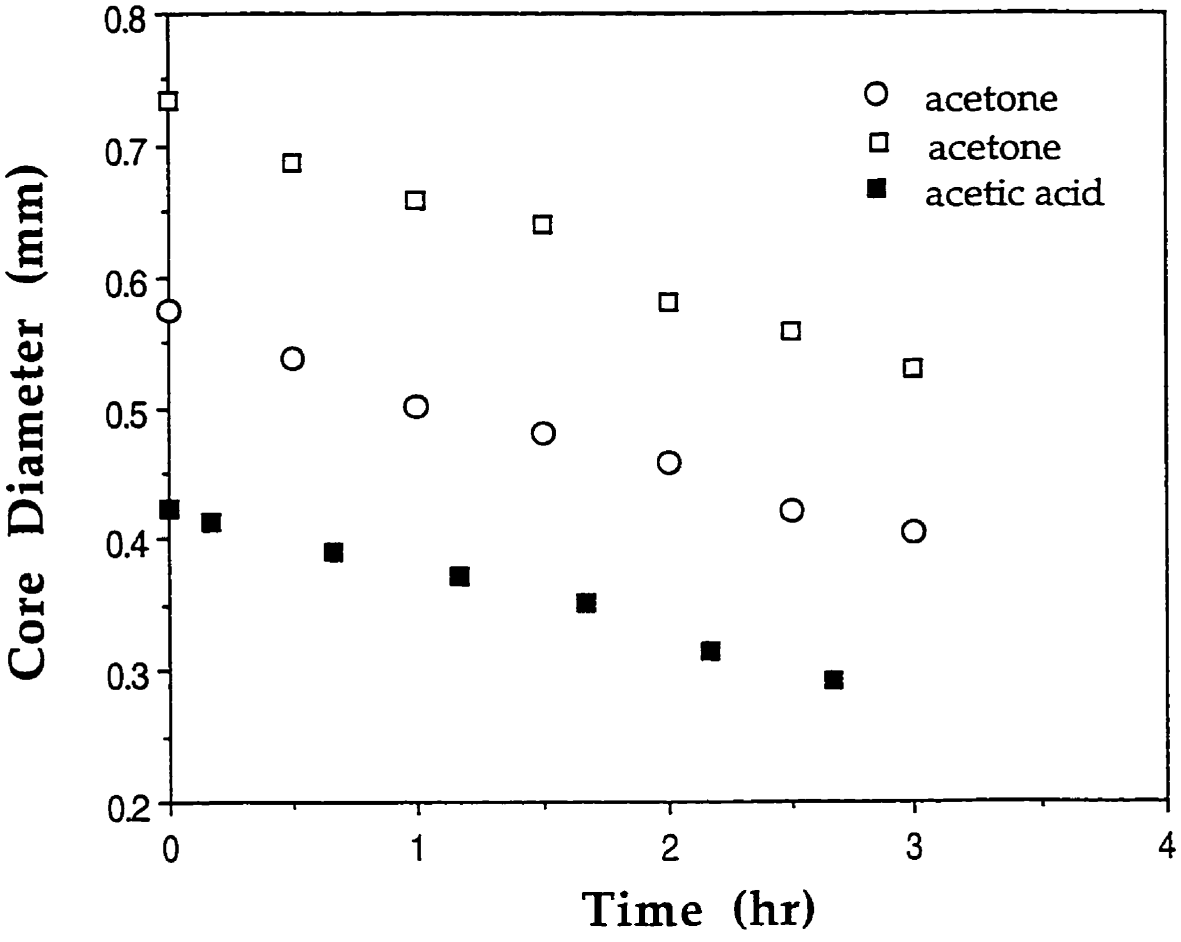

Figure 4.1 Dissolution profiles of uncrosslinked PMMA beads in acetone and acetic acid at 25°C

penetration rate of dissolution front into the center of beads remained constant throughout the dissolution process. Beads of different diameters were tested in the dissolution experiment. As shown in Figure 4.2, the dissolution rate appears to be independent of the bead diameter. This constant dissolution rate, similar to the penetration rate of the swelling front during Case II sorption, may serve as another indirect evidence that there is no detectable effect of spatial distribution of molecular weight within the beads. The beads can be considered uniform for both diffusion and dissolution.

The molecular weight of a crosslinked polymer is considered infinitely high. The swelling of crosslinked polymer in a penetrant can be used to demonstrate if the molecular weight of a polymer has any significant effect on the resulting Case II behavior. The results of methanol penetration in crosslinked PMMA beads are shown in Figures 4.3 and 4.4. The induction time and front penetration rate, and their dependence on the diameter of the crosslinked beads are essentially identical to the results of uncrosslinked beads under identical conditions.

Data collected so far indicates that the effect of molecular weight on induction time and penetration rate is not significant within the limit of our tests. It is therefore reasonable to conclude that the possible difference in the molecular weight distribution in beads with different sizes is not likely to be the cause for the observed size effect.

4.3.2 No Effect of Morphological Differences

SEM and Atomic Force Microscopy (AFM) were used to examine the correlation between surface morphology of the bead and disc samples in order to detect any

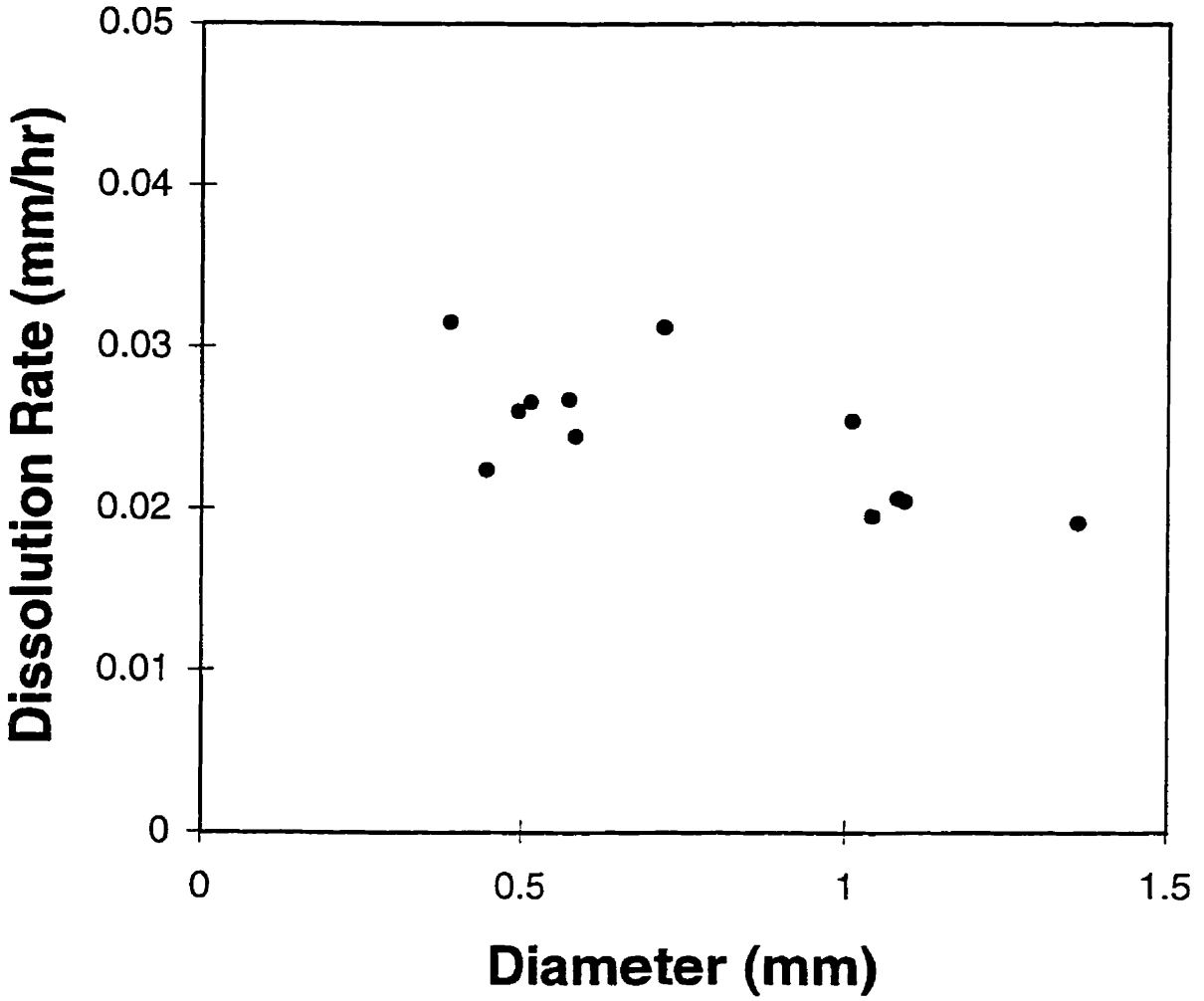

Figure 4.2 Effect of the diameter of PMMA beads on dissolution rate in acetone at 25°C

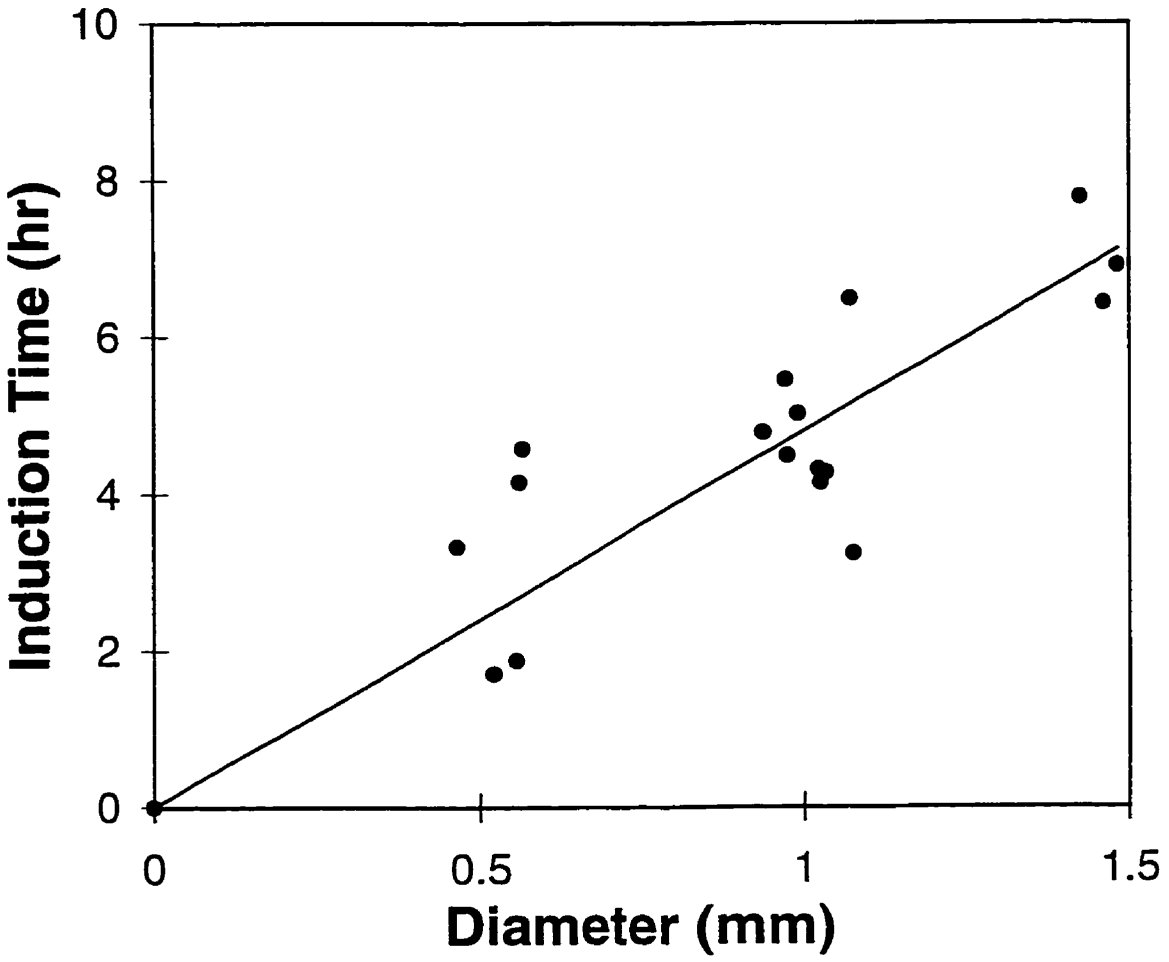

Figure 4.3 Size effect on induction time for methanol sorption in crosslinked PMMA beads at 25°C. The crosslinked PMMA beads were annealed at 130°C and cooled to room temperature at 5°C/min

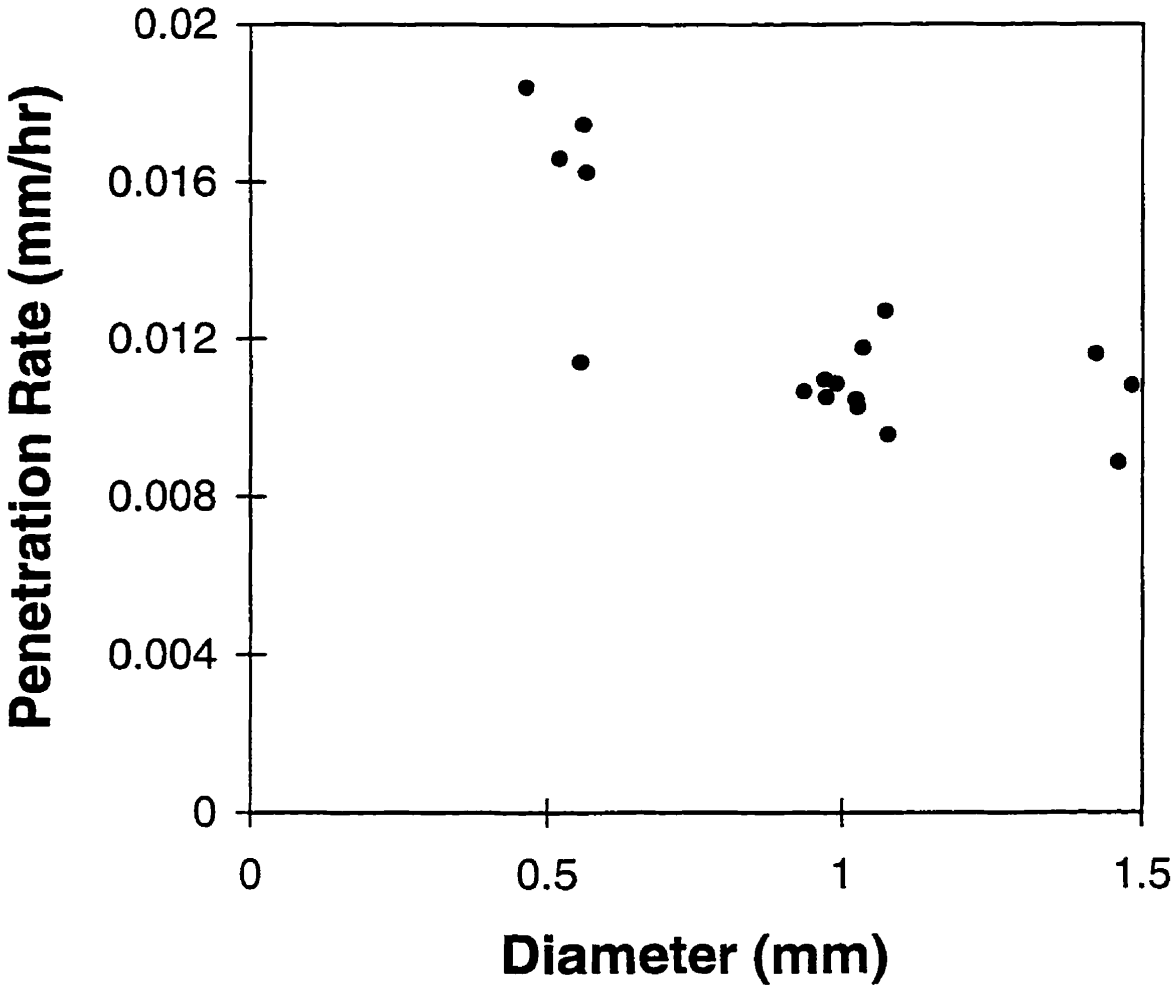

Figure 4.4 Size effect on methanol penetration rate in crosslinked PMMA beads at 25°C. The crosslinked PMMA beads were annealed at 130°C and cooled to room temperature at 5°C/min

correlation with their penetration behavior.

SEM images show that voids were observed on the surface of PMMA beads without heat treatment. The size and number of these voids were reduced after annealing above the glass transition temperature of the polymer as shown in Figures 4.5 and 4.6. This helps to explain the observation that heat treatment increases the induction time while reducing the front penetration rate. Furthermore, the size and the number of voids do not vary significantly with the diameter of the beads. This implies that the size effect is not due to morphological differences among beads with different sizes. Therefore, SEM can be employed to establish the effect of heat treatment on the density, and size of voids on the surface of these beads.

On the other hand. AFM enables the direct observation of swollen polymer surface without the influence of vacuum as encountered in SEM. The surface morphology of swollen beads and slabs was also compared with that of the dehydrated ones using AFM. It was observed that the size of the voids increased in the swollen states as shown in Figures 4.7 and 4.8.

4.3.3 Effect of Polymer Composition

To further explore the generality of the size effect, penetration test was conducted in polystyrene (PS) beads immersed in n-hexane, another system exhibiting typical Case II behavior. The results are summarized in Figures 4.9 and 4.10. The induction time of n-hexane in PS beads increased with increasing bead diameter, with a much stronger dependence on size as compared with that of PMMA. The penetration rate of n-hexane in

Figure 4.5 Surface characteristics of a PMMA bead before annealing, as observed under SEM

Figure 4.6 Surface characteristics of a PMMA bead after annealing above the glass transition temperature of the polymer, as observed under SEM

Figure 4.7 The surface morphology of a dry PMMA bead observed under AFM

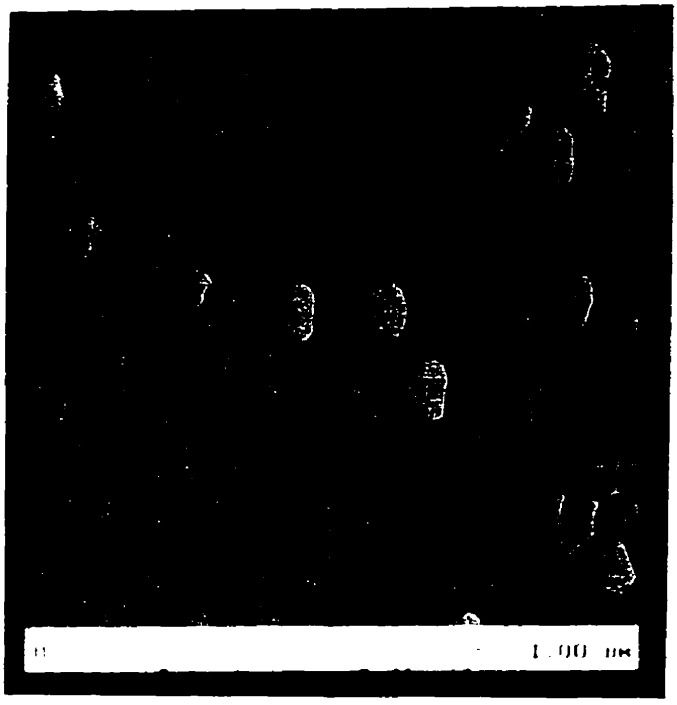

Figure 4.8 The surface morphology of a swollen bead observed under AFM

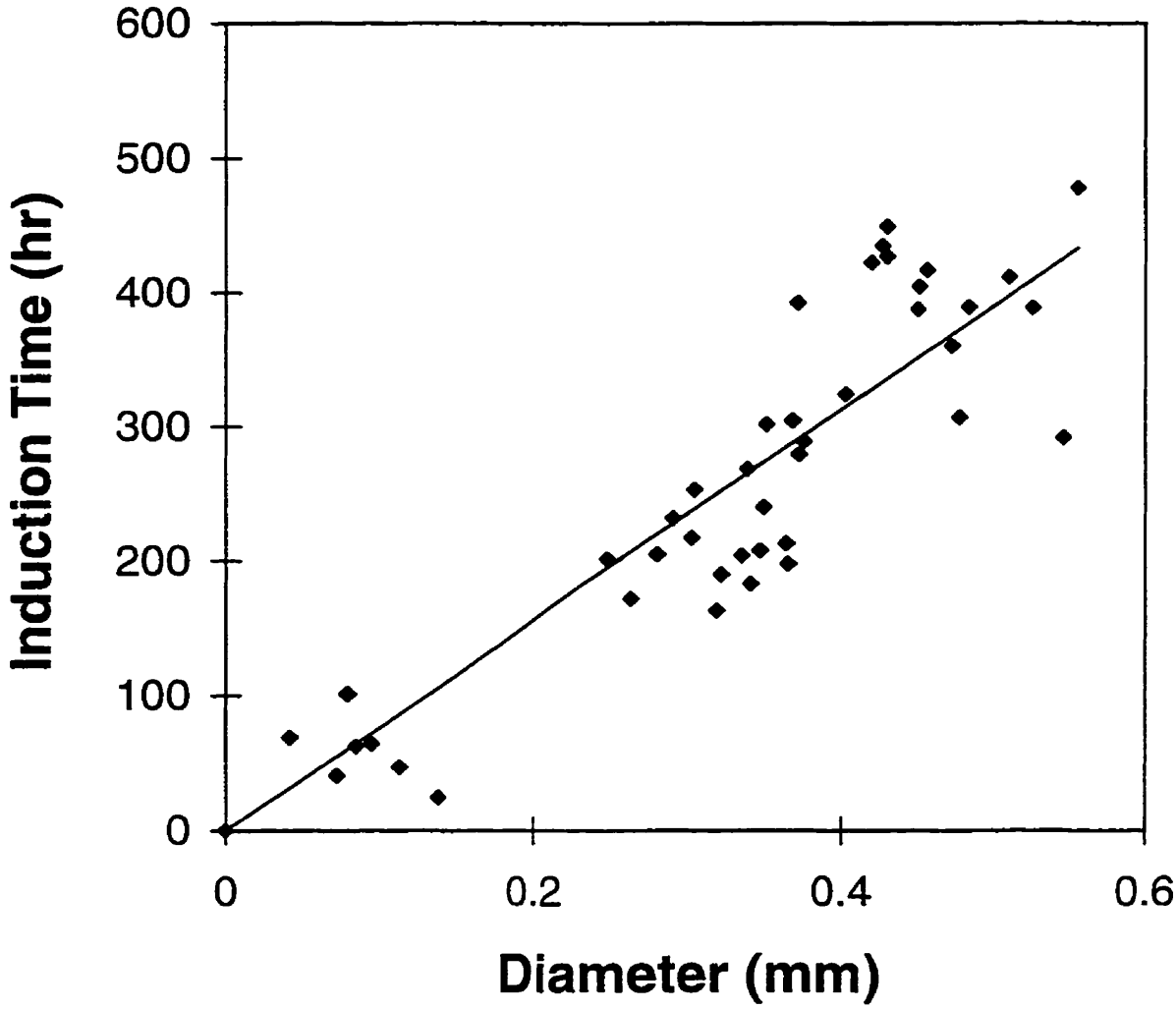

Figure 4.9 Size effect on induction time for n-hexane sorption in uncrosslinked PS beads at 25°C. The uncrosslinked PS beads were annealed at 130°C and cooled to room temperature at 5°C/min

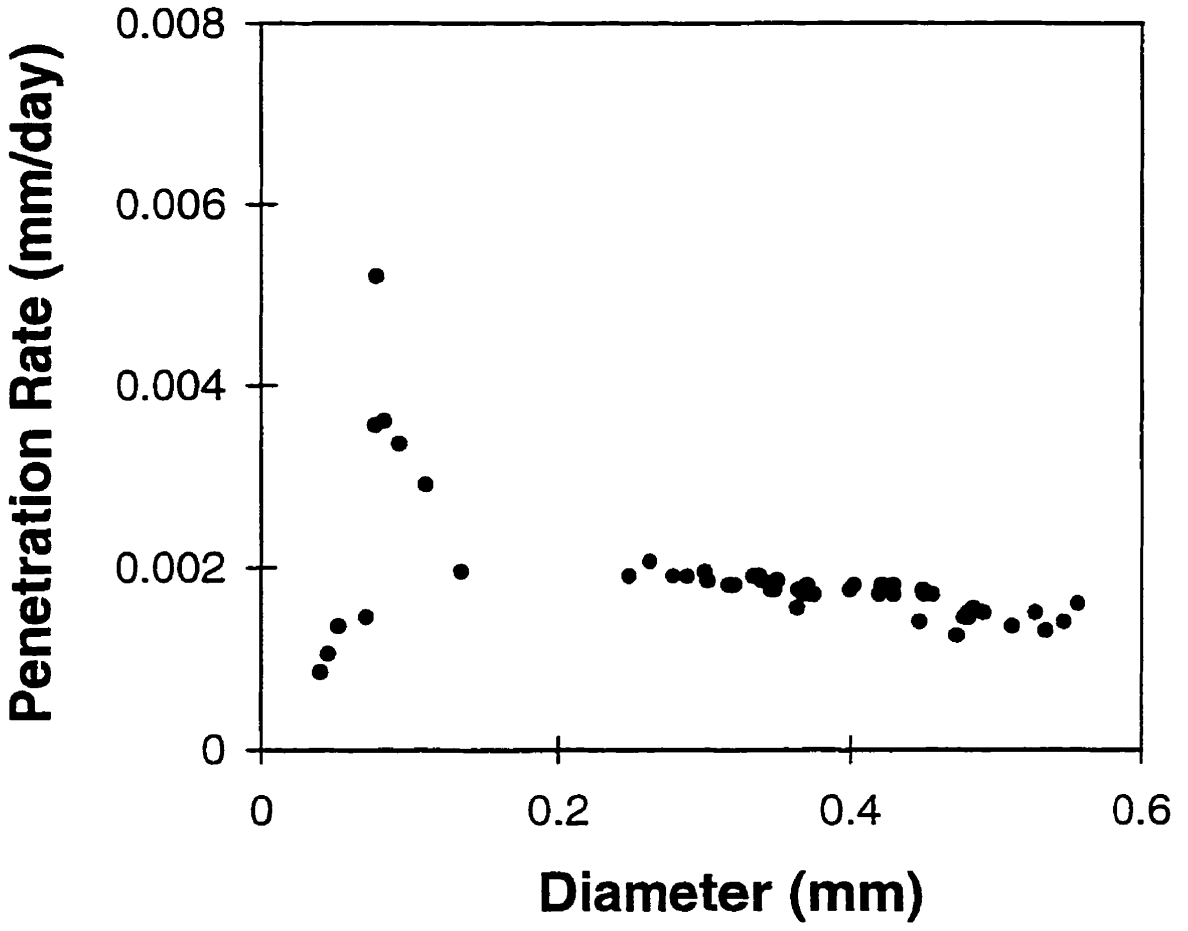

Figure 4.10 Size effect on n-hexane penetration rate in uncrosslinked PS beads at 25°C. The uncrosslinked PS beads were annealed at 130°C and cooled to room temperature at 5°C/min

PS beads did not seem to depend on the diameter of the PS beads.

The penetration of water or methanol in PHEMA beads does not exhibit typical Case II behavior (Lee and Kim. 1992). It is conceivable that the size effect is not merely caused by sample geometry.

4.3.4 Effect of Geometry

Experiments were conducted to determine whether the size effect occurred in beads would occur in cylindrical or slab samples.

The samples used in the test included cylindrical Plexiglas discs of the same thickness with different diameters, Plexiglas slabs and Acrylite slabs with different thickness (same area). As are shown in Figure 4.11 and 4.12, the experimental results did not show a significant dependence of induction time on disc diameter or thickness of the samples. This indicates that the induction time for slab and cylindrical geometry approaches that of the semi-infinite geometry more than that of the spherical geometry. The size effect is thus insignificant when the dimension of slab or cylinder is comparable to that of the spherical beads in the penetration direction.

In the present study, discs with different diameters (3-11 mm) were machined from the same sheet. There is a possibility that even the smallest diameter of the disk is still large when compared with its thickness (1 mm), as a result the discs all behave like infinitely large discs. Therefore, the diameter of the disc does not affect induction time. This also suggests that the effect of the differential swelling stress on penetration rate may not be dominant in this case.

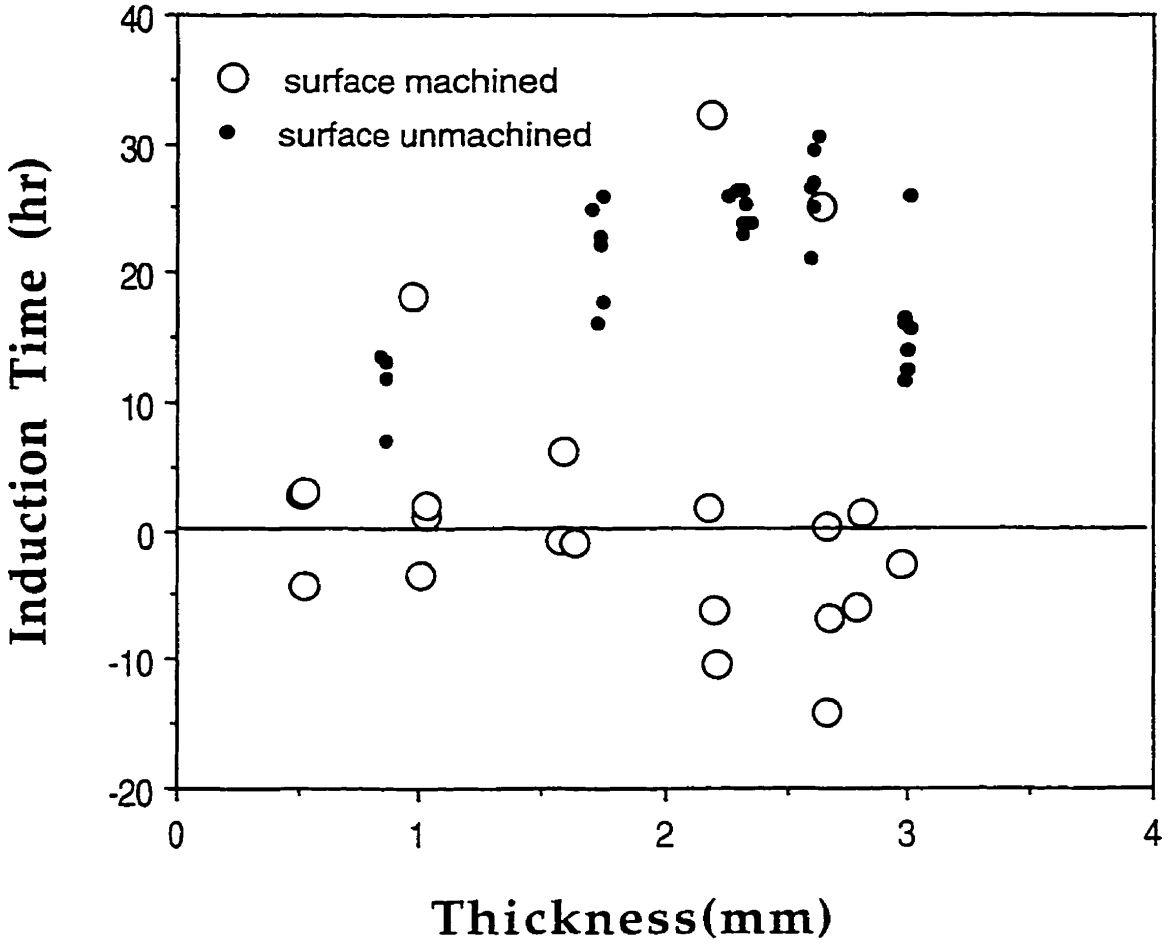

Figure 4.11 Size effect on induction time for methanol sorption in Plexiglas slabs at 25°C. The Plexiglas slabs were annealed at 130°C and cooled to room temperature at 5°C/min

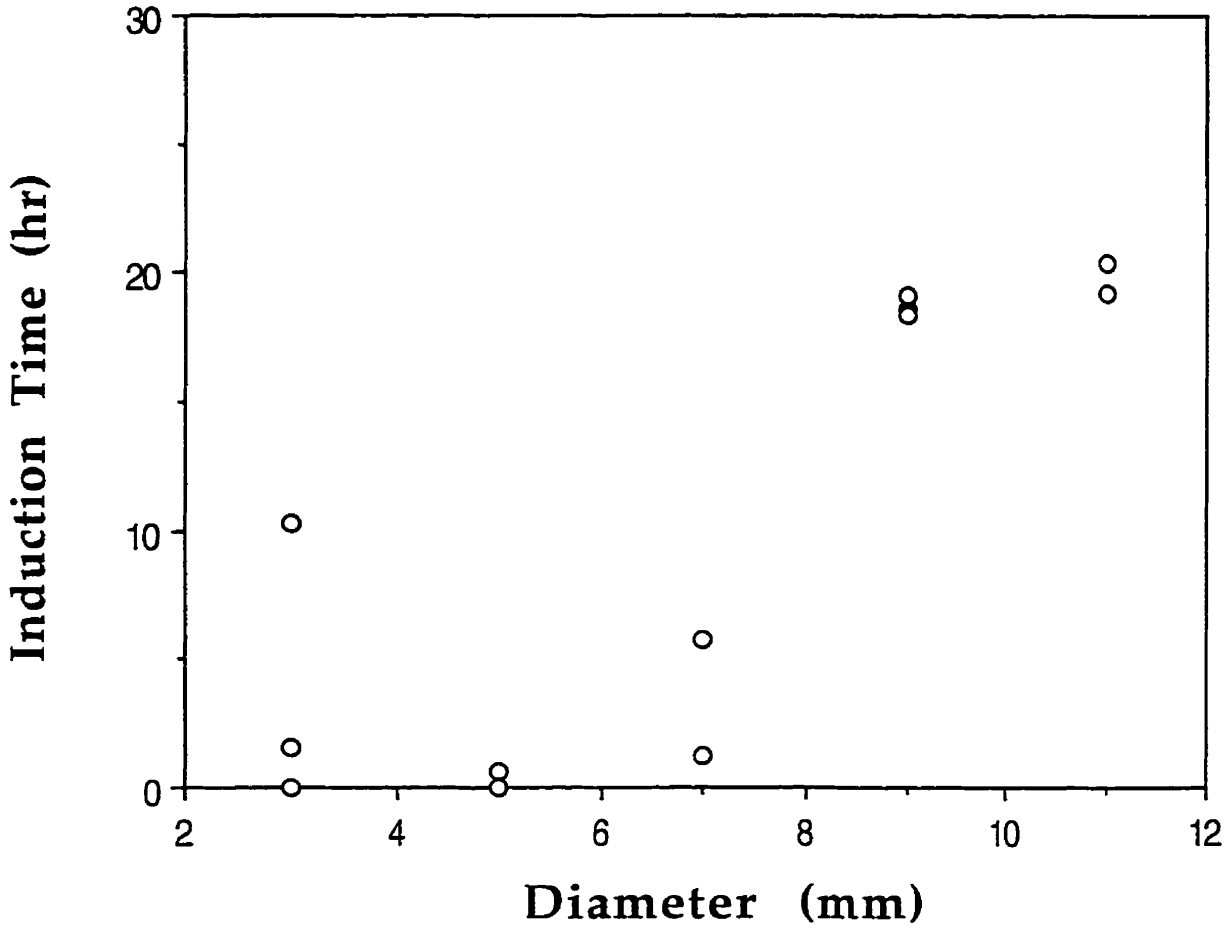

Figure 4.12 Size effect on induction time for methanol sorption in Plexiglas discs with a thickness of 1.0 mm at 25°C. The Plexiglas discs were annealed at 130°C and cooled to room temperature at 5°C/min

During Plexiglas sample preparation, one side of the slab was machined to change the thickness of the slab. The roughness of the machined surface and the associated deformation due to machining showed no apparent effect on either induction time or penetration rate as compared with the penetration from unmachined smooth surface.

4.3.5 Effect of Extractables

To further verify whether there is a size dependence in slab geometry, experiment was conducted to test if such a dependence can be revealed by reducing the scattering of sorption data through purification of the Plexiglas slabs. Methanol penetration test was performed before and after the purification. The results are shown in Figure 4.13 and 4.14.

The Plexiglas slabs were extracted extensively in methanol in a Soxhlet. The extract was concentrated by evaporation and the components were then separated by TLC. UV and IR spectra were obtained for the extractable components. It appears that the extract consists of long carbon chain esters.

The front penetration rate of the extracted slabs in methanol was lower than that of the unextracted ones with a reduced data scattering. However, no obvious dependence of penetration rate on slab thickness was observed. In addition, negative values of induction time were obtained from extrapolation of some of the experimental data, which is not typical of Case II sorption and no obvious dependence of induction time on slab thickness can be discerned. Some Plexiglas slabs were distorted during extraction. Cracks were present on the surface of the Plexiglas slabs after extraction. This may have contributed to the abnormal trend of some measured induction time.

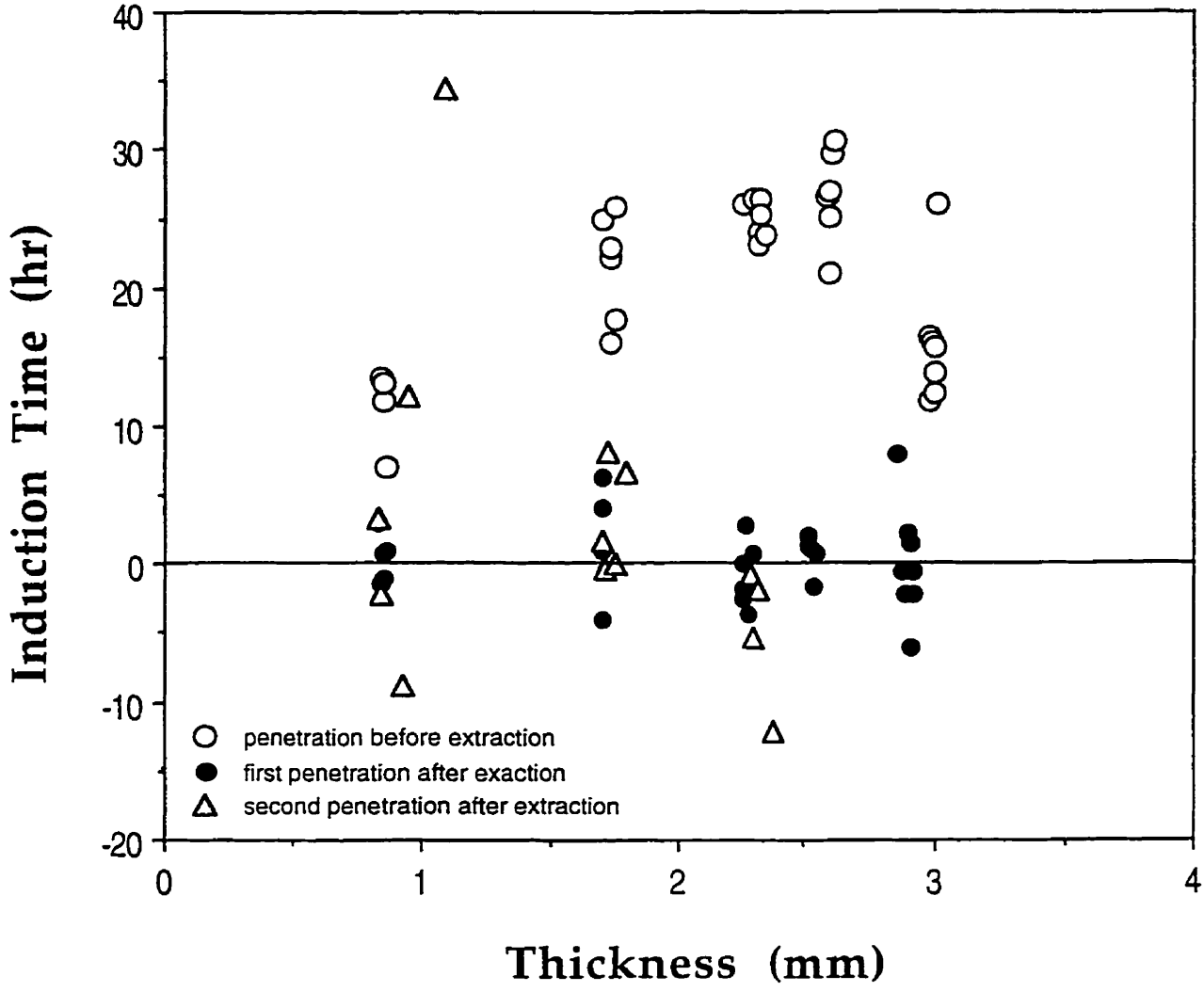

Figure 4.13 Size effect on induction time for methanol sorption in Plexiglas slabs at 25°C. The Plexiglas slabs were annealed at 130°C and cooled to room temperature at 5°C/min

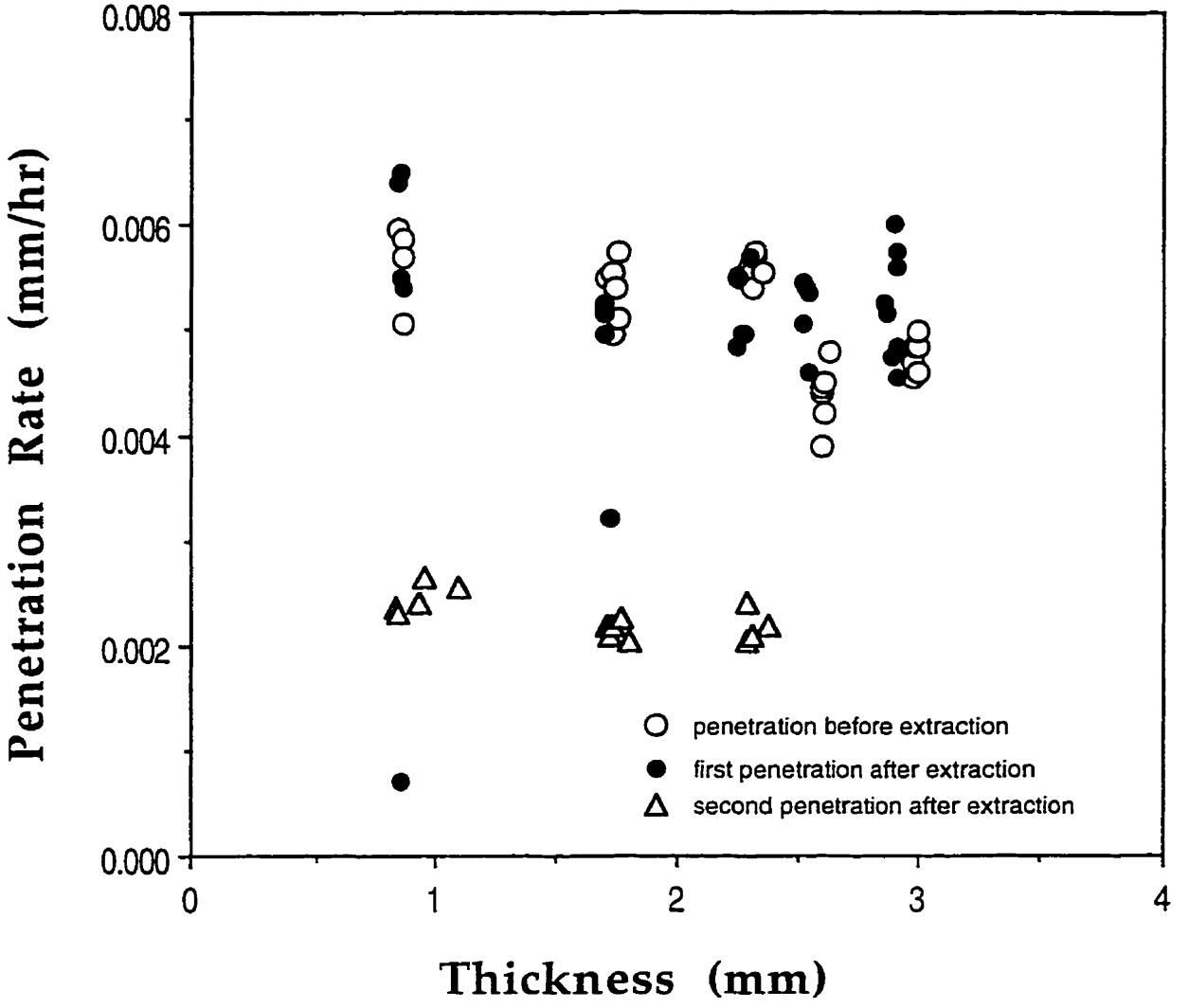

Figure 4.14 Size effect on methanol penetration rate in Plexiglas slabs at 25°C. The Plexiglas slabs were annealed at 130°C and cooled to room temperature at 5°C/min before each penetration test

4.3.6 Effect of Stress Distribution

Fringes due to the distribution of differential swelling stress in swelling spheres could be observed under polarized light like those published in the literature, as is shown in Figure 4.15.

The birefringence in a swelling slab due to differential swelling stress can also be observed under polarized light. This is shown in Figure 4.16. The color is related to the size of the slab and the concentration distribution in the slab. In the later stage of the penetration experiments, the contrast of color of the swollen region to the unswollen region is not obvious. In fact, residual birefringence exists after the disappearance of the unswollen core, indicating that the relationship between stress and strain is not elastic. The color disappears eventually as reorientation and rearrangement in the swollen polymer proceeded.

The partially penetrated slab has a laminate sandwich structure. According to the lamination theory of composites (Tsai and Hahn, 1980), the stress in homogeneous lamina can be considered as uniform. This is supported by the fact that the color of the swollen region is uniform but different from that of the unswollen region when observed under polarized light.

Based on the experimental results of Thomas and Windle (1978; 1980; 1981; 1982,), and the theoretical treatment of Cohn and Marom (1982; 1983), the change of slab sample thickness does not affect the value of the induction time. According to More *et al.* (1992), however, both induction time and penetration rate are stress-dependent. If this were true, a change in sample size will result in the change of differential stress state in a

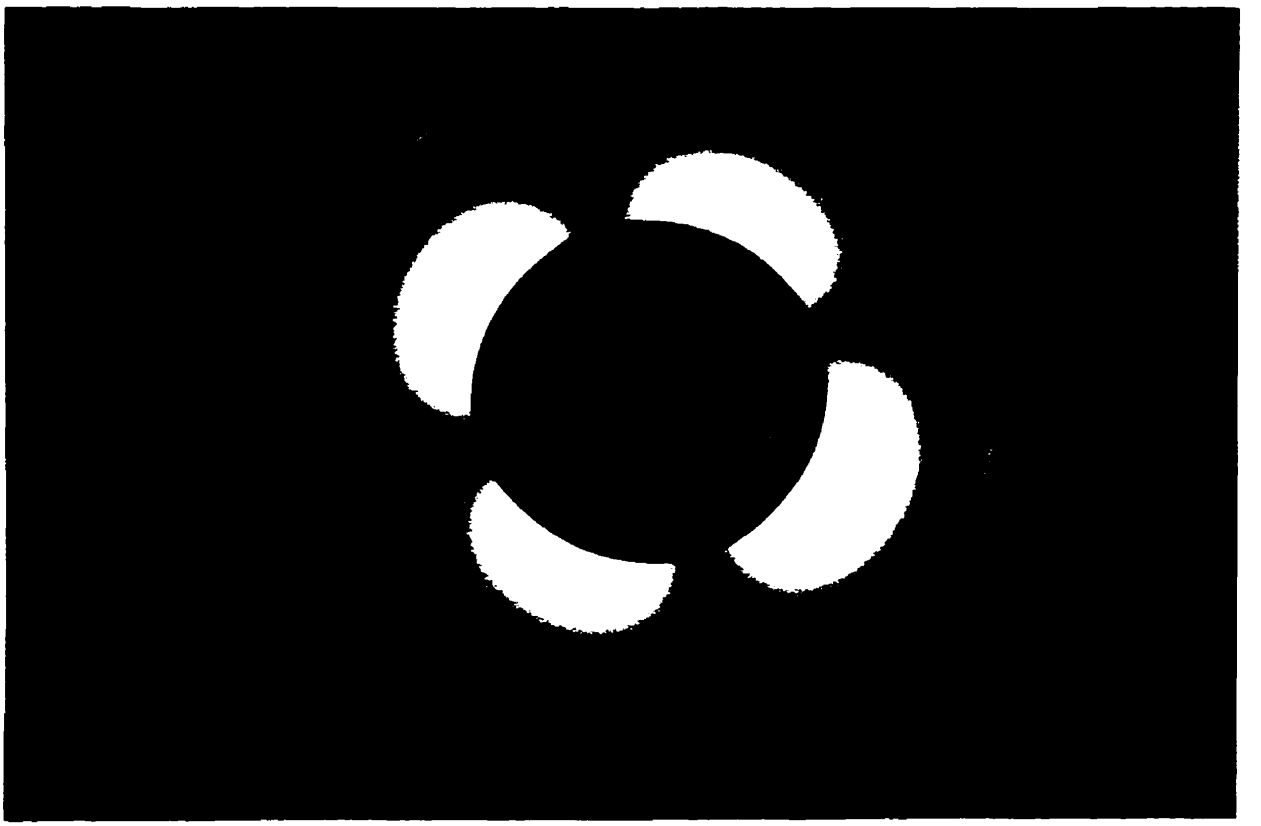

Figure 4.15 Fringes due to the distribution of differential swelling stress in a swelling PMMA bead as observed under polarized light

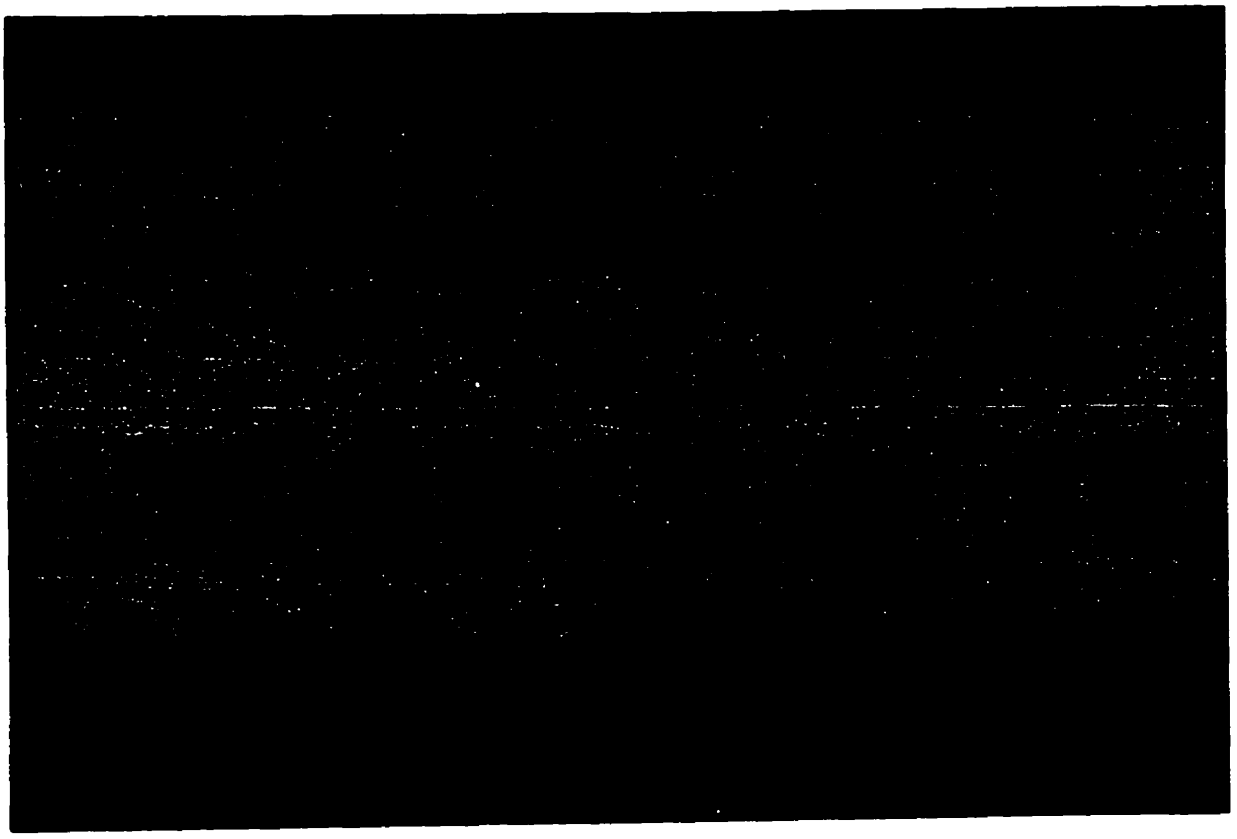

Figure 4.16 The birefringence in a swelling Plexiglas slab due to the distribution of differential swelling stress as observed under polarized light

swelling polymer, consequently, both induction time and penetration rate should show size dependency, However this is not consistent with current experimental observations relating to Case II sorption. Moreover, since the stress distribution changes as the front moves towards the center, and the front penetration rate for beads with various diameters maintains about the same value regardless of the position of the front, it may be reasonable to conclude that the effect of differential swelling stress on the characteristics of Case II sorption may not be significant.

4.4 Conclusions

- The dependence of induction time on bead sample size cannot be attributed to differences in surface morphology since there is no detectable difference in the surface morphology for beads of different diameters, as measured by SEM and AFM.
- This size dependence occurs in bead samples of homogeneous structure as both dissolution and penetration tests suggest that the uncrosslinked beads appear to be uniform. Crosslinked PMMA beads also exhibit typical Case II behavior. In this case, the dependence of induction time on the diameter of crosslinked PMMA beads is identical to that of the uncrosslinked PMMA beads. It is therefore reasonable to assume that the observed size effect is not likely to be sensitive to differences in polymer molecular weight or its distribution.
- The effect of differential swelling stress on the characteristics of Case II sorption may not be significant since the stress distribution changes as the front moves towards the center, while front penetration rate stays at about the same value regardless of the front position and the bead size.

- The size effect on induction time is also determined by sample geometry. The value of induction time for slab and cylindrical geometry approaches that of the semi-infinite geometry more than that of the spherical geometry. Consequently the size effect may become insignificant when the dimension of slab or cylinder is comparable to that of the spherical beads in the penetration direction.
- The presence of extractable impurities in the polymer may facilitate the front propagation. The front penetration rate of the extracted PMMA slabs in methanol was lower than that of the unextracted ones.
- The size effect can also be observed in the penetration of n-hexane in PS beads, which suggests that this size effect is a characteristic of Case II sorption regardless of the chemical composition of the glassy polymer.

Chapter 5

Summary of Conclusions and Suggestions

5.1 Summary of Conclusions

Our results show that the induction time and front penetration rate associated with Case II sorption of methanol in PMMA beads appear to depend on the diameters of the beads, which is not predicted by existing theories. This implies that the characteristic parameters for Case II sorption are not material properties. Consequently, the induction time and penetration rate become dependent on the sample geometry and history; the latter may be well associated with free volume changes. In this case, the induction time increases with decreasing cooling rate, while the dependence of penetration rate on cooling rate follows the opposite trend.

We have derived and experimentally confirmed the phenomenological relationship between induction time and front penetration rate. The induction time and front penetration rate are inversely related by the extrapolated normalized penetration, which appears to be independent on the bead size and cooling rate.

Our results also show that the volume swelling ratio in the swollen region of the bead remains constant during the propagation of the penetration front. This offers additional supporting evidence for the uniform concentration distribution in the swollen region during Case II sorption. This volume swelling ratio also shows a slight increase with the swelling temperature. No significant dependence of volume swelling ratio on the molecular size of a homologous series of alcohols was observed.

The effect of differential swelling stress on the characteristics of Case II sorption does not appear to be significant since the stress distribution changes as the front moves towards the center, while front penetration rate and volume swelling ratio maintain about the same value regardless of the spatial position of the front and the size of the bead.

The dependence of induction time on bead size is not caused by differences in surface morphology since there is no detectable differences in surface morphology for PMMA beads of different diameters, as confirmed by SEM and AFM observation.

This size dependence occurs in PMMA beads with homogeneous structure because both dissolution and penetration tests indicate that uncrosslinked beads can be considered uniform throughout. Crosslinked PMMA beads also exhibit typical Case II behavior where the dependence of induction time on the diameter of crosslinked PMMA beads is similar to that of the uncrosslinked PMMA beads. It is also reasonable to conclude that the size effect may not be caused by differences in the molecular weight or its distribution.

The size effect on induction time is determined by sample geometry. The value of induction time for slab and cylindrical geometry approaches that of the semi-infinite geometry more than that of the spherical geometry. Consequently the size effect may become insignificant when the dimension of slab or cylinder is comparable to that of the spherical beads in the penetration direction.

The size effect has also been observed during the penetration of n-hexane in PS beads, which demonstrates that this size effect is a characteristic of Case II sorption, regardless of the chemical composition of the polymer.

The relationship between induction time and penetration derived from a molecular theory agrees with the results of other phenomenological analysis under the imposed constant flux boundary condition. It is also demonstrated that the induction time of Case II sorption depends on the geometry and size of the glassy polymer. Consequently, the induction time should not be considered as a material constant. Based on our results, a quantitative criterion has been formulated for the occurrence of Case II diffusion. Typical trend of Case II front penetration can be recreated when the surface resistance boundary condition is used. This suggested that Case II sorption can be regarded as a pseudo steady state transport process. The initial flux of the penetrant into the glassy polymer during the induction period may be limited to a much lower finite value, due to the coupling between diffusion and differential swelling stress in a viscoelastic glassy polymer.

A new phase diagram has been constructed to predict the occurrence of Case II behavior. It provides a qualitative definition of the upper temperature limit for Fickian diffusion or lower temperature limit for anomalous diffusion in glassy polymers (see appendix).

5.2 Suggestions for Future Work

The inability of the classical Fick's law in describing anomalous diffusion again reveals that Fick's law and consequently Fourier's law are perhaps limiting laws. They can be used as a first approximation for simple diffusion process. As in Newton's law, the adoption of the first derivative is not supported by any universal principle or method.

Despite the intensive research effort in this area, it is generally agreed that a complete physical picture of diffusion in glassy polymer is not yet available. It should be emphasized here

again that a glass transition is not essential for the occurrence of Case II behavior. The exact nature of relaxation involved in Case II sorption is still not clear, though it has been unduly associated with glass transition. Since the front penetration rate remains constant as the distributions of internal stresses change, the effect of internal stresses might not be dominant in Case II sorption. More systematic and creative experimental investigation is needed to quantitatively test some of the existing models and theories, to examine the synergy between relaxation, swelling (internal stress or gradient of internal stress) and diffusion, to elucidate the micro-mechanism or macro-mechanism of Case II behavior, and ultimately to establish a criterion for the occurrence of Case II behavior.

Existing theories are generally *ad hoc* and the predicted trends are only in qualitative agreement with some experiments. The seemingly controversial or intriguing experimental results have not been explained by a consistent theory. So far, no model has been successful both qualitatively and quantitatively in predicting this synergistic effect. A more realistic physical picture for Case II sorption in glassy polymer is still lacking. Both the boundary conditions and governing equations need to be re-formulated according to the physical scenario of Case II behavior, consistent with the spectra of known anomalous transport behaviors. In particular, the theory for Case II sorption should be a special case of a unified theory for anomalous transport.

The practical exploitation of Case II behavior for the design of zero-order drug release device may be questionable, since the transport process involved in drug release from glassy hydrogels is more likely to be multi-component diffusion, involving mechanisms different from typical Case II sorption. Furthermore, the drug release rate from such device may be too slow to

be useful for high molecular weight drugs, such as proteins and peptides. Moreover, zero-order release may not necessarily the optimal profile to pursue as dictated by chronopharmacokinetics.

References

Alfrey T. (1965) Glassy Polymer Diffusion Is Often Tractable, Chemical & Engineering News, October, 64-65

Alfrey T, Gurnee EF and Lloyde WG. (1966) Diffusion in Glassy Polymers, Journal of Polymer Science, Part C, 12:249-261

Arnould D and Laurence RL. (1992) Size Effects on Solvent Diffusion in Polymers, Industrial & Engineering Chemistry Research, 31:218-228

Astarita G and Joshi S. (1978) Sample Dimension Effects in the Sorption of Solvents in Polymers. A Mathematical Models, Journal of Membrane Science, 8:165-182

Astarita G and Sarti GC. (1978) A Class of Mathematical Models for Sorption of Swelling Solvents in Glassy Polymers, Polymer Engineering and Science. 18:319-395

Auerbach I, Miller WR, Kuryla WC and Gehman SD. (1958) A Diffusivity Approach for Studying Polymer Structure, Journal of Polymer Science, 28:129-150

Baird BR, Hopfenberg HB and Stannett VT. (1971) The Effect of Molecular Weight and Orientation on the Sorption of n-Pentane by Glassy Polystyrene, Polymer Engineering and Science, 11:274-283

Bellenger V, Kaltenecker-Commercon J, Verdu J and Tordjeman P. (1997) Interactions of Solvents with Poly (methyl methacrylate), Polymer, 38:4175-4184

Berens AR and Hopfenberg HB. (1978) Diffusion and Relaxation in Glassy Polymer Powders: 2. Separation of Diffusion and Relaxation Parameters, Polymer, 19:489-496

Berens AR and Hopfenberg HB. (1979) Induction and Measurement of Glassy-State Relaxations by Vapor Sorption Techniques, Journal of Polymer Science, Part B, Polymer Physics, 17:1757-1770

Billovits GF and Durning CJ. (1988) Penetrant Transport in Semicrystalline Poly (ethylene terephthalate), Polymer, 29:1468-1484

Bray JC and Hopfenberg HB. (1969) The Effect of Polymer Molecular Weight on the Solvent Crazing of Polystyrene, Polymer Letters, 7:679-684

Brochard F and de Gennes PG. (1983) Kinetics of Polymer Dissolution, PCH PhysicoChemical Hydrodynamics, 4:313-322

Brown HR. (1989) A Model of Environmental Craze Growth in Polymers, Journal of Polymer Science, Part B, Polymer Physics, 27:1273-1288

Cairncross RA and Durning CJ. (1996) A Model for Drying of Viscoelastic Polymer Coatings, AIChE Journal, 42:2415-2425

Carbonell RG and Sarti GC. (1990) Coupled Deformation and Mass-Transport Processes in Solid Polymers, Industrial & Engineering Chemistry Research, 29:1194-1204

Carslaw HS and Jaeger JC. (1959a) Conduction of Heat in Solids, Oxford Press, pp.75

Carslaw HS and Jaeger JC. (1959b) Conduction of Heat in Solids, Oxford Press, pp.112

Carslaw HS and Jaeger JC. (1959c) Conduction of Heat in Solids, Oxford Press, pp.71

Camera-Roda G and Sarti GC. (1990) Mass Transport with Relaxation in Polymers, AIChE Journal, 36:851-860

Carbonell RG and Sarti GC. (1990) Coupled Deformation and Mass-Transport Processes in Solid Polymers, Industrial & Engineering Chemistry Research, 29:1194-1204

Cohen DS and Erneux T. (1990) Changing Time History in Moving Boundary Problems, SIAM Journal of Applied Mathematics, 50:483-489

Cohen DS and White Jr. AB. (1989) Sharp Fronts Due to Diffusion and Stress at the Glass Transition in Polymers, Journal of Polymer Science, Part B, Polymer Physics, 27:1731-1747

Cohn D and Marom G. (1982) Anisotropic Hygroelastic Behavior of Poly (methyl methacrylate) under Case II Diffusion, Polymer Engineering and Science, 22:870-877

Cohn D and Marom G. (1983) Deformation and Failure of Polymeric Matrices under Swelling Conditions, Journal of Applied Polymer Science, 28:1981-1992

Cole JV and Lee HH. (1989) A Criterion for Case II Diffusion in Resist Development by Dissolution, Journal of Electrochemical Society, 136:3872-3873

Cox RW. (1990) Shocks in a Model for Stress-Driven Diffusion, SIAM Journal of Applied Mathematics, 50:1284-1299

Cox RW and Cohen DS. (1989) A Mathematical Model for Stress-Driven Diffusion in Polymers, Journal of Polymer Science, Part B, Polymer Physics, 27:589-602

Crank J. (1953) Influence of Molecular Relaxation and Internal Stress on Diffusion in Polymer, Journal of Polymer Science, 11:151-168

Crank J. (1975a) The Mathematics of Diffusion, Clarendon Press, pp.61-62

Crank J. (1975b) The Mathematics of Diffusion, Clarendon Press, pp.81

Crank J. (1975c) The Mathematics of Diffusion, Clarendon Press, pp.96-97

Crank J. (1975d) The Mathematics of Diffusion, Clarendon Press, pp. 36

Crank J. (1975e) The Mathematics of Diffusion, Clarendon Press, pp. 60

Crank J. (1975f) The Mathematics of Diffusion, Clarendon Press, pp. 80

Doghieri F, Camera-Roda G and Sarti GC. (1993) Rate Type Equations for the Diffusion in Polymers: Thermodynamic Constraints, AIChE Journal, 39:1847-1858

Downes S. (1991) Methods for Improving Drug Release from Poly (methyl methacrylate) Bone Cement, Clinical Materials, 7:227-231

Drake PA and Bohn PW. (1994) Localized Raman Scattering Probes of Molecular-Scale motions in Case II Swelling of Polystyrene in n-Hexane, Analytical Chemistry, 66:79-84

Drake PA and Bohn PW. (1995) Anomalous Diffusion. Surface Plasmon Resonance Measurements as Probes of Nanometer-Scale Film-Swelling Dynamics for CH_3OH in Poly(methyl methacrylate), Analytical Chemistry, 67:1766-1771

Drake PA and Bohn PW. (1996) Interfacial Events Associated with Case II Diffusion in the Poly(methyl methacrylate)/CH_3OH System, Applied Spectroscopy, 50:1023-1029

Durning CJ, Edwards DA and Cohen DS. (1996) Perturbation Analysis of Thomas and Windle's Model of Case II Transport, AIChE Journal, 42:2025-2035

Durning CJ, Hassan MM, Tong HM and Lee KW. (1995) A Study of Case II Transport by Laser Interferometry, Macromolecules, 28:4234-4248

Durning CJ Spencer JL and Tabor M. (1985) Differential Sorption and Permeation in Viscous Media, Journal of Polymer Science, Polymer Letters Edition, 23:171-181

Durning CJ and Tabor M. (1986) Mutual Diffusion in Concentrated Polymer Solutions, Macromolecules, 19:2220-2232

Edwards DA. (1996) Non-Fickian Diffusion in Thin Polymer Films, Journal of Polymer Science, Part B, Polymer Physics, 34:981-997

Edwards DA and Cohen DS. (1995a) An Unusual Moving Boundary Condition arising in Anomalous Diffusion Problems, SIAM Journal of Applied Mathematics, 55:662-676

Edwards DA and Cohen DS. (1995b) A Mathematical Model for a Dissolving Polymer, AIChE Journal, 40:2345-2355

Enscore DJ, Hopfenberg HB and Stannett VT. (1977a) Effect of Particle Size on the Mechanism Controlling n-Hexane Sorption in Glassy Polystyrene Microspheres, Polymer, 18:793-800

Enscore DJ, Hopfenberg HB, Stannett VT and Berens AR. (1977b) Effect of Prior Sample History on n-Hexane Sorption in Glassy Polystyrene Microspheres, Polymer, 18:1105-1110

Ercken M, Adriaensens P, Reggers G, Carleer R, Vanderzande D and Gelan J. (1996) Use of Magnetic Resonance Imaging to Study Transport of Methanol in Poly(methyl methacrylate) at Variable Temperature, Macromolecules, 29:5671-5677

Fahmay AA and Hurt JC. (1980) Stress Dependence of Water Diffusion in Epoxy Resin, Polymer Composites, 1:77-80

Fieldson GT and Barbari TA. (1995) Analysis of Diffusion in Polymers Using Evanescent Field Spectroscopy, AIChE Journal, 41:795-804

Friedman A and Rossi G. (1997) Phenomenological Continuum Equations to Describe Case II Diffusion in Polymeric Materials, Macromolecules, 30:153-154

Frisch HL. (1964) Isothermal Diffusion in Systems with Glasslike Transitions, The Journal of Chemical Physics, 41:3679-3683

Frisch HL. (1980) Sorption and Transport in Glassy Polymers - A Review, Polymer Engineering and Science, 20:2-13

Frisch HL, Wang TT and Kwei TK. (1969) Diffusion in Glassy Polymers. II, Journal of Polymer Science, Part A-2, 7:879-887

Fu TZ and Durning CJ. (1993) Numerical Simulation of Case II Transport, AIChE Journal, 39:1030-1044

Gall TP, Lasky RC and Kramer EJ. (1990) Case II Diffusion: Effect of Solvent Molecule Size, Polymer, 31:1491-1499

Gent AN and Liu GL. (1991) Diffusion of Polymer Molecules into Polymer Networks: Effect of Stress and Constraints, Journal of Polymer Science: Part B: Polymer Physics, 29:1313-1319

Gostoli G and Sarti GC. (1983) Influence of Rheological Properties in Mass Transfer Phenomena: Super Case II Sorption in Glassy Polymers, Chemical Engineering Communication, 21:67-79

Govindjee S and Simo JC. (1993) Coupled Stress-Diffusion: Case II, Journal of Mechanics and Physics of Solids, 41:863-887

Graessley WW. (1982) Entangled Linear, Branched and Network Polymer Systems - Molecular Theories, Advances in Polymer Science, 47:67-117

Grinsted RA, Clark L and Koenig JL. (1992) Study of Cyclic Sorption-Desorption into Poly (methyl methacrylate) Rods Using NMR Imaging, Macromolecules, 25:1235-1241

Harmon JP, Lee S and Li JCM. (1987) Methanol Transport in PMMA: The Effect of Mechanical Deformation, Journal of Polymer Science, Part A, Polymer Chemistry, 25:3215-3229

Hayes CK and Cohen DS. (1992) The Evolution of Steep Front in Non-Fickian Polymer-Penetrant Systems, Journal of Polymer Science, Part B, Polymer Physics, 30:145-161

Herman MF and Edwards SF. (1990) A Reptation Model for Polymer Dissolution, Macromolecules, 23:3662-3671

Hopfenberg HB. (1978) The Effect of Film Thickness and Sample History on the Parameters Describing Transport in Glassy Polymers, Journal of Membrane Science, 3:215-230

Hopfenberg HB and Frisch HL. (1969) Transport of Organic Micromolecules in Amorphous Polymers, Polymer Letters, 7:405-409

Hopfenberg HB, Holley RH and Stannett V. (1969) The Effect of Penetrant Activity and Temperature on the Anomalous Diffusion of Hydrocarbons and Solvent Crazing in Polystyrene, Part I: Biaxially Oriented Polystyrene, Polymer Engineering and Science, 9:242-249

Hopfenberg HB and Hsu KC. (1978) Swelling-Controlled, Constant Rate Delivery Systems, Polymer Engineering and Science, 18:1186-1191

Hui C-Y, Wu K-C, Lasky RC. and Kramer J. (1987a) Case II Diffusion in Polymer. I. Transient Swelling, Journal of Applied Physics, 61:5129-5136

Hui C-Y, Wu K-C, Lasky RC and Kramer J. (1987b) Case II Diffusion in Polymer. II. Steady-State Front Motion, Journal of Applied Physics, 61:5137-5149

Jacques CHM and Hopfenberg HB. (1974a) Vapor and Liquid Equilibria in Glassy Polyblends of Polystyrene and Poly(2,6-Dimethyl-1,4-Phenylene Oxide): Part I. Polymer Engineering and Science, 14:441-448

Jacques CHM and Hopfenberg HB. (1974b) Kinetics of Vapor and Liquid Transport in Glassy Polyblends of Polystyrene and Poly(2,6-Dimethyl-1,4-Phenylene Oxide): Part II, Polymer Engineering and Science, 14:449-455

Janacek J. and Kolarik J. (1976) Secondary Relaxation of Swollen Polymethacrylates and Methacrylate Copolymers, International Journal of Polymeric Materials, 5:71-88

Joshi S and Astarita G. (1979) Mathematical Model of the Desorption of Swelling Solvents from Swollen Polymer Films, Polymer, 20:1217-1220

Jou D, Camacho J and Grmela M. (1991) On the Nonequilibrium Thermodynamics of Non-Fickian Diffusion, Macromolecules, 3597-3602

Jou D, Casas-Vázquez J and Lebon G. (1996) Extended Irreversible Thermodynamics, Second Edition, Springer-Verlag Berlin Heidelberg New York, 299-304

Kalospiros NS, Ocone R, Astraria G and Meldon JH. (1990) Analysis of Anomalous Diffusion and Relaxation in Solid Polymers, Industrial & Engineering Chemistry Research, 30:851-864

Kalospiros NS, Astraria G and Paulaitis ME. (1993) Coupled Diffusion and Morphological Change in Solid Polymers, Chemical Engineering Science, 48:23-40

Kausch HH and Plummer CJG. (1994) The Role of Individual Chains in Polymer Deformation, Polymer, 35:3848-3856

Kim D-J, Caruthers JM and Peppas NA. (1996) Experimental Verification of a Predictive Model of Penetrant Transport in Glassy Polymers, Chemical Engineering Science. 51:4827-4841

Kim M and Neogi P. (1984) Concentration-Induced Stress Effects in Diffusion of Vapors through Polymer Membranes, Journal of Applied Polymer Science, 29:731-742

Kip GAM, Busscher HJ, van Silfhout A and Arends J. (1985) Surface Layer Relaxation in PMMA during n-Propanol Adsorption and Desorption: An Ellipsometric Study, Polymer Communication, 26:215-217

Klier J and Peppas NA. (1987) Anomalous Penetrant Transport in Glassy Polymer: 4. Stresses in Partially Swollen Polymers, Polymer, 28:1851-1859

Larché FC and Cahn JW. (1982) The Effect of Self-Stress on Diffusion in Solids, Acta Metallurgica, 30:1835-1845

Lasky RC, Kramer J and Hui C-Y. (1988a) The Initial Stages of Case II Diffusion at Low Penetrant Activities. Polymer, 29:673-679

Lasky RC, Kramer J and Hui C-Y. (1988b) Temperature Dependence of Case II Diffusion, Polymer. 29:1131-1135

Lee PI. (1993) Temperature Dependence of Methanol Transport in Spherical PMMA Beads, Polymer. 34:2397-2400

Lee PI and Kim C-J. (1992) Effect of Geometry on Solvent Front Penetration in Glassy Polymers. Journal of Membrane Science. 65:77-92

Lee S and Li JCM. (1981) Dislocation-Free Diffusion Processes, Journal of Applied Physics, 52:1336-1346

Li JCM. (1978) Physical Chemistry of Some Microstructural Phenomena. Metallurgical Transactions A, 9A:1353-1380

Lin CB, Lee S and Liu KS. (1990) Methanol-Induced Crack Healing in Poly (methyl methacrylate), Polymer Engineering & Science. 30:1399-1406

Lin CB, Liu KS and Lee S. (1991) Methanol-Induced Opacity in Poly (methyl methacrylate), Journal of Polymer Science, Part B, Polymer Physics, 29:1457-1466

Long FA and Richman D. (1960) Concentration Gradients for Diffusion of Vapours in Glassy Polymers and Their Relation to Time-Dependent Diffusion Phenomena, Journal of American Chemical Society, 82:513-519

Lustig SR, Caruthers JM and Peppas NA. (1992) Continuum Thermodynamics and Transport Theory for Polymer-Fluid Mixtures. Chemical Engineering Science, 47:3037-3057

Mark HF. (1985) Encyclopedia of Polymer Science and Engineering, A Wiley-Interscience publication, 1:234-299

McAfee KB. (1958) Stress-Enhanced Diffusion in Glass. I. Glass under Tension and Compression; II. Glass under Shear, The Journal of Chemical Physics, 28:218-229

McGarel OJ and Wool RP. (1987) Craze Growth and Healing in Polystyrene. Journal of Polymer Science, Part B, Polymer Physics, 25:2541-2560

McLeish TCB, Plummer CJG and Donald AM. (1989) Crazing by Disentanglement: Non-Diffusive Reptation. Polymer, 30:1651-1655

More AP, Donald AM and Henderson A. (1992) Stress Modified Case II Diffusion in Poly (methyl methacrylate), Polymer, 33:3759-3761

Neogi P. (1983) Anomalous Diffusion of Vapors through Solid Polymers, AIChE Journal, 29:829-839

Neogi P. (1993) A Hole-Filling Theory of Anomalous Diffusion in Glassy Polymers: Effects of Microvoids, Journal of Polymer Science: Part B: Polymer Physics, 31:699-710

Neogi P, Kim M and Yang Y. (1986) Diffusion in Solids under Strain, with Emphasis on Polymer Membranes, AIChE Journal, 32:1146-1157

Neumann S and Marom G. (1987) Prediction of Moisture Diffusion Parameters in Composite Materials under Stress, Journal of Composite Materials, 21:68-80

Papanu JS, Hess DW, Soane DS and Bell AT. (1990) Swelling of Poly(methyl Methacrylate) Thin Films in Low Molecular Weight Alcohols, Journal of Applied Polymer Science, 39:803-823

Peterlin A. (1965) Diffusion in a Network with Discontinuous Swelling, Journal of Polymer Science, Part B, Polymer Physics, 3:1083-1087

Peterlin A. (1980) Diffusion with Discontinuous Swelling. IV. Type II Diffusion into Spherical Particles, Polymer Engineering and Science, 20: 238-243

Petropoulos JH and Roussis PP. (1978) The Influence of Transverse Differential Swelling Stresses on the Kinetics of Sorption of Penetrants by Polymer Membranes, Journal of Membrane Science, 3:343-356

Plummer CJG and Donald AM. (1990) Disentanglement and Crazing in Glassy Polymers, Macromolecules, 23:3929-3937

Rossi G, Pincus PA and de Gennes P-G. (1995) A Phenomenological Description of Case II Diffusion in Polymeric Materials, Europhysics Letters, 35:391-396

Samus MA and Rossi G. (1996) Methanol Absorption in Ethylene-Vinyl Alcohol Copolymers: Relation between Solvent Diffusion and Changes in Glass Transition Temperature in Glassy Polymeric Materials, Macromolecules, 29:2275-2288

Sarti G and Doghieri F. (1994) Non-Fickian Transport of Alkyl Alcohols through Prestretched Poly (methyl methacrylate), Chemical Engineering Science, 49:733-748

Sauer BB and Walsh DJ. (1991) Use of Neutron Reflection and Spectroscopic Ellipsometry for the Study of the Interface between Miscible Polymer Films, Macromolecules, 24:5948-5955

Sauer BB and Walsh DJ. (1994) Effect of Solvent Casting on Reduced Entanglement Density in Thin Films Studied by Ellipsometry and Neutron Reflection, Macromolecules, 27:432-440

Shankar V. (1981) Influence of Interfacial Resistance on Kinetics of Sorption, Polymer, 22:748-752

Sih GC, Michopoulos JG and Chou SC. (1986) Hygrothermoelasticity, Martinus Nijhoff Publishers

Smith TL and Adam RE. (1981) Effect of Tensile Deformation on Gas Transport in Glassy Polymer Films, Polymer, 22:299-304

Thomas NL. (1978) Transport Mechanism Associated with the Swelling of PMMA by Methanol, Ph. D thesis, University of Cambridge

Thomas NL and Windle AH. (1977) Discontinuous Shape Changes Associated with Case II Transport of Methanol in Thin Sheets of PMMA, Polymer, 18:1195

Thomas NL and Windle AH. (1978) Transport of Methanol in Poly(methyl methacrylate), Polymer, 19:255-265

Thomas NL and Windle AH. (1980) A Deformation Model for Case II Diffusion, Polymer, 21:613-619

Thomas NL and Windle AH. (1981) Diffusion Mechanics of the System PMMA-Methanol, Polymer, 22:627-639

Thomas NL and Windle AH. (1982) A Theory of Case II Diffusion, Polymer, 23:529-542

Treloar LRG. (1976) Swelling of Bonded-Rubber Cylinders, Polymer, 17:142-146

Truesdell C. (1984) Rational Thermodynamics, 2nd Edition, Springer, New York

Tsai SW and Hahn HT. (1980) Introduction to Composite Materials, Technomic Publishing Company Inc.

Umezawa K, Gibson WM, Welch JT, Araki, K, Barros G and Frisch HL. (1992) A Study of Case II Diffusion of a Fluorinated Hydrocarbon in Poly(styrene) by Resonance Nuclear Reaction Analysis, Journal of Applied Physics, 71:681-684

Unger DJ and Aifantis EC. (1983) On the Theory of Stress-Assisted Diffusion, II, Acta Mechanica, 47:117-151

Vrentas JS and Duda CM. (1977) Diffusion of Polymer-Solvent Systems. III. Construction of Deborah Number Diagrams, Journal of Polymer Science, Part B, Polymer Physics, 15:441-453

Vrentas JS, Jarzebski CM and Duda JL. (1975) A Deborah Number for Diffusion in Polymer-Solvent Systems, AIChE Journal, 21:894-901

Weitsman Y. (1990) A Continuum Diffusion Model for Viscoelastic Materials, Journal of Physical Chemistry, 94:961-968

Williams DRG, Allen, PEM and Truong VT. (1986) Glass Transition Temperature and Stress Relaxation of Methanol Equilibrated Poly(methyl methacrylate), European Polymer Journal, 22:911-919

Wilson RK and Aifantis EC. (1982) On the Theory of Stress-Assisted Diffusion, I, Acta Mechanica, 45:273-296

Windle AH. (1984) The Influence of Thermal and Mechanical Histories on Case II Sorption of Methanol by PMMA, Journal of Membrane Science, 18:87-97

Windle AH. (1985) Case II Sorption, in "Polymer Permeability" (Edited by J Comyn), Elsevier Applied Science, London, 75-118

Witelski TP. (1996) Traveling Wave Solutions for Case II Diffusion in Polymers, Journal of Polymer Science, Part B, Polymer Physics, 34:141-150

Wu JC and Peppas NA. (1993) Modeling of Penetrant Diffusion in Glassy Polymers with an Integral Sorption Deborah Number, Journal of Polymer Science, Part B, Polymer Physics, 31:1503-1518

Yaniv G and Ishai O. (1987) Coupling between Stresses and Moisture Diffusion in Polymeric Adhesives, Polymer Engineering & Science, 27:731-739

Appendix

A Graphic Presentation of Diffusion Behavior in Glassy Polymers

Introduction

The sorption of small molecules in glassy polymer is not a simple mixing or diffusion process, except for sorption involving penetrant at very low activity or at very high temperatures (far above T_g). The interaction of penetrant and polymer may induce different changes in the polymer structures within various parts of the specimen during sorption. The structural changes of polymer can be reversible or irreversible depending on the diffusion temperature, type and activity of the penetrant, the chemical and physical structure of the polymer, and consequently a spectrum of diffusion behavior is observed, which cannot always be described by Fick's law.

The chemical structure and T_g of poly (methyl methacrylate) (PMMA) and poly-hydroxylethylmethacrylate (PHEMA) are very close. Under ambient conditions, the penetration of methanol into PMMA is purely Case II in contrast to the anomalous or non-Fickian sorption behavior of water in PHEMA. It is not clear as to how the difference in diffusion behavior in PMMA and PHEMA arises. To understand what makes them different, it is necessary to examine physicochemical factors relevant to diffusion of solvent in glassy polymers. Although experimental and theoretical efforts have been made to delineate the transport processes involved in the absorption of small molecules in polymers (Alfrey, 1965; Alfrey et al., 1966; Hopfenberg and Frisch, 1969; Cole and Lee, 1989), criteria available for the prediction of transport behavior under a given set of conditions are generally unsatisfactory. To elucidate the mechanism of Case II sorption, it is desirable to re-examine the criteria for conditions under which Case II sorption will occur.

Alfrey (1965), Hopfenberg and Frisch (1969) attempted to describe the full spectrum of diffusion behaviors for a given polymer-penetrant system in a phase diagram with temperature and penetrant activity as independent variables. This systematic phase

diagram, however, does not encompass all experimental observations. For example, immediately following the complete desorption of methanol from PMMA, the reabsorption of methanol is no longer Case II. But according to the phase diagram of Hopfenberg and Frisch (1969), if the absorption temperature and the penetrant activity are the same, one should expect the same Case II behavior. This is certainly not consistent with experimental observations. It should also be noted that diffusion of penetrant into glassy polymer will cease at 0 K, and Hofenberg's experimental results show that the thickness of the polymer will determine the mode of diffusion (Enscore *et al.*, 1977a, 1977b; Hopfenberg, 1978, Thomas and Windle, 1978). These facts are not included in the reported phase diagram. Therefore, there is a need for a generalized new phase diagram for the polymer-penetrant system.

Vrentas, Duda and co-workers correlated the appearance of non-Fickian behavior with a diffusional Deborah number $\theta=\alpha D/L^2$, the ratio of a characteristic relaxation time to a characteristic diffusion time (Vrentas *et al.*, 1975). Here, α is the mean relaxation time; D is a diffusion coefficient and L is a characteristic length. L^2/D represents a characteristic time for sorption determined by molecular mechanism. They showed that the anomalous behavior appears at intermediate Deborah numbers. The size of a swelling sample and the relaxation behavior of polymer will play an important role in determining the Deborah number and the corresponding transport kinetics. Although Deborah number diagrams were constructed to predict the diffusion pattern, they cannot be used to predict the occurrence of Case II behavior, because Deborah number can be well defined only in differential sorption and, as a result, integral sorption cannot be characterized by a single Deborah number (Vrentas and Duda, 1977; Wu and Peppas, 1993). An integral Deborah number has been defined as the ratio of the characteristic relaxation time in the glassy region to the characteristic time in the swollen region in order to characterize integral sorption with a single value (Wu and Peppas, 1993).

Although Deborah number has been widely used to interpret experimental observations, the soundness of these ideas was challenged based on physical considerations (Samus and Rossi, 1996). For example, according to the Deborah number diagram, when a PMMA slab is immersed in methanol, Case II behavior should occur at

room temperature for samples with a thickness of about 1 mm, whereas Fickian behavior may take place when a sufficiently thick slab of PMMA is used. However, when extending this approach to other Fickian systems such as natural rubber or polyethylene, unrealistic prediction of "non-Fickian" or even Case II behavior for thin films would result. Since Case II behavior only occurs during integral sorption when the polymer is in glassy state, the extent of utility of the Deborah number diagram is therefore open to interpretation.

Available experimental evidence suggests that during Case II sorption the swollen polymer can be either glassy or rubbery. Since the state of a swollen polymer is related to the penetrant concentration in the polymer, it is obvious that the criterion for Case II sorption cannot be based solely on penetrant concentrations affecting the glass transition. There is good evidence that the maximum penetrant concentration gradient in a polymer may determine the transport pattern through its influence on osmotic pressure.

A new phase diagram has been constructed to illustrate the temperature-dependent diffusion behavior, which provides a qualitative definition of the upper temperature limit for Fickian diffusion or lower temperature limit for anomalous diffusion in glassy polymers.

Phase Diagram and Criterion

Although experimental and theoretical efforts have been made to delineate the transport process involved in the absorption of small molecules in polymers, at present, no practical criteria are available to predict the transport behavior or conditions for the transformation of diffusion behavior under a given set of conditions. It is not surprising that no satisfactory theory can predict the conditions under which Case II sorption would occur.

It is well known that existing diffusion of small molecules proceeds with the fluctuation of the free volume distribution within the polymer. The interaction between polymer and penetrant certainly depends on the temperature since it determines the dynamics of the fluctuation and the equilibrium concentration of the system. Depending

on the type and activity of the penetrant, swelling of the polymer may occur. The physical state of the penetrated polymer and its transition will depend on the concentration of the penetrant and temperature as well as on time and position. The diffusion behavior will be significantly influenced by the physical state of the penetrated polymer. Although the criteria are still unknown, it is reasonable to expect that good solvent will enable the dissolution of polymer through the oriented reptation of polymer chains, poor solvent may induce crazing of polymer through forced reptation of polymer chains or cracking of polymer involving scission of polymer chains. The structural changes in the polymer will affect the pattern of subsequent penetrant uptake.

In Figure A1, a new diagram is constructed to predict the local diffusion pattern of a penetrant (activity=1.0) into a polymer solid. In this diagram, C_t is the local concentration of the penetrant inside the polymer at time t which is related to the polymer volume change due to swelling. C_e is the equilibrium (maximum) concentration of the penetrant in the polymer which increases with increasing temperature. C_g is the penetrant concentration at which the transition of polymer from glassy to rubbery state occurs. C_l is the minimum concentration at which the polymer changes into liquid or the maximum concentration at which the polymer remains rubbery.

T_β is the temperature at the onset of β relaxation of the polymer. At temperature below T_β, the penetrated polymer will remain in its glassy state. The change of C_t is essentially Fickian. The diffusion is realized through the fluctuation of the free volume distribution related to γ relaxation. The activation energy for diffusion is generally less than 10 kcal/mol.

T_α is the temperature at which glass transition of polymer occurs when it is in equilibrium with the penetrant. At temperatures between T_β and T_α, the change of C_t is initially Fickian. Deviation from Fickian behavior will occur due to changes in the penetrated polymer structure at higher penetrant concentration. Maximum osmotic pressure is expected in this temperature range due to an increased equilibrium penetrant concentration and a relatively restricted polymer mobility. Anomalous diffusion such as Case II sorption, Super Case II sorption may occur due to the generation of microvoids,

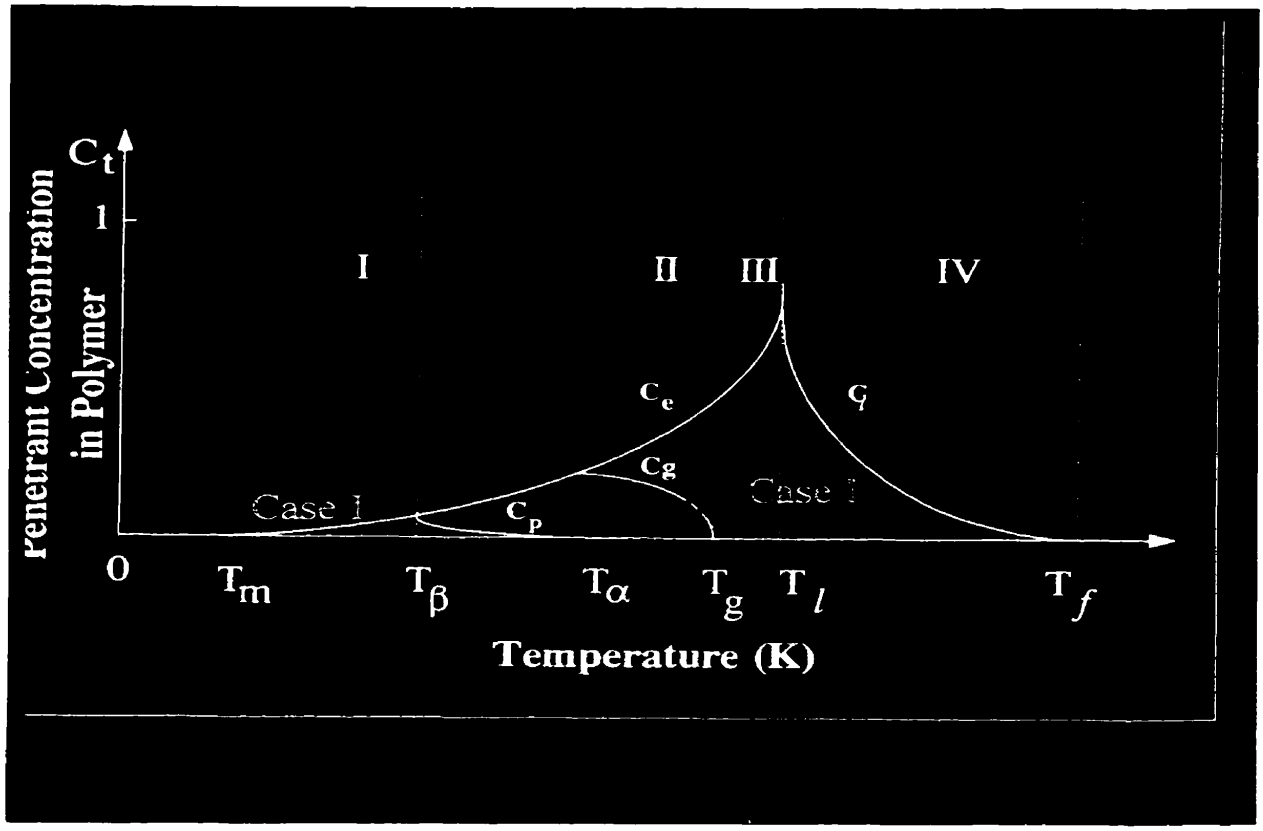

Figure A1 Phase diagram for transport of penetrant in polymers

crazes or cracks in various parts of the polymer through forced reptation of polymer chains related to β relaxation, mainly driven by the osmotic pressure. The activation energy ranges from 20 to 50 kcal/mol, corresponding to the range of the activation energy from β relaxation of the polymer to primary chain scission.

Between T_α and the glass transition temperature of the unpenetrated polymer, T_g, anomalous diffusion will eventually occur due to the transition of polymer state induced by the high degree of penetrant sorption. In this case, a significant increase in the volume of the swelling polymer is expected. Case II sorption may also occur when the swollen polymer is rubbery.

T_l is the onset temperature at which polymer starts to flow. Between T_g and T_l, the polymer initially remains in the rubbery state. The change of C_t is initially Fickian. Concentration dependent diffusion is expected at higher penetrant concentration. Between T_l and T_f, dissolution or flow of polymer will eventually occur. Here the diffusion behavior is completely Fickian.

Conclusions

A new phase diagram is constructed to predict the occurrence of Case II behavior. It provides a qualitative definition of the upper temperature limit for Fickian diffusion or lower temperature limit for anomalous diffusion in glassy polymers.

IMAGE EVALUATION
TEST TARGET (QA–3)

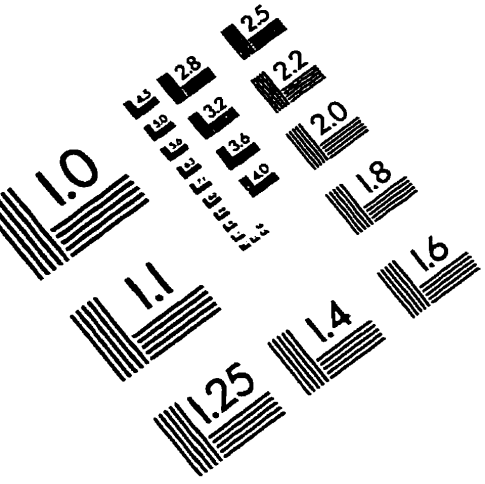

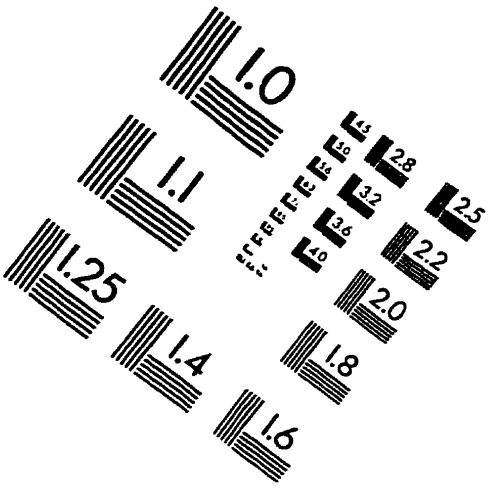

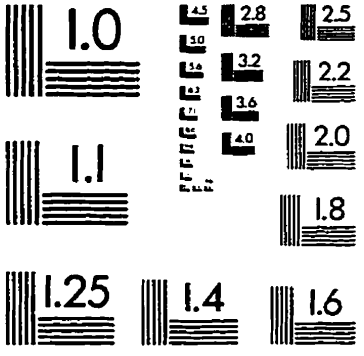

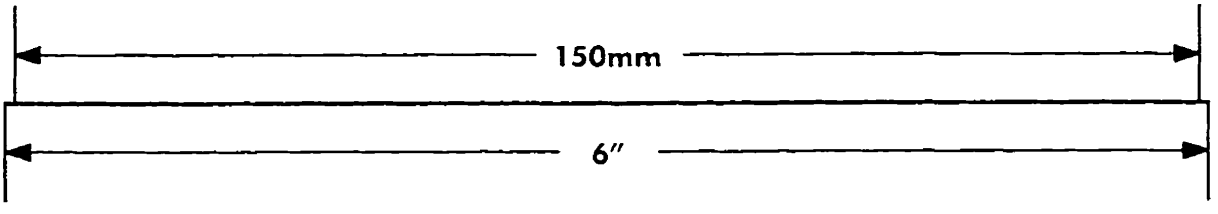

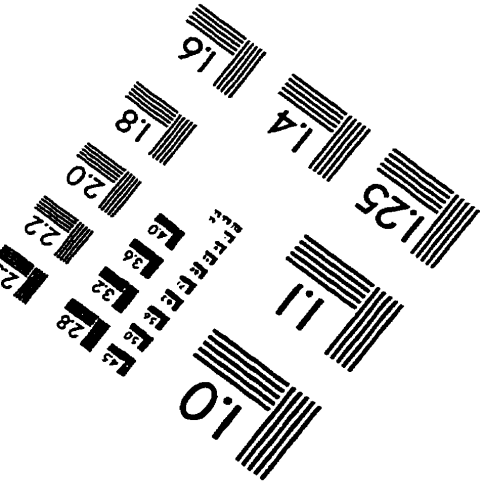

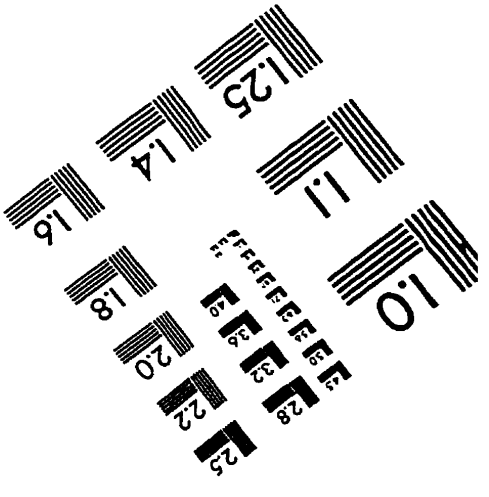

APPLIED IMAGE, Inc
1653 East Main Street
Rochester, NY 14609 USA
Phone: 716/482-0300
Fax: 716/288-5989